

Mitochondria and Cellular Cytochromes as Oxygen Sensors in Hypoxic Pulmonary Vasoconstriction

Inaugural Dissertation

Submitted to the Faculty of Medicine

in partial fulfillment of the requirements

for the PhD-Degree

of the Faculties of Veterinary Medicine and Medicine

of the Justus Liebig University Giessen

by

Sommer, Natascha

of

Nürnberg

Germany

Giessen 2011

From the Department of Medicine
Director: Prof. Dr. Werner Seeger
of the Faculty of Medicine of the Justus Liebig University Giessen

First Supervisor and Committee Member: Prof. Dr. Norbert Weissmann

Second Supervisor and Committee Member:

Committee Members:

Date of Doctoral Defense:

I declare that I have completed this dissertation single-handedly without the unauthorized help of a second party and only with the assistance acknowledged therein. I have appropriately acknowledged and referenced all text passages that are derived literally from or are based on the content of published or unpublished work of others, and all information that related to verbal communications. I have abided by the principles of good scientific conduct laid down in the charter of the Justus Liebig University of Giessen in carrying of the investigations described in the dissertation.

I. Table of contents

1	Introduction	12
1.1	Hypoxic pulmonary vasoconstriction (HPV).....	12
1.1.1	Physiological relevance	12
1.1.2	Characteristics of HPV - effector and sensor cell type	13
1.1.3	Mechanism of HPV - effectors, mediators, sensors.....	14
1.1.3.1	Effector pathway	14
1.1.3.2	Mediators: Reactive oxygen species (ROS) and redox state	16
1.1.3.2.1	Application of oxidants and antioxidants.....	17
1.1.3.2.2	Measurement of ROS	18
1.1.3.3	Other mediators: ATP, AMP kinase, protein kinases, carbon monoxide (CO), hydrogen sulfide (H ₂ S).....	19
1.1.3.4	Oxygen sensors in HPV - location and dynamic range.....	20
1.1.3.4.1	Mitochondria as oxygen sensor: ATP production – ROS metabolism – calcium buffering.....	21
1.1.3.4.1.1	Inhibition of complex IV	22
1.1.3.4.1.2	Mitochondrial ROS production	23
1.1.3.4.1.3	Calcium homeostasis	28
1.1.3.4.2	NAD(P)H oxidase	28
1.1.3.4.3	Cytochrome P450, EETs and HETEs.....	29
1.1.3.4.4	Hemeprotein related to potassium channels	30
1.2	Measurement of mitochondrial function in HPV.....	31
1.2.1	Respiration.....	31
1.2.2	Redox state of mitochondrial cytochromes.....	32
1.3	Measurement of NADPH oxidase, cytochrome P 450 and other heme proteins in HPV.....	33
1.4	Aim of the study.....	34
2	Material and Methods.....	36
2.1	Materials	36
2.1.1	Animals	36
2.1.2	Equipment.....	36
2.1.3	Chemicals and reagents.....	37
2.1.4	Antibodies	38
2.2	Methods.....	39
2.2.1	Isolated lung models.....	39
2.2.1.1	Isolated perfused and ventilated rabbit lung	39
2.2.1.2	Isolated perfused and ventilated mouse lung	40
2.2.2	Isolated cell experiments	40

2.2.2.1	Isolation of pulmonary and renal arterial smooth muscle cells	40
2.2.2.2	Isolation of aortal smooth muscle cells	41
2.2.2.3	Cell culture and preparation for respirometric measurement.....	41
2.2.2.4	Immunoflourescence staining	42
2.2.3	Remission spectrophotometry	42
2.2.3.1	Principle of spectral measurements.....	42
2.2.3.2	Measurement of redox state in isolated rabbit and mouse lungs.....	44
2.2.3.2.1	Setup for measurement in isolated lungs	44
2.2.3.2.2	Experimental procedure.....	47
2.2.3.3	Measurement in cell suspensions.....	48
2.2.3.3.1	Experimental setup	48
2.2.3.3.2	Experimental procedure.....	50
2.2.4	High-resolution respirometry and O ₂ kinetics.....	50
2.2.5	Mitochondrial membrane potential and mitochondrial matrix superoxide measurement	53
2.2.6	Statistics	53
3	Results	54
3.1	Remission spectrophotometry in isolated lungs and cell suspensions.....	54
3.1.1	Evaluation of tissue cytochrome spectra	54
3.1.2	Evaluation of scattering, reflection and water content in tissue	55
3.1.3	Evaluation of cellular cytochrome spectra	56
3.1.4	Evaluation of scattering interference in cell suspensions	59
3.1.5	Semiquantitative analysis of cytochrome redox state based on difference spectra.....	61
3.2	Mitochondria as oxygen sensors	62
3.2.1	Mitochondrial complex IV in oxygen sensing of HPV	62
3.2.1.1	Hypoxia-induced inhibition of the mitochondrial electron transport system and HPV in the isolated lung	62
3.2.1.2	Hypoxia-induced inhibition of the mitochondrial electron transport system and HPV in isolated PASMCM	64
3.2.1.2.1	Redox changes in isolated PASMCM.....	64
3.2.1.2.2	Respiration in isolated PASMCM.....	66
3.2.2	Mitochondrial complex III in oxygen sensing of HPV	67
3.2.3	Comparison of PASMCM to arterial smooth muscle cells of the systemic vasculature	69
3.2.4	Correlation of HPV to respiration and redox state during application of mitochondrial inhibitors.....	72

3.2.4.1	Correlation of HPV with redox state of mitochondrial cytochromes	72
3.2.4.1.1	Application of cyanide	72
3.2.4.1.2	Application of 2-n-heptyl-4-hydroxyquinoline-N-oxide (HQNO)	73
3.2.4.1.3	Application of rotenone	74
3.2.4.1.4	Application of FCCP	75
3.2.4.2	Correlation of HPV with mitochondrial respiration during application of cyanide, HQNO, rotenone and FCCP	76
3.3	Identification of non-mitochondrial cytochromes.....	78
3.3.1	Cytochrome <i>b₅₅₈</i> of the NADPH oxidase.....	78
3.3.2	Cytochrome P450	80
3.3.3	Soluble guanylate cyclase	80
3.3.4	Myoglobin	81
3.3.5	Hemoglobin.....	81
4	Discussion.....	84
4.1	Remission spectrophotometry	85
4.2	Mitochondrial complex IV in oxygen sensing of HPV	88
4.3	Mitochondrial complex III in oxygen sensing of HPV.....	90
4.4	Comparison of PASMC to arterial smooth muscle cells of the systemic vasculature	92
4.5	Mitochondrial inhibition and HPV.....	93
4.6	Identification of non-mitochondrial cytochromes.....	94
4.7	Conclusion	96
5	Summary.....	98
6	Zusammenfassung.....	99
7	References.....	101
8	Appendix	115
8.1	Published reference spectra	115
8.2	Measured reference spectra.....	115
9	Curriculum vitae	116
10	Acknowledgements.....	119

II. List of figures and tables

Figure 1.1	Ventilation-perfusion matching.....	13
Figure 1.2	Effector mechanisms of HPV.....	16
Figure 1.3	Possible role of mitochondria in oxygen sensing of HPV.....	22
Figure 1.4	Mechanisms of mitochondrial ROS production.....	25
Figure 1.5	Heme oxygenase and carbon monoxide in oxygen sensing.....	30
Figure 1.6	Aim of the study.....	35
Figure 2.1	Spectrum of reduced mitochondria.....	43
Figure 2.2	Spectrum of oxidized mitochondria.....	43
Figure 2.3	Difference spectrum of reduced minus oxidized mitochondria.....	43
Figure 2.4	Reduction and oxidation of mitochondrial cytochromes.....	44
Figure 2.5	Schematic setup for measurement of remission difference spectra.....	45
Figure 2.6	CytoSPEC II.....	46
Figure 2.7	LEA flat and endoscopic probe.....	46
Figure 2.8	Setup for measurement in isolated lungs.....	47
Figure 2.9	Experimental procedure for redox measurement in isolated lungs.....	48
Figure 2.10	Schematic setup for measurement in cell suspension.....	49
Figure 2.11	Light fibre probe for Oxygraph-2k (O2k) chamber.....	49
Figure 2.12	Setup of redox measurement in cell suspension.....	50
Figure 2.13	Oxygraph-2k (O2k) from Oroboros for high-resolution respirometry.....	51
Figure 2.14	Mitochondrial and non-mitochondrial respiration.....	52
Figure 2.15	Determination of O ₂ affinity (p50).....	52
Figure 3.1	Cytochrome spectra in the isolated lung.....	54
Figure 3.2	Spectrum of white light backscattered by milk.....	55
Figure 3.3	Influence of tissue water content on difference spectrum.....	56
Figure 3.4	Reference spectra and anoxic difference spectrum.....	57
Figure 3.5	Mitochondrial reduction by anoxia and cyanide.....	58
Figure 3.6	Spectral changes induced by addition of digitonin and medium.....	59
Figure 3.7	Cytochrome c concentration in comparison to light attenuation.....	60
Figure 3.8	Analysis of redox state at different wavelength ranges.....	60
Figure 3.9	Fitting of mitochondrial spectra.....	61
Figure 3.10	O ₂ dependency of HPV.....	62
Figure 3.11	Hypoxia-dependent alterations of remission spectra.....	63
Figure 3.12	O ₂ -dependent alterations of remission difference spectra in PASMC.....	64
Figure 3.13	O ₂ dependency of cytochrome redox alterations in PASMC.....	65
Figure 3.14	O ₂ dependency of respiration in PASMC.....	66
Figure 3.15	Differential regulation of mitochondrial cytochromes in PASMC.....	67
Figure 3.16	Hypoxia-dependent alterations of mitochondrial superoxide concentration in PASMC.....	68
Figure 3.17	Hypoxia-dependent changes of mitochondrial membrane potential in PASMC.....	68
Figure 3.18	Comparison of redox alterations of cytochrome <i>aa3</i> , <i>b_{1/11}</i> , <i>c</i> in PASMC, ASMC and RASMC.....	69
Figure 3.19	O ₂ affinity of PASMC, ASMC, and RASMC.....	70
Figure 3.20	Hypoxic mitochondrial superoxide concentration in PASMC, ASMC and RASMC.....	70
Figure 3.21	Hypoxic mitochondrial membrane potential in PASMC, ASMC and RASMC.....	71
Figure 3.22	HPV and redox state at different cyanide concentrations in the isolated lung.....	72
Figure 3.23	HPV and redox state at different cyanide concentrations in PASMC.....	73
Figure 3.24	HPV and redox state at different HQNO concentrations in the isolated lung.....	73
Figure 3.25	HPV and redox state at different HQNO concentrations in PASMC.....	74
Figure 3.26	HPV and redox state at different rotenone concentrations in the isolated lung.....	74
Figure 3.27	HPV and redox state at different rotenone concentrations in PASMC.....	75
Figure 3.28	HPV and redox state at different FCCP concentrations in PASMC.....	76
Figure 3.29	HPV and mitochondrial respiration in isolated PASMC in presence of mitochondrial inhibitors.....	78
Figure 3.30	Spectrum of cytochrome <i>b₅₅₈</i> of NADPH oxidase.....	79
Figure 3.31	Identification of NADPH oxidase in isolated lungs.....	79
Figure 3.32	Carbon monoxide (CO) in isolated lungs and PASMC.....	80
Figure 3.33	Fitting of hemoglobin in isolated lungs.....	82
Figure 3.34	Correlation of HPV and oxygenation state of hemoglobin.....	82

Figure 3.35	Correlation of HPV and amount of hemoglobin	83
Figure 4.1	Proposed mitochondrial pathway of oxygen sensing in HPV	97
Figure 8.1	Published reference difference spectra	115
Figure 8.2	Measured reference difference spectra	115
Table 1	Effect of cyanide and azide (inhibitors of complex IV) on HPV.....	23
Table 2	Mitochondrial inhibitors and HPV.....	27
Table 3	Cytochromes in mammalian tissue.....	33

III. List of abbreviations

[Ca ²⁺] _i	intracellular calcium concentration
3-NPA	3-nitropropionic acid
AA	Arachidonic acid
ADP	adenosine diphosphate
AMP	adenosine monophosphate
ANT	adenine nucleotide translocase
ARDS	acute respiratory distress syndrome
ASMC	aortic smooth muscle cell
ATP	adenosine triphosphate
AU	arbitrary units
BKCa	calcium- and voltage-activated potassium channel
BSA	bovine serum albumin
Ca ²⁺	calcium
CaCl ₂	calcium chloride
cADP	cyclic adenosine diphosphate
CCE	capacitative calcium entry
cGMP	cyclic guanosine monophosphate
cmH ₂ O	centimeter of hydrostatic head
CO	carbon monoxide
CoA	coenzyme A
COPD	chronic obstructive pulmonary disease
Cu/Zn-SOD	copper/zinc superoxide dismutase
cyt	cytochrome
DAG	diacylglycerol
DAPI	4',6-diamidino-2-phenylindole
DCFH	dichlorofluorescein
DMSO	dimethylsulfoxide
DPBS	Dulbecco's phosphate buffered saline
DPI	diphenyliodonium
EDTA	ethylenediaminetetraacetic acid
EET	epoxyeicosatrienoic acids
ESR	electron spin resonance
ETS	electron transport system
FADH	reduced flavin adenine dinucleotide
FCCP	p-trifluoromethoxy carbonyl cyanide phenyl hydrazone
FCS	fetal calf serum
FITC	fluorescein isothiocyanate
FRET	fluorescence resonance electron transfer
g	gram
G	gauge
GSH	reduced glutathione
GSSG	oxidized glutathione
H ₂ O ₂	hydrogen peroxide
H ₂ S	hydrogen sulfide
Hb	hemoglobin
HEPES	2-(4-(2-hydroxyethyl)-piperazinyl)-1-ethansulfonate
HETE	hydroxyeicosatetraenoic acid
HIF	hypoxia-inducible factor
HO-2	heme oxygenase 2
HPV	hypoxic pulmonary vasoconstriction
HQNO	2-n-heptyl-4-hydroxyquinoline-N-oxide
IMAC	inner membrane anion channel

IP ₃	inositol trisphosphate
J _(O₂)	O ₂ consumption (at a specific pO ₂)
k/o	knock out
KCl	potassium chloride
kg	kilogram
KH ₂ PO ₄	potassium dihydrogen phosphate
K _v	voltage dependent potassium
l	liter
LV	left ventricle
M	molar
Mb	myoglobin
MgCl ₂	magnesium chloride
min	minute
ml	milliliter
mM	millimolar
mmHg	millimeter of mercury
Mn-SOD	magnesium superoxide dismutase
n	number of experiments
N ₂	nitrogen
Na ₂ HPO ₄	sodium hydrogen phosphate
NaCl	sodium chloride
NADH	reduced nicotinamide adenine dinucleotide
NAD ⁺	oxidized nicotinamide adenine dinucleotide
NADPH	reduced nicotinamide adenine dinucleotide phosphate
NADP ⁺	oxidized nicotinamide adenine dinucleotide phosphate
nM	nanomolar
NO	nitric oxide
NSCC	non specific cation channel
O ₂	oxygen
O ₂ ⁻	superoxide radical
P/S	penicillin/streptomycin
p50	oxygen concentration at half maximal respiration
PA	pulmonary artery
PAP	pulmonary arterial pressure
PASMC	pulmonary arterial smooth muscle cell
PBS	phosphate buffer saline
pCO ₂	partial pressure of carbon dioxide
PK	protein kinase
PMA	phorbol myristate acetate
pmol	picomol
pO ₂	partial pressure of oxygen
Q	ubiquinone
QH ₂	ubiquinol
Q _i	quinone reductase site of complex III
Q _o	quinol oxidase site of complex III
RASMC	renal arterial smooth muscle cells
ROC	receptor-operated channel
ROS	reactive oxygen species
rpm	rotations per minute
RyR	ryanodine sensitive receptor
sEH	soluble epoxide hydrolase
SEM	standard error of mean
sGC	soluble guanylate cyclase
s	second
SOC	store-operated channel

SOD	superoxide dismutase
TRP	transient receptor potential
U	Units
VDAC	voltage dependent anion channel
VOCC	voltage operated calcium channel
vWF	von Willebrand factor
x g	times gravity
$\Delta\psi$	plasma membrane potential
$\Delta\psi_{\text{mito}}$	mitochondrial membrane potential
μM	micromolar

1 Introduction

1.1 Hypoxic pulmonary vasoconstriction (HPV)

1.1.1 Physiological relevance

Hypoxic pulmonary vasoconstriction (HPV), also known as the von-Euler-Liljestrand-mechanism, is an essential physiological response of the lung in order to match blood perfusion to alveolar ventilation. It optimizes pulmonary gas exchange under conditions of local alveolar hypoxia. Impairment of this mechanism during pathological situations in pulmonary and systemic diseases (e.g. adult respiratory distress syndrome [ARDS] [1], hepatopulmonary syndrome [2]) or during anesthesia [3], may result in insufficient arterial blood oxygenation. Under conditions of chronic hypoxia, as it occurs at high altitude or during respiratory diseases (e.g. chronic obstructive pulmonary disease [COPD], lung fibrosis) generalized vasoconstriction of the pulmonary vasculature in combination with hypoxia-induced vascular remodeling may lead to pulmonary hypertension with subsequent right heart hypertrophy.

HPV is a highly conserved mechanism, present in most mammals [4-7], partially in reptiles [8] and probably even in fish [9]. Although an increase in pulmonary arterial pressure (PAP) in response to alveolar hypoxia was recognized over 100 years ago [10, 11], it was von Euler and Liljestrand in 1946 who suggested [12], that ventilation-perfusion matching was the purpose of this response. Subsequently HPV was demonstrated to be present in humans, determined by a 50% increase in pulmonary arterial resistance to an alveolar pO_2 below 50 mmHg ($\sim 7\% O_2$) [13].

Despite the recognition of this mechanism decades ago, the underlying O_2 sensing and signal transduction processes have not been fully resolved. Neither the O_2 sensing process nor the exact pathway underlying HPV has been fully deciphered yet. As O_2 sensors mitochondria, nicotinamide adenine dinucleotide (phosphate) oxidases (NAD[P]H oxidases) and cytochrome P450 have been proposed. They are thought to communicate with the effectors, which are different ion channels of the plasma membrane via redox state, reactive oxygen species (ROS) or other mediators.

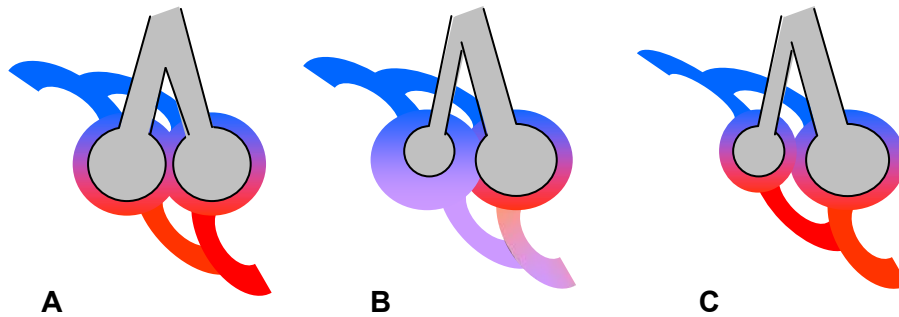


Figure 1.1 Ventilation-perfusion matching

Under physiological conditions, alveoli are equally ventilated and perfused, so that the blood is optimally oxygenated (A). During alveolar hypoxia less well oxygenated blood decreases total oxygenation of systemic arterial blood (B). HPV provides for lower perfusion of badly ventilated areas, thereby decreasing the amount of less well oxygenated blood in the systemic arterial blood (C).

1.1.2 Characteristics of HPV - effector and sensor cell type

HPV occurs within seconds and has been found *in vivo* and in explanted lungs of different species to start at mild hypoxia, in rabbit lungs at alveolar O_2 concentrations $\leq 10\%$ ($pO_2 \leq 75$ mmHg) [5, 14]. It shows a sigmoidal stimulus-response relationship to different degrees of alveolar hypoxia with an onset at 7-10% O_2 ($\sim pO_2$ 50-75 mmHg) and half-maximal response at 3-7% O_2 ($\sim pO_2$ 25-50 mmHg) [5, 7].

Although there are divergent results regarding the influence of precapillary pO_2 on HPV, it is commonly accepted that HPV is mainly determined by alveolar pO_2 . In studies in rabbits neither retrograde nor anterograde perfusion of vessels with hypoxic buffer (3% O_2 , pO_2 23 mmHg) with or without blood did influence vessel tone, whereas inhaled gas changes from 21-0% O_2 (pO_2 158 to 0 mmHg) resulted in a sigmoidal dose-response of HPV [5].

The precapillary smooth muscle cell layer of the resistance vessels with a size of 80-600 μm depending on the species, which is located at the entrance of the acinus in close contact with alveoli has been identified as the effector and sensor cell-type for HPV [15-18]. Less importance was assigned to the conduit arteries, smaller, partially muscularized [15] and postcapillary vessels [16-20].

In line with these studies, hypoxic exposure causes isolated pulmonary arterial smooth muscle cells (PASMC) 1) to contract, 2) to increase their intracellular calcium concentration, and 3) to decrease their plasma membrane potential difference. In contrast, smooth muscle cells derived from isolated cerebral arteries and renal artery rings expand upon exposure to hypoxia [21-23] and mesenteric arteries do not decrease their plasma membrane potential difference in response to hypoxia [24].

Hypoxia-induced responses in PASMC occur at O_2 levels below O_2 concentrations of 3-7% O_2 ($\sim pO_2$ 20-50 mmHg) [21, 25, 26]. The discrepancy to the hypoxic level initiating HPV in isolated organs of 7-10 O_2 ($\sim pO_2$ 50-75 mmHg) may be due to diffusion limitation of O_2 from the alveoli to PASMC in precapillary vessel of the isolated organ or priming factors in the isolated organ.

Factors modulating HPV include gender, local and circulating vasoactive substances, pH, pCO_2 [27, 28] and red blood cells, but there was an early consensus that the mechanism itself was independent from neural [29] or humoral [30, 31] triggers.

In contrast to the response in acute hypoxia, for sustained hypoxia, that lasts several minutes to hours, a contribution of endothelial cells must also be taken into account [32, 33]. Sustained HPV may be a transitory state leading to chronic hypoxic alterations, like vascular remodeling and chronic pulmonary hypertension.

1.1.3 Mechanism of HPV - effectors, mediators, sensors

The effector pathway is suggested to include L-type calcium channels, non-specific cation channels (NSCC) and voltage-dependent potassium (K_v) channels, whereas mitochondria and NADPH oxidases are discussed as O_2 sensors. ROS, redox couples, and adenosine-monophosphate-kinase (AMP kinase) are under investigation as mediators of HPV.

1.1.3.1 Effector pathway

The pathways leading to contraction of the PASMC converge in an intracellular calcium increase and include the influx of extracellular calcium and probably release of intracellularly stored calcium [34].

There is evidence that calcium influx from the extracellular space is achieved by both, L-type calcium channels [35, 36] and NSCC. Consistent with this suggestion, inhibition of L-type calcium channels only partially abolished HPV [37, 38], whereas inhibition of NSCC completely inhibited HPV [39-41]. Hypoxic regulation of the L-type calcium channels may be achieved by direct modulation via ROS or membrane depolarisation via potassium channels (as stated very early [42-44]) and NSCCs.

Different types of potassium channels have been demonstrated to be involved in hypoxia-associated membrane depolarization, particularly the K_v channels, $K_v2.1$, $K_v1.5$, $K_v9.3$ [45-47], which have been suggested to initiate HPV. The concept of K_v channels being directly regulated by redox-changes has been proposed early [43]. The K_v channels may be

regulated by 1) reducing agents [48-51] like reduced glutathione (GSH) [52] 2) an associated hemeprotein [24], 3) membrane depolarization, 4) phosphorylation by kinases [53], 5) mitochondrial adenosine triphosphate (ATP) [54] or 6) calcium increase triggered by intracellular calcium release from intracellular stores or via NSCCs [53]. This is consistent with the observation, that the intracellular calcium increase induced by hypoxia has been proposed to play an obligatory role in hypoxic inhibition of potassium currents [55, 56]. Furthermore, only partial inhibition of HPV in potassium channel knock-out animals suggests that this may not be the sole mechanism of HPV [57].

Thus NSCCs may be key channels for hypoxic signaling as e.g. in the regulation of potassium channels, of L-type calcium channels or the calcium level [41]. They consist of a group of store-operated (SOCs) and receptor-operated calcium channels (ROCs), and their molecular identity has been revealed as transient receptor potential (TRP) channels. The ROCs can be activated by protein kinases and diacylglycerol (DAG). Recently it was demonstrated that this mechanism is essential for acute HPV, occurring within seconds to minutes, as TRPC6 knock-out mice have no HPV or hypoxia-induced intracellular calcium increase or membrane depolarisation [58].

The SOCs play a role in capacitative calcium entry (CCE), a calcium influx from the extracellular space that can be induced by emptying intracellular stores, and has been shown to be activated in HPV [41, 59]. While CCE is a phenomenon observed in several types of systemic arteries, its coupling to contraction appears to be of particular importance in pulmonary arteries [60], but its exact impact on HPV has not yet been resolved, especially due to the lack of specific experimental manipulation methods [41].

An initial release of calcium from intracellular stores was also suggested as a key trigger for HPV as an hypoxia-induced increase in intracellular calcium even after removal of extracellular calcium has been shown. The initial intracellular calcium increase was proposed to originate from a calcium release from ryanodine-sensitive (RyR) calcium stores [61] with calcium buffering of inositolphosphate 3 (IP_3) sensitive stores [26, 62, 63]. Recently it was shown, that hypoxia-induced calcium release and contraction was reduced in PASMC of type-3 ryanodine receptors knock-out mice [64]. Debate continues regarding how they might be regulated and if the observed increase of intracellularly released calcium may be restricted to PASMC of non-resistance pulmonary arteries with a large diameter [58]. Ryanodine-sensitive receptor channels in other cell types are modulated by calcium [64], redox-regulating systems [65], ROS [66, 67] and cyclic adenosine diphosphate (cADP)-ribose [68], whereas IP_3 receptor channels are regulated via cyclic guanosine monophosphate (cGMP) and reduced nicotinamide adenine dinucleotide (NADH) [69].

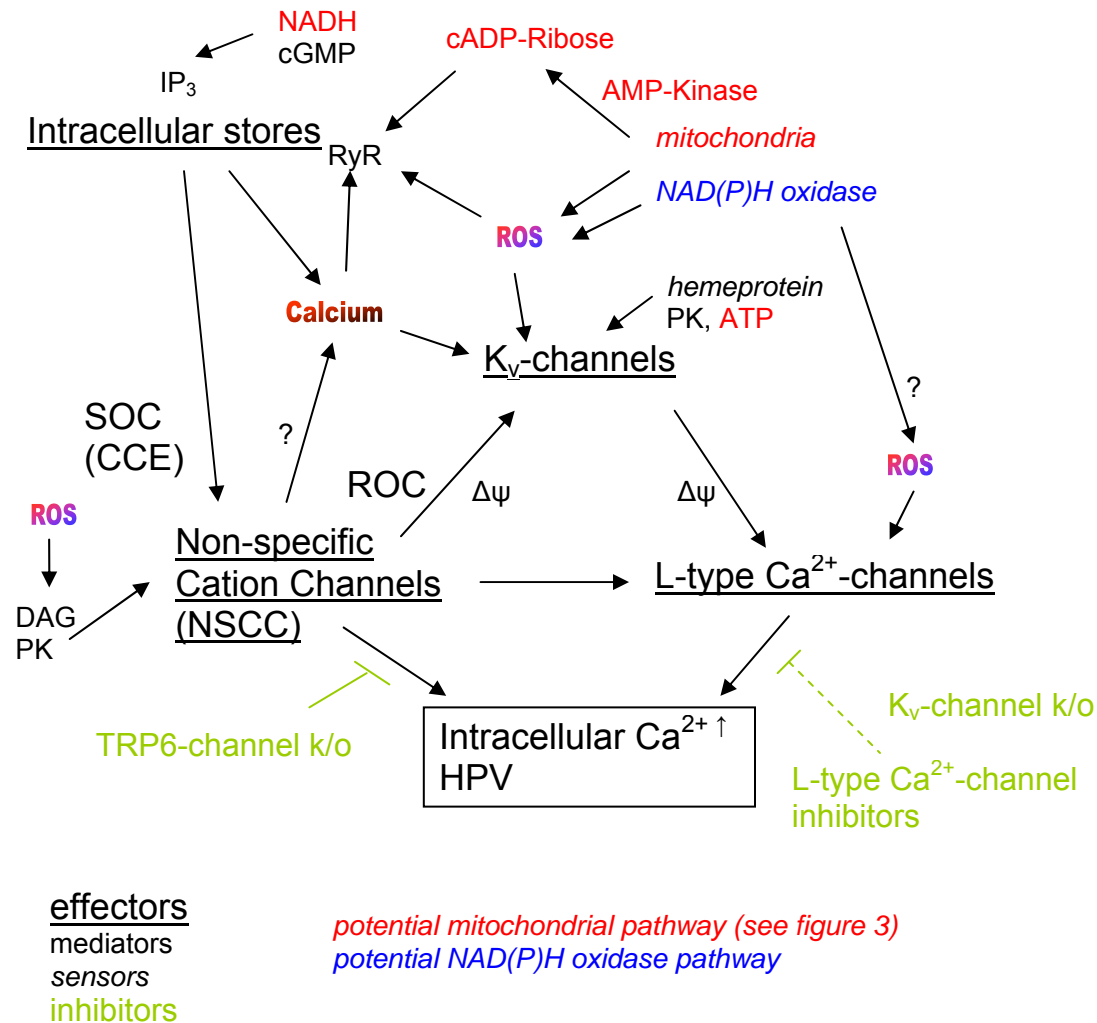


Figure 1.2 Effector mechanisms of HPV

Intracellular calcium increase might be triggered by non-specific cation channels, L-type Ca^{2+} -channels and K_v -channels. However, only genetical deletion of the TRP6 subtype of NSCC, results in a complete inhibition of HPV (full line), in contrast to K_v -channel deletion or L-type Ca^{2+} -channel inhibition (dashed line).

AMP: adenosine monophosphate, ATP: adenosine triphosphate, Ca^{2+} : calcium, cADP: cyclic adenosine diphosphate, CCE: capacitative calcium entry, cGMP: cyclic guanosine monophosphate, DAG: diacylglycerol, HPV: hypoxic pulmonary vasoconstriction, IP_3 : inositol triphosphate, K_v : voltage dependent potassium, k/o. knock-out, NADH: reduced nicotinamide adenine dinucleotide, NADPH: reduced nicotinamide adenine dinucleotide phosphate, PK: protein kinase, ROC: receptor-operated channel, ROS: reactive oxygen species, RyR: ryanodine receptor, SOC: store-operated channel, TRP: transient receptor potential, $\Delta\psi$: plasma membrane potential.

1.1.3.2 Mediators: Reactive oxygen species (ROS) and redox state

As concluded from the above, one main modulator of the effector pathway could be the cellular redox state and/or ROS. The overall redox state of the cell is determined by the concentration of ROS and the availability of reducing equivalents, such as reduced/oxidized nicotinamide adenine dinucleotide (phosphate) (NAD[P]H/NAD[P]^+), reduced/oxidized glutathione (GSH/GSSG), and is compared to extracellularly rather reduced.

ROS, possibly involved in O₂ sensing, include superoxide (O₂⁻), hydrogen peroxide (H₂O₂), and reactive nitrogen species. Besides being highly toxic for the cell in high concentrations and being regarded rather as by-products in O₂ metabolism, in low concentrations of the pico- or low nanomolar ranges they now have been postulated to play a role as diffusible mediators in intracellular signal transduction.

ROS interfere with cellular functions by modifying mainly heme or thiol redox-regulated systems, including guanylate cyclase, cytochromes of the mitochondrial electron transport system, cyclooxygenases, protein kinases like protein kinase C (PKC) and calcium/potassium channels [70, 71]. Important ROS producing systems are NAD(P)H-oxidases, mitochondria, nitric oxide (NO) synthases and cytochrome P450. Intracellular balance of the ROS concentration is achieved by detoxification through catalase, superoxide dismutases (SODs) and redox systems of the cell, like glutathione and NAD(P)H.

ROS concentration is therefore a result of the homeostasis between activation of ROS producing systems, O₂ tension and ROS degrading processes.

Although there is wide consensus regarding the importance of ROS in O₂ sensing, two opposing hypothesis are offered for ROS regulation during HPV: Whereas one concept favors K_v channel modification by a reduced level of ROS as trigger for contraction, another concept proposes an increase in ROS during hypoxia originating from mitochondria or NAD(P)H oxidases (for review see: [72-76]).

1.1.3.2.1 Application of oxidants and antioxidants

Application of oxidants and antioxidants was used to elucidate the reactivity of the pulmonary vascular system with regard to HPV.

Based on studies with the relatively unspecific oxidizing agent diamide causing vasodilation and inhibiting HPV in the isolated lungs [77, 78], a decrease of ROS in HPV was early suggested [79]. In line with this finding, antioxidants contract normoxic pulmonary artery vessel and inhibit potassium channels [48]. These results were challenged in isolated lungs by studies with antioxidants and inhibitors of SOD that specifically inhibit HPV, but do not induce vasoconstriction during normoxia, suggesting an increase of H₂O₂ during hypoxia [80, 81]. In isolated pulmonary arteries increase of ROS by xanthine oxidase reaction during normoxia was shown to cause contraction through activation of PKC [82]. Application of the thiol-reducing agent dithiothreitol during the sustained phase of HPV reversed hypoxic vasoconstriction, whereas the superoxide scavenger nitroblue tetrazolium prevented further pulmonary vasoconstriction during the sustained phase of HPV, but did not reverse it [66].

Studies with exogenous H₂O₂, suggesting an increase of ROS during HPV, for example in isolated pulmonary arteries [83], have to be judged critically with regard to rather multiple

effects of H_2O_2 in the cell and use of supra-physiologic dosages. In general the discrepancies of the studies may result from the possibility that the applied agents reach only parts of the vasoreactive pathways without necessarily affecting the physiologic pathway activated during hypoxia.

Another study demonstrated that overexpression of glutathione peroxidase, cytosolic or mitochondrial catalase attenuated the hypoxia-induced increase in ROS signaling and intracellular calcium, whereas mitochondrial matrix-targeted Mn-SOD (which decreases superoxide, but increases H_2O_2) augmented intracellular calcium [84]. This suggests that superoxide production, leading to H_2O_2 being released from mitochondria, contributes to the hypoxia-induced increase in intracellular calcium.

In summary, detailed pharmacological interventions provided evidence for both an upregulation as well as for a downregulation of superoxide, and subsequently H_2O_2 , as the underlying pathway of HPV.

1.1.3.2.2 Measurement of ROS

The lack of valid techniques for ROS measurement may be one reason for the opposing results in investigations of their role in HPV [85]. Technical limitations of different fluorescent probes with regard to their specificity and autooxidation [86] have been the major drawbacks in the past. Also, artefacts due to a non-physiological environment of isolated arteries and PASMC have to be considered. For example, pretone may influence ROS production by activation of stretch-sensitive NAD(P)H oxidases [87] and some investigators believe that healthy mitochondria do not release ROS under baseline conditions at all [88]. Furthermore, most of the measurements do not take into account the possibility that the alterations of ROS occur localized in the cell and are dependent on O_2 concentration and time course of the experiment [70]. This could even lead to opposite reactions of different ROS producing systems, the experimental setup pronouncing the one or the other [73].

Arguments for a decrease in ROS production are provided by studies in the isolated lung indicating a decrease of superoxide in hypoxia, but are limited in their validity by the use of luminol and lucigenin enhanced chemiluminescence [89], that is influenced by media conditions [90], edema of the lung [91] and induction of superoxide [92]. To overcome the limitations that are related to the use of one specific dye and localization of ROS production in the lung, measurements were performed in denuded pulmonary arterial rings with three different optical methods (Amplex Red, dichlorofluorescein (DCFH) and lucigenin) and confirmed the decrease of ROS during hypoxia [23].

In contrast, measurements in isolated pulmonary arteries with chemiluminescence and electron spin resonance transfer (ESR), a technique to overcome limitation of dye related detection methods, showed an increase of hydroxyl and alkyl radicals during hypoxia [93]. The same discrepancy occurs in measurements of PASMC [94-96]. Measurements with a new fluorescence resonance energy transfer (FRET) method and ESR support the theory of a localized, hypoxia-dependent ROS increase during HPV [84, 97-99]. An overview is provided by Sommer et al. [85].

Therefore, the apparently conflicting conclusions concerning ROS in HPV may be explained by the hypothesis that a local, subcellular and compartmentalized regulation of ROS triggers HPV, e.g. by localization of mitochondria close to K_v -channels [100].

1.1.3.3 Other mediators: ATP, AMP kinase, protein kinases, carbon monoxide (CO), hydrogen sulfide (H₂S)

It was early suggested that ATP acts a second messenger for HPV, as 1) inhibitors of the mitochondrial chain and of glycolysis caused pulmonary vasoconstriction and 2) oxidative phosphorylation is the main O₂ consumption process [24, 101]. However, the role of ATP was again rejected, as changes in ATP content or deterioration of energy state during hypoxia could not be detected [102, 103], O₂ affinity (p50) of cytochrome c oxidase seemed to be too high to enable ATP to be influenced by mild hypoxia [104] and inhibitors of the mitochondrial cytochrome c oxidase did induce pulmonary vasoconstriction, but did not abolish HPV [105], an effect, that was not consistently found by different investigations (see Table 1).

Still there has also been evidence, that oxidative ATP production might be impaired and energy state is maintained by upregulation of glycolysis [106], especially in sustained HPV [102, 107]. A decrease in energy state was considered to be responsible for hypoxic relaxation, after an initial rise in vascular tone during hypoxia. In contrast to femoral arteries, pulmonary arteries recovered after that and constricted again. This was postulated to be due to accelerated glycolytic ATP production in pulmonary arteries [102].

Small and/or localized changes in ATP production might act - beyond deterioration of energy state - as second messenger via activation of AMP activated protein kinase α 1 (AMPK) by an increase of the AMP/ATP ratio. AMPK can elevate cADP-ribose that releases calcium through ryanodine-sensitive calcium stores. This effect is enhanced by additional increase of β -NADH/NAD⁺ relationship, that leads to inhibition of cADP-ribose-hydrolase and also

increases intracellular cADP-ribose [68, 108]. As ATP would be necessary for change of AMP/ATP relationship, but also for phosphorylation of AMPK during activation, low decrease of ATP was supposed to activate the AMPK-cADP-ribose pathway, whereas a high decrease would block the pathway again. This effect could possibly explain dose dependent results of studies with cyanide on HPV. However, inhibition of AMP kinase has been shown to preferentially inhibit sustained HPV [109]. Furthermore the importance of decrease ATP was challenged by the finding that oxidative stress and not an increase in the AMP/ATP ratio is required for hypoxic activation of AMPK [110].

Besides AMP kinase, several other protein kinases have been suggested as modulators of HPV [111]. Especially PKC via activation of NADPH oxidase [112] might be involved. PKC activation might be induced by mitochondrial ROS production [113]. The recently suggested second messenger diacylglycerol (DAG) that regulates TRP6 channel activity [58] might be increased by ROS activated phospholipase C or mitochondrial DAG production [114]. Also inhibition of mitochondrial beta-oxidation might increase DAG concentrations due to increased acetyl-CoA concentration which is converted to DAG via glycerol-3-phosphate.

As CO has been shown to inhibit HPV, a role for cytochrome P450 dependent hydroxyeicosatetraenoic acid (HETE) production and a pathway depending on heme oxygenase and large-conductance calcium- and voltage-activated potassium channels (BKCa) had been proposed. This will be discussed below.

Recently, decreased mitochondrial H₂S oxidation during hypoxia has been speculated to be the O₂ sensing mechanism of HPV [115].

.

1.1.3.4 Oxygen sensors in HPV - location and dynamic range

For the triggering mechanism of HPV, two main requirements are necessary: 1) the sensor has to respond to changes in O₂ with a sensitivity in the range of mild hypoxia and 2) the sensor has to be able to utilize the above mentioned mediators for signaling to the effector pathways. This emphasizes the problem of defining hypoxia. HPV in the isolated lung exhibits a sigmoidal stimulus-response relationship with an onset at 7-10% O₂ (~ pO₂ 50-75 mmHg) and half-maximal response at 3-7% O₂ (~ pO₂ 25-50 mmHg) [5, 7]. Isolated cells were shown to contract in response to O₂ concentrations of 3-7% O₂ (~ pO₂ 20-50 mmHg) [21, 22], whereas studies with measurement of intracellular calcium were usually performed at pO₂ levels below 4% O₂ (pO₂ 30 mmHg) [40, 105, 116]. Therefore, it is clear that a sensor must exhibit sensitivity to at least 7% O₂ (~ pO₂ 50 mmHg) and below. Although HPV might depend on priming factors, the primary O₂ sensor is obviously located in the PASMC themselves as 1) isolated PASMC contract in response to hypoxia and 2) increase their intracellular calcium.

1.1.3.4.1 Mitochondria as oxygen sensor: ATP production – ROS metabolism – calcium buffering

Mitochondria, as the primary O₂-consuming organelle of the cell, have long been thought to play a key role in the O₂ sensing process of HPV, for two main experimental reasons: First, inhibitors of the mitochondrial chain block specifically HPV in isolated lungs and pulmonary arteries, secondly PASMC depleted of mitochondria do not show hypoxia specific reactions [105]. In general, mitochondria have diverse functions in the cell. They produce energy, control calcium homeostasis of the cell and act as a source and scavenger of ROS. Energy is produced by reducing NADH and flavin adenine dinucleotide (FADH) and building up a proton gradient across the inner mitochondrial membrane, which is used for ATP synthesis by shuttling back protons through the mitochondrial ATP-Synthase (complex V). The energy for the proton gradient is provided by electrons being passed along a system of redox enzymes with increasing redox potential (=increasing electron affinity), the electron transport system, finally reducing O₂ to water (see Figure 1.3 and 1.4). Members of the electron transport system are complex I and II providing electrons, complex III passing on electrons via cytochrome c, and complex IV including the final reduction centre of O₂. The electrochemical gradient is also used to drive other membrane-embedded ion or protein exchangers, like the calcium uniporter. Electron transfer onto O₂ not occurring in complex IV can result in incomplete reduction of O₂ and production of ROS. Cellular calcium concentration can be influenced directly by buffering of cytosolic calcium or indirectly via regulation of capacitative calcium entry. In summary, mitochondria could trigger or modulate HPV via hypoxic inhibition of complex IV, disturbed ROS metabolism or change in calcium handling (see Figure 1.3).

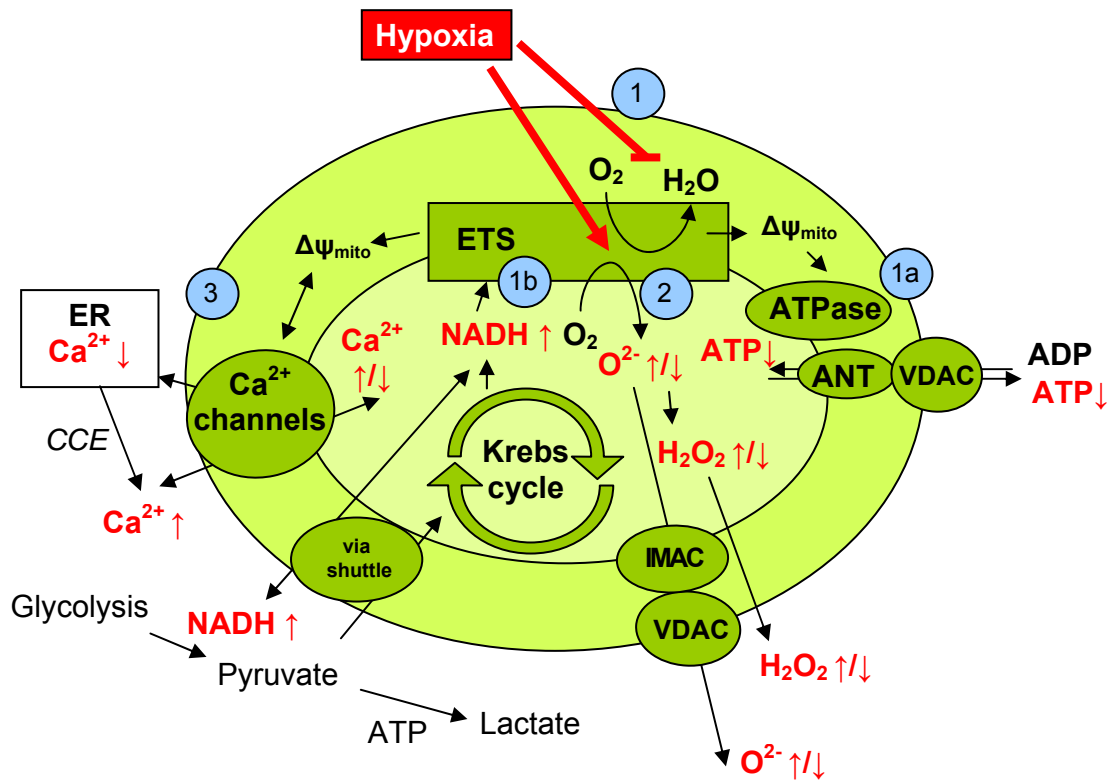


Figure 1.3 Possible role of mitochondria in oxygen sensing of HPV

Hypoxia can interfere with mitochondrial metabolism by 1a) inhibition of oxidative phosphorylation, 1b) change in mitochondrial redox state, 2) superoxide production or 3) calcium homeostasis.

ANT: adenine nucleotide translocase, ADP: adenosine diphosphate, ATP: adenosine triphosphate, Ca²⁺: calcium, Ca²⁺-channels: mitochondrial calcium channels (mitochondrial calcium uniporter, mitochondrial ryanodine receptor, permeability transition pore, sodium- and proton exchanger), CCE: capacitative calcium entry, ER: endoplasmic reticulum, ETS: Electron transport system, IMAC: inner membrane ion channel, NADH: reduced nicotinamide adenine dinucleotide, O₂⁻: superoxide, VDAC: voltage dependent anion channel, Δψ_{mito}: mitochondrial membrane potential.

1.1.3.4.1.1 Inhibition of complex IV

Inhibition of complex IV as a mechanism for HPV was early suggested, as inhibitors of the mitochondrial chain mimicked the effects of hypoxia in the pulmonary vasculature and inhibited HPV [24, 101]. However, the mechanism by which mitochondria elicit HPV was soon discussed to be beyond simple inhibition of complex IV, as 1) complex IV and mitochondria of isolated non-pulmonary cells are largely functional at very low O₂ concentrations (= have high O₂ affinity) [117], but HPV occurs at mild hypoxia and 2) application of inhibitors of complex IV suggested the O₂ sensing mechanism to be upstream of complex IV [84, 118, 119].

As already discussed above, in line with this, no ATP depletion [103, 120] was evident in the whole lung during hypoxia, although this might be due to a shift from oxidative phosphorylation to glycolytic ATP production [106]. However, slight inhibition of complex IV

that regulates ROS production, calcium signaling, NADH concentration or AMP/ATP ratio [108] could act as a signal for HPV beyond ATP depletion.

This might be supported by a lower O₂ affinity of mitochondria in PASMC compared to other cell types or by modulation of affinity by NO or CO, so that mitochondria of PASMC are inhibited at mild hypoxia. Neither O₂ affinity of PASMC nor O₂ affinity in the isolated lung has been investigated before. A hint for a certain degree of inhibition of the mitochondrial respiratory chain during hypoxia is the high NADH/NAD⁺ ratio during acute hypoxia (2% O₂, pO₂ 15-18 mmHg) [107], but not NADPH/NADP⁺ ratio (5-8% O₂, pO₂ 35-60 mmHg) [121] in isolated pulmonary arteries.

Despite this consideration, the failure of the complex IV inhibitor cyanide to inhibit HPV in some investigations (see Table 1) questioned the general importance of hypoxic inhibition of complex IV. However, in most investigations cyanide mimicked hypoxic effects and at least in isolated lung experiments inhibitory effects on HPV seem to be dose-dependent (Table 1).

	ROS	Normoxic effect	HPV/hypoxia induced cellular effects	Model
Cyanide	↑, inhibited by SOD	↑ tone, inhibited by SOD	--	0.15μM-1.5μM, buffer perfused rat lung, PASMC [96]
		↑ tone, inhibited by ebselen and myxothiazol	↑	10 μM, buffer perfused rat lung [95]
		↑ tone	inhibited: 25 μM specifically, 80 μM unspecifically	25-80μM, buffer perfused rabbit lung [122]
		↑ tone	inhibited, unspecifically	1 mM, buffer and blood perfused rat lung [123]
	-- during hypoxia		↑ [Ca ²⁺] _i	1 μM, PASMC [84]
		--	no effect on phase 1, potentiates phase 2	100 μM, PA [107]
		↑ [Ca ²⁺] _i , also in non-PASMC	not investigated	10 mM, PASMC [124]
Azide		↑ tone	inhibited, unspecifically	isolated rat lung [123]
	--		inhibited, unspecifically	vessel wall [125, 136]

Table 1: Effect of cyanide and azide (inhibitors of complex IV) on HPV

[Ca²⁺]_i: intracellular calcium, SOD: superoxide dismutase, PA: pulmonary artery, PASMC: pulmonary arterial smooth muscle cells, specifically: HPV was inhibited, unspecifically: HPV and vasoconstriction induced by a vasoconstrictive substance was inhibited

1.1.3.4.1.2 Mitochondrial ROS production

Due to above mentioned high O₂ affinity of mitochondria, ATP maintenance during hypoxia, conflicting results regarding complex IV blockade and generally accepted importance of ROS

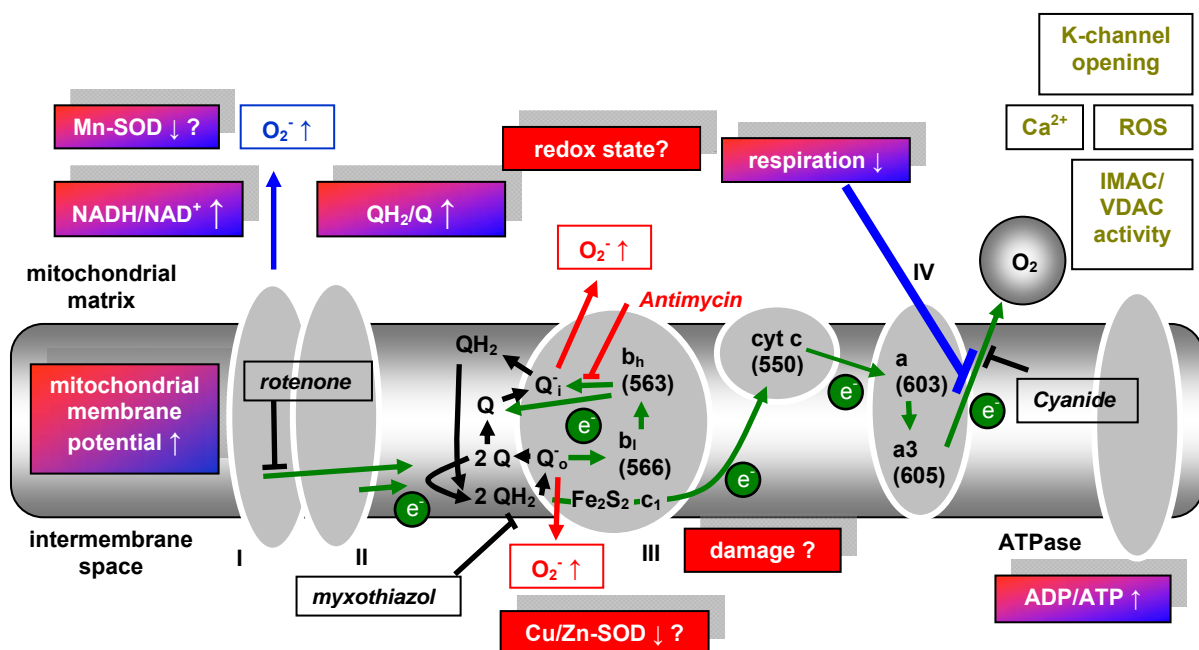
in O₂ sensing, studies focused on an O₂ sensing mechanism via mitochondrial ROS production independent of complex IV.

Mitochondria are known to produce ROS as by-products during electron transfer at complex I, II or III. Single electrons are passed on to O₂, producing a superoxide radical, which is detoxified by mitochondrial SODs located in the mitochondrial matrix and intermembrane space. The resulting H₂O₂ can readily diffuse through membrane into the cell, but also superoxide can diffuse through an inner membrane ion channel (IMAC) and a voltage dependent anion channel (VDAC) located in the matrix and intermembrane space, respectively [126, 127].

However, there is currently much discussion about whether mitochondrial ROS release is increased or decreased during hypoxia to trigger HPV [14]. A decrease in ROS production at complex I or III can be caused by a lack of O₂ as substrate due to decreased pO₂. ROS production at complex I is inhibited by a decreased NADH/NAD⁺ ratio, reduced/oxidized ubiquinone (QH₂/Q) ratio or a decreased mitochondrial membrane potential [128].

Increased ROS production is favored by high membrane potential with concomitantly slowed down distal electron flow and a highly reduced ubiquinone (= high ubiquinol) pool. This is the case in so called "state 4" respiration characterized by inhibition of complex V due to high ADP/ATP ratio [128, 129]. A similar condition which might result in high ROS production is the combination of high electron inflow (high NADH concentration) and inhibition of complex IV as occurring during ischemia or NO mediated inhibition of cytochrome c oxidase [128, 130, 131]. The latter condition supports ROS production by high membrane potential, probably caused by reverse function of complex V due to high glycolytic ATP production [130]. However, the contribution of complex I or III to ROS production under these conditions is under debate, but believed to be relatively low for complex III [128, 132]. Discrepant results may be caused by interference of ROS production with ROS detoxifying systems, allowing mitochondrial matrix ROS produced by complex I or quinone reductase (Q_i) site of complex III to be eliminated very fast in intact mitochondria [133]. Therefore, in intact mitochondria the quinol oxidase (Q_o) site of complex III might be the dominant site of ROS production, because it releases ROS into the intermembrane space, away from the antioxidant defense of the matrix [133]. This process can be provoked by inhibition of complex III downstream of the Q_o site of semiubiquinone by antimycin A hereby increasing life time of semiubiquinone. In contrast, further downstream inhibition of complex IV is believed to lead to ROS production at complex I, but not ROS production of complex III, as reduced cytochrome c₁ cannot dock to the iron-sulfur cluster and thus prevents electron entry into complex III [133]. Therefore inhibition of complex IV seems to require additional mechanism to induce ROS production at complex III. Additional damage of the Q_o site and iron-sulfur protein, e.g. by ischemia, has

been suggested to result in increased electron leak at this site [133], but also unspecific interference of O_2 with the mitochondrial membrane during hypoxia [134]. However, intrinsic hypoxic ROS production of mitochondria was questioned and additional cellular factors, like regulation of SOD activity or redox state of mitochondrial cytochromes by NO were suggested to be a prerequisite for increased ROS production at complex III [128, 135]. Other sites of hypoxic ROS production might include complex II [136], glycerol-1-phosphate dehydrogenase, and dihydroorotate dehydrogenase [129]. Generally ROS can also be increased by mitochondrial calcium influx [137] or activation of mitochondrial potassium channels [138]. However, also release of ROS, e.g. via membrane potential dependent VDACs could act as a mechanism for ROS regulation in hypoxia (see Figure 1.4) [126].



Factors favoring ROS production at Complex I

Factors favoring ROS production at Complex III

Factors favoring ROS production generally

Mitochondrial inhibitors

Figure 1.4 Mechanisms of mitochondrial ROS production

For details see text.

ADP: adenosine diphosphate, ATP: adenosine triphosphate, Ca^{2+} : calcium, Cu/Zn-SOD: copper-zinc superoxide dismutase, e^- : electron, Fe_2S_2 : iron sulfur cluster, IMAC: inner membrane ion channel, K-channel: potassium channel, Mn-SOD: manganese superoxide dismutase, NADH/NAD⁺: reduced/oxidized nicotinamide adenine dinucleotide, O_2^- : superoxide, Q^- : semiubiquinone at the quinol oxidase site, Q_i^- : semiubiquinone at the quinone reductase site, QH_2/Q : reduced/oxidized ubiquinone, ROS: reactive oxygen species, VDAC: voltage dependent anion channel, I/II/III/IV: complex I/II/III/IV, $b_h/b_l/c_1/aa3$: cytochrome $b_h/b_l/c_1/aa3$ with absorption peaks in nm in brackets.

For an involvement of mitochondrial ROS in HPV, the original redox hypothesis was proposed by Weir, Archer and colleagues assuming a decrease in the production of mitochondrial ROS, resulting in the inhibition of K_v channels mediated by redox couples like GSH/GSSH, NADH/NAD⁺ [96, 139]. In contrast, Schumacker, Chandel and co-workers suggested that an increase in ROS production during hypoxia from the semiubiquinone binding site in mitochondrial complex III triggers subsequent intracellular calcium release and thus HPV [74, 95]. Main discrepancies emerge due to different results regarding the effects of mitochondrial inhibitors on normoxic or hypoxic vessel tone and regarding measurement of ROS (see Table 2). In Archer's studies rotenone inhibited HPV or K_v channel activity, decreased ROS and increased the normoxic tone. As antimycin A led to similar reactions, whereas cyanide did not inhibit HPV, Archer concluded that a decrease in ROS at Complex I or III triggers HPV. In contrast, Schumacker did not find a specific attenuation of the hypoxia-induced calcium increase and HPV by antimycin, but an inhibition of HPV and decrease of ROS with myxothiazol. His group therefore concluded that an increase of ROS at complex III induced HPV. The effects of the inhibitors seem to depend on several variables, like respiration substrate, inhibitor concentration or pre-blockade by mitochondrial inhibitors. Generally the results generated with antimycin and myxothiazol have to be judged critically, as both substances seem to inhibit HPV by interaction with the NO system, which is not thought to be involved in O₂ sensing (see Table 2). A more convincing approach recently showed by using cytochrome b depleted cells, that mitochondrial ROS production at complex III is necessary for hypoxic hypoxia-inducible factor (HIF) stabilization [140].

	ROS	Normoxic tone	HPV	Model
Rotenone	↓	↑	inhibited	isolated lung/PASMC, bolus of 1µM/0.1µM [96]
	↓	↑	inhibited	PA/PASMC, 5µM, opposite in renal tissue [23]
		↑	inhibited, unspecifically	isolated lung, 0.5 µM [123]
	↓	↑		vessel wall, 10µM [136]
		↑	inhibited, specifically	isolated rat lungs/PASMC, ~0.1 µM (50ng/ml) [95]
		-- with inhibited NO	inhibited, specificity pronounced under blocked NO	isolated rabbit lung, 30-350 nM [118]
		--	inhibited	PA, 100 nM [107]
3-NPA	prevents hypoxia-induced increase	↑	inhibited	Intraacinar arteries [125, 136]
		--	inhibited	isolated lung [118]
Succinate		--	reverses effect of rotenone	PA [107]
Antimycin A	↓ in normoxia and hypoxia	↑	inhibited, unspecifically	whole lung/PASMC [96], bolus of 5µM/0.1 µM
	↓	↑	inhibited	PA/PASMC, 50µM, opposite in renal tissue [23]
		↑	inhibited, unspecifically	isolated rat lung, 5-10µM [123]
		↑	inhibited unspecifically at 10ng/ml, no change at 1 ng/ml	isolated lung, ~ 20 nM/2 nM (10ng/ml/1 ng/ml) [95]
	↓ in normoxia and hypoxia	↑	pronounced vasodilation	vessel wall, ~ 6 µM (3 µg/ml) [125, 136]
		-- with inhibited NO	inhibited unspecifically under blocked NO	isolated lung, 1-4 nM [118]
HQNO		↑	inhibited specifically	isolated lung [118]
Myxothiazol	↓ during hypoxia		decreased $[Ca^{2+}]_i$ during hypoxia	PASMC, 100 nM [84]
	↓ during hypoxia	--	inhibited	isolated rat lungs/PASMC, 50 ng/ml, ~0.1 µM [95]
		--	inhibited	PA, 100 nM [107]
		-- with inhibited NO	HPV inhibited unspecifically, especially under preblocked NO	isolated lung, 50-80 nM [118]

Table 2: Mitochondrial inhibitors and HPV

rotenone: inhibitor of complex I, 3-NPA (3-nitropropionic acid): inhibitor of complex II, succinate: substrate of complex II, antimycin A/HQNO (2-n-heptyl-4-hydroxyquinoline-N-oxide): inhibitor of Q_i site of complex III, myxothiazol: inhibitor of Q_o site of complex III, PA: pulmonary artery, PASMC: pulmonary arterial smooth muscle cell, $[Ca^{2+}]_i$: intracellular calcium, NO: nitric oxide, specifically: HPV was inhibited, unspecifically: HPV and vasoconstriction induced by a vasoconstrictive substance was inhibited.

1.1.3.4.1.3 Calcium homeostasis

Calcium homeostasis of the cell is balanced by mitochondria, that buffer calcium [141-143] and regulate capacitative calcium entry [144]. They take up calcium via a calcium uniporter, that is driven by mitochondrial membrane potential and the concentration of cytosolic calcium [137]. It was suggested, that inhibition of mitochondrial calcium uptake by p-trifluoromethoxy carbonyl cyanide phenyl hydrazone (FCCP) or hypoxia augmented intracellular calcium increase [144], which fits to the observation that mitochondrial uncouplers increase normoxic tone and enhance HPV in isolated lungs [118].

1.1.3.4.2 NAD(P)H oxidase

In vascular smooth muscle cells, NAD(P)H-dependent ROS production occurs mainly intracellularly [145] and has been proposed to be the main ROS producing system compared to other cellular systems, therefore probably playing a role in HPV [146]. The classical leukocyte NADPH oxidase is composed of the transmembrane subunits gp91 phox (now also termed NOX2) and p22, which include cytochrome *b₅₅₈*, and the cytosolic subunits p47phox, p67phox and p40phox. In contrast to the leukocytic NADPH oxidase certain non-phagocytic NADPH oxidases, that substitute gp91 (NOX2) e.g. by the isoforms NOX1 and NOX4, produce low amounts of superoxide in the intracellular compartment not only after activation, but also constitutively [145, 147].

Leukocytic NADPH oxidase superoxide production was shown to be dependent on pO₂, with a slow decrease of ROS release with decreasing pO₂ and a sharp decline at an O₂ concentration lower than 1% (pO₂ 8 mmHg) [148]. However, its activity also depends on cellular membrane potential and the NADPH concentration [149, 150]. Activation can be induced by phosphorylation, which may involve phospholipase A2 and PKC [112, 151].

Marshall and colleagues first described a NAD(P)H oxidase in PAs, that had an unusually low redox potential and might play a role in HPV. Isolated PASMC demonstrated an increase in superoxide production under hypoxic conditions, which was suggested to be derived from that NAD(P)H oxidase [152]. Several subsequent studies showed inhibition of HPV by inhibitors of the NAD(P)H oxidase, which were partially limited by specificity of the inhibitors, like diphenyliodonium (DPI), which also inhibits mitochondrial enzymes [153-156] or apocynin, which seems to be a ROS scavenger in general. More specificity was proposed for 4-(2-aminoethyl)benzenesulfonyl fluoride, which selectively inhibited HPV in isolated rabbit lungs [154] and cadmium sulphate which inhibited HPV in isolated pulmonary arteries [157]. However, the role of NADPH oxidases in O₂ sensing then seemed to become negligible due to a study that demonstrated that gp91phox-deficient mice fully exhibit HPV [158]. Although

this clearly excludes the phagocytic NADPH oxidase type to be the O₂ sensor in HPV, it was demonstrated that mice deficient of the cytosolic NADPH oxidase subunit p47 had a ~25% reduced acute, but unchanged sustained HPV [122]. Therefore isoforms of the leukocytic NADPH oxidase may, at least in part, function as O₂ sensors in HPV.

Whereas some investigations proposed decreased ROS production by NADPH oxidases during HPV [159], others supported the initial hypothesis of increased ROS production during hypoxia by an activation of a NADPH oxidases, as all the inhibitors of NADPH oxidases inhibited, but did not mimic HPV [81]. In isolated perfused lungs, intravascular NADPH oxidase dependent superoxide concentration increased during graded hypoxia peaking at 5% O₂ (pO₂ 38 mmHg), when NADPH oxidase was maximally stimulated with phorbol myristate acetate (PMA), although under non-stimulated conditions superoxide release decreased with hypoxia. Therefore it was concluded that regulation of electron flux rather than O₂ may be the rate-limiting step in superoxide formation from non phagocytic NADPH oxidase [97]. NADPH oxidases might be activated in HPV by PKC [112] or phospholipase A₂ [151, 160].

1.1.3.4.3 Cytochrome P450, EETs and HETEs

Cytochrome P450 monooxygenases (P450 hydroxylase [CYP4A] and P450 epoxygenase [CYP2C]) that produce 19- and 20-hydroxyeicosatetraenoic acids (HETEs) and epoxyeicosatrienoic acids (EETs) by oxidizing arachidonic acid (AA) have been postulated to play a specific role in HPV [161]. 20-HETEs dilated isolated pulmonary arteries of the human [162] and rabbit pulmonary artery rings [163]. In contrast they constricted kidney, brain and striate muscle vessels [164]. EETs decreased tone of isolated lungs of the rabbit [165] and the dog [166], but also have been shown to constrict pulmonary vessels [167].

Because of their heme moiety the activity of cytochrome P450 enzymes is highly O₂ dependent and hypoxia could block conversion of AAs into 20-HETE and EETs with subsequent decrease of vasodilatory prostanoids. Administration of inhibitors of CYP4A showed normoxic vasoconstriction and subsequent increase of HPV [163]. Inhibition of Cytochrome P-450 also reversibly inhibited potassium currents and depolarized PA cells [168]. In contrast, increasing the concentration of EETs by inhibition of soluble epoxide hydrolase (sEH) inhibitors or use of sEH knock-out mice enhanced HPV and caused normoxic vasoconstriction by a mechanism dependent on transient receptor potential 6 (TRP6) signaling [169].

However, the specificity for blockade of HPV can be questioned [170], as well as the necessity for an intact P450 system for HPV, as the specific inhibitor 1-aminobenzotriazole

attenuated HPV, but during following washout the activity of P450, but not the strength of HPV is still decreased [171]. Recently inhibition of CYP2C29, has been shown to decrease, but not abolish HPV [172].

Cytochrome P450 can be identified by characteristic carbon monoxide spectrum (see appendix) or spectral alterations due to substrate binding [173].

1.1.3.4.4 Heme protein related to potassium channels

A common physiologic mechanism to detect O_2 , NO and CO for signal transduction is the use of a great variety of heme-based proteins, that respond to a wide range of O_2 concentrations [174]. Besides the already discussed ones, that are cytochromes of the respiratory chain and the NADPH-oxidase, it was recently suggested, that heme oxygenase-2 (HO-2) might play a role in O_2 sensing via cytochrome P450 reductase dependent production of CO [175]. A large conductance calcium and voltage dependent potassium channel (BKCa) is co-localized with HO-2 and activated by HO-2 produced CO during normoxia [176]. Hypoxia therefore could inhibit HO-2, decrease CO and lead to vasoconstriction. However, recently this concept has been challenged by an investigation showing that mice deficient of the gene for HO-2 and BKCa have no limitation of HPV [177].

CO is well known to specifically inhibit HPV in isolated lungs [178], but it has a wide spectrum of interaction partners. It also may modulate hypoxic reactions by binding to cytochrome P450 (see above), mitochondrial cytochrome c oxidase [179] and activation of sGC [180].

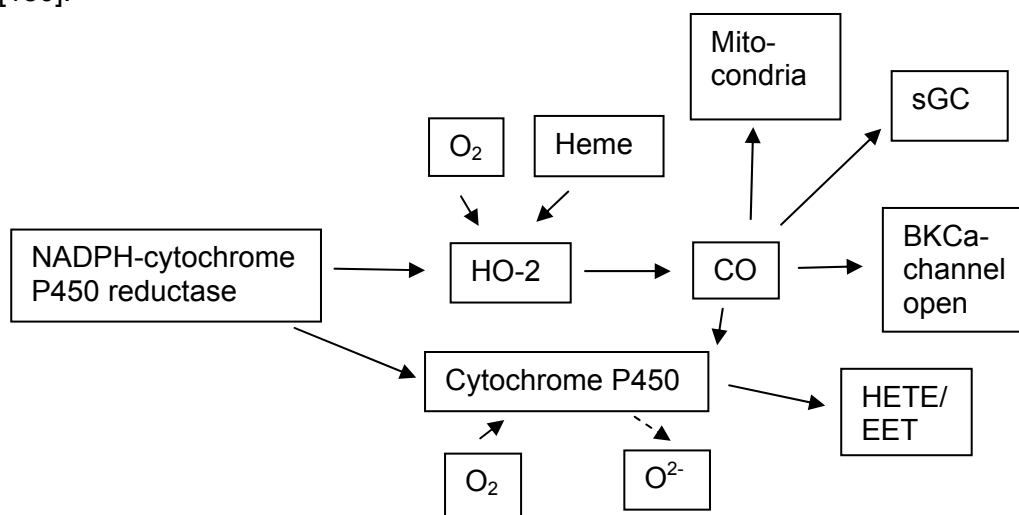


Figure 1.5 Heme oxygenase and carbon monoxide in oxygen sensing

In the presence of O_2 heme oxygenase-2 (HO-2) uses electrons from heme and NADPH-cytochrome P450 reductase to produce carbon monoxide (CO), which maintains opening of large conductance calcium and voltage dependent potassium channel (BKCa). Cytochrome P450 enzymes also use electrons from NADPH-cytochrome P450 reductase to produce hydroxyeicosatetraenoic acids (HETE), epoxyeicosatrienoic acids (EET) and possibly superoxide (O_2^-) in the presence of O_2 . CO interferes with BKCa-channel, but also cytochrome P450, soluble guanylate cyclase (sGC) and cytochrome c oxidase of mitochondria.

1.2 Measurement of mitochondrial function in HPV

Mitochondrial respiratory chain activity is dependent on substrate supply, activity of single mitochondrial chain enzymes, O₂ concentration and ADP concentration. Under physiological conditions, ADP concentration is of major importance for regulation of respiration in order to adjust cellular ATP production to demand. Therefore, maximal respiration can be achieved in isolated mitochondria with maximal ADP concentration, which is the so called "state 3" respiration, in contrast to "state 4" respiration under conditions of ADP depletion [181, 182]. However, fine-tuning mitochondrial respiration can be achieved by mitochondrial calcium concentration and metabolites controlling complex IV activity (e.g. NO, CO, ATP) [137, 183]. Mitochondrial respiratory chain activity can be directly monitored by either measurement of mitochondrial O₂ consumption (i.e. mitochondrial respiration), or under hypoxia and specific inhibitors by measurement of cytochrome redox state [117, 184, 185]. Indirect parameters for its activity can be mitochondrial membrane potential or ATP production [181, 182]. However, both of these parameters are also dependent on other factors, like mitochondrial proton leak and glycolytic ATP production. As direct measurement of mitochondrial respiratory chain function O₂ consumption (i.e. respiration) and redox state are therefore most suitable. Both parameters can be determined isolated cells, whereas redox measurements can also be performed in isolated organs. Measurements in isolated lungs offer the advantage, that mitochondrial function can be directly compared to the strength of HPV. Furthermore the influence of other cell types surrounding PASMC and the O₂ gradient from alveoli to mitochondria of PASMC can be taken into account. Isolated PASMC on the other hand, may be more specific for the O₂ response, as they represent the O₂ sensor cell type. Isolated PASMC should be preferred to isolated mitochondria, as they represent better physiological conditions without the need of artificial application of external substrate and ADP.

1.2.1 Respiration

Mitochondrial O₂ consumption (= respiration) can be determined by measurement of the rate of decreasing O₂ concentration in a closed chamber. O₂ consumption in relation to O₂ concentration is a measure for O₂ affinity of the mitochondria, usually expressed as O₂ concentration at half maximal O₂ consumption (= p50 value). O₂ concentration can be measured with pO₂-electrodes based on different methodological background. However, the measurement technique is limited by 1) precision of the pO₂ electrode, particularly in the low O₂ range, 2) O₂ consumption and backdiffusion of the surrounding material of the chamber

and 3) artefacts due to non-mitochondrial O₂ consumption, resulting in a biphasic O₂ kinetics during mild hypoxia [186].

Furthermore, in whole organs mitochondrial O₂ consumption cannot be determined.

1.2.2 Redox state of mitochondrial cytochromes

If electron transfer of the mitochondrial respiratory enzymes to O₂ is limited by hypoxia, cytochrome *aa3* of complex IV, and subsequently cytochrome *c* and cytochrome *b_{lh}* located in complex III will become reduced, which can be detected by a change in absorption characteristics (= difference spectrum, see methods Figure 2.4). Thus inhibition of mitochondrial respiration by hypoxia will be reflected by reduction of mitochondrial cytochromes, specifically cytochrome *aa3*, which can be detected in tissue or isolated cells by remission spectrophotometry (see methods 2.2.3.1). Moreover, measurement of the redox state of cytochrome *b_{lh}* can provide insight into mechanisms of ROS production at complex III. An increased electron transfer to produce superoxide could be reflected by an increased oxidation state of this cytochrome.

An overview of mitochondrial and non-mitochondrial cytochromes is given in table 3.

1.3 Measurement of NADPH oxidase, cytochrome P 450 and other hemeproteins in HPV

Besides mitochondrial cytochromes, also non-mitochondrial cytochromes can be observed by remission spectrophotometry, depending on their concentration and strength of absorption (absorption coefficient).

Cytochrome	Source	Absorption peaks	Inhibitors
cytochrome <i>aa3</i>	complex IV of ETS	reduced minus oxidized: 445/420/605 nm [181] (see appendix)	cyanide, azide, CO, NO
cytochrome <i>b</i>	hemoglobin	HbCO minus HbO ₂ : 423/525/565 nm HbCO minus HbN ₂ : 420/533/570 nm HbN ₂ minus HbO ₂ : 435/560/592 nm (presented study)	
	myoglobin	MbO ₂ : 582, 544 [187] MbCO minus MbO ₂ : 421/540/580nm [188]	
	sGC	sGC-O ₂ minus sGC-N ₂ : 437 nm [189] sGC-CO: 423/541/567 nm [190]	
	complex II	reduced minus oxidized: 560 nm [191]	
	complex III of ETS	anoxia minus normoxia: cyt. <i>b_h</i> : 430/532/562 nm cyt. <i>b_i</i> : 430/532/566 nm (see appendix) [181, 192]	antimycin A, myxothiazol, HQNO
	NADPH oxidase	reduced minus oxidized: cyt. <i>b₅₅₈</i> : 425-427/558 nm [193, 194]	SDT
	cytochrome P450	P450-CO minus P450-SDT: 450 nm [195]	CO
cytochrome <i>c</i>	soluble protein of ETS	reduced minus oxidized: 416/521/550 nm [181] (see appendix)	
cytochrome <i>c1</i>	complex III	reduced minus oxidized: 418/520/553 nm [181]	

Table 3: Cytochromes in mammalian tissue

CO: carbon monoxide, ETS: electron transport system, Hb: hemoglobin, HQNO: 2-n-heptyl-4-hydroxyquinoline-N-oxide, Mb: myoglobin, NADPH: nicotinamide adenine dinucleotide phosphate, N₂: nitrogen, NO: nitric oxide, O₂: oxygen, SDT: sodium dithionite, sGC: soluble guanylate cyclase

1.4 Aim of the study

Although the response of the pulmonary vasculature to acute hypoxia has been described long since, the O₂ sensing mechanism still remains to be elucidated.

In order to identify the role of mitochondria in O₂ sensing of HPV, the aim of the present study was to examine,

- 1) if complex IV can act as an O₂ sensor of HPV. This question should be addressed by correlating O₂ dependent mitochondrial respiratory chain function to the strength of HPV,
 - a) in the isolated lung (measurement of mitochondrial cytochrome redox state by remission spectrophotometry),
 - b) in isolated PASMC (measurement of respiration and redox state by combination of spectrophotometry and respirometry)
- 2) if complex III can act as an O₂ sensor of HPV. This question should be addressed by measurement of changes in the redox state of cytochrome *b₅₅₉* that can be attributed to altered ROS production during HPV,
- 3) if cytochromes of PASMC behave differently or similarly to those from the systemic circulation (aortic smooth muscle cells [ASMC] and renal smooth muscle cells [RASM]), and
- 4) if yet undescribed or non-mitochondrial cytochromes involved in O₂ sensing can be identified.

The aim of the study is summarized in figure 1.6.

Until now these uncertainties have not been resolved due to methodological limitations. In isolated organs mitochondrial O₂ affinity (i. e. pO₂ dependent mitochondrial respiration) cannot be determined, and in isolated cells simple determination of O₂ affinity by O₂ consumption measurements is hampered by artefacts due to non-mitochondrial O₂ consumption resulting in biphasic O₂ kinetics during mild hypoxia [186].

To overcome these limitations, in this work

- 1) the technique of remission spectroscopy was adapted in order to examine the redox state of the mitochondrial respiratory system in intact lungs and in isolated PASMC, ASMC and RASM,
- 2) high-resolution respirometry was used in PASMC, ASMC and RASM.

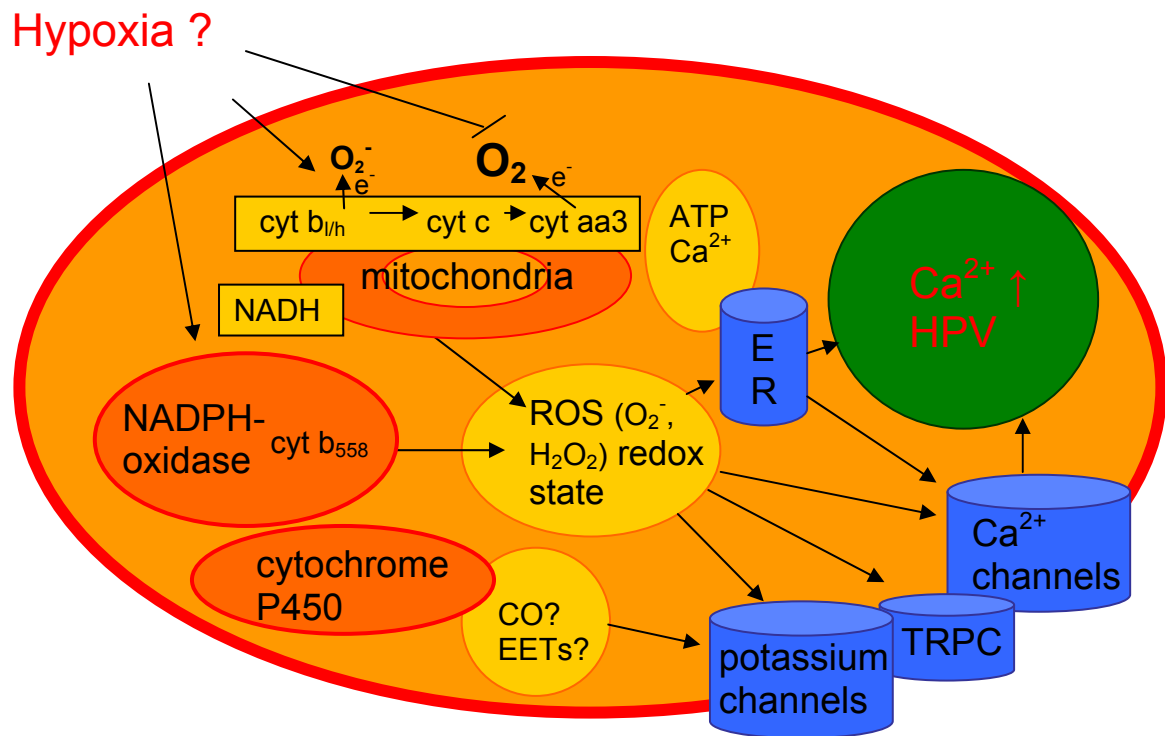


Figure 1.6 Aim of the study

How does hypoxia influence the function of mitochondrial respiratory chain enzymes and non-mitochondrial cytochromes and can this be related to hypoxia-induced reactions in the isolated lung and PASM?C?

ATP: adenosine triphosphate, CO: carbon monoxide, EET: epoxyeicosatrienoic acids, ER: endoplasmatic reticulum, NADH: reduced nicotinamide adenine dinucleotide, ROS: reactive oxygen species, TRPC: transient receptor potential channels.

2 Material and Methods

2.1 Materials

2.1.1 Animals

Chinchilla bastard rabbits of either sex (2.5–3.2 kg body weight) and C57BL/6J mice (21–30 g body weight, Jackson Laboratory) were used for the investigations. All animal experiments were approved by the local Governmental Commission.

2.1.2 Equipment

For isolated lung experiments:

Air tight tubings	Cole-Parmer Instruments Company (Vernon Hills, USA)
Amplifier (Plugsy DBA 660)	Hugo Sachs Elektronik (March-Hugstetten, Germany)
BP 742 Fresenius Roller Pump, Pulsatile Flow Cat-Rabbit Ventilator UV 6025	Fresenius (Bad Homburg, Germany) Hugo Sachs Elektronik (March-Hugstetten, Germany)
Chart recorder (Rikadenki R 50 Series)	Rikadenki Electronics (Freiburg, Germany)
Force Transducer, Load Cell	Hottinger Balowin Messtechnik (Darmstadt, Germany)
Frigomix-U	Braun Melsungen AG (Melsungen, Deutschland)
Gas mixing chamber (KM 60–3/6MESO)	WITT (Witten, Germany)
Gas (normoxic gas mixture, N ₂ , O ₂ , CO ₂ , CO)	Air Liquide Deutschland GmbH, (Ludwigshafen, Deutschland)
Glassware	Glassblowing (University of Giessen, Germany)
Oszillographic recorder	Hugo Sachs Elektronik (March-Hugstetten, Germany)
Pressure transducers Combitrans	Braun Melsungen AG (Melsungen, Germany)
Respirator research setup system: Isolated Perfused Lung for Mouse Size 1, IL-1 Threats	Hugo Sachs Elektronik (March-Hugstetten, Germany) Coats GmbH (Kenzingen, Germany)
<i>For remission spectrophotometry:</i>	
CytoSPEC II	LEA Medizintechnik (Giessen, Germany)
LEA flat probe	LEA Medizintechnik (Giessen, Germany)
LEA endoscopic probe	LEA Medizintechnik (Giessen, Germany)
LEA O2k probe	LEA Medizintechnik (Giessen, Germany)

For respirometry:

Oxygraph-2k
Hamilton Syringes

OROBOROS (Innsbruck, Austria)
OROBOROS (Innsbruck, Austria)

For fluorescence measurements:

Olympus BX50 WI
IMAGO CMOS-Kamera
Software TILLvision
Hypoxic chamber flow through system

Olympus (Hamburg, Germany)
Till Photonics (Martinsried, Germany)
Till Photonics (Martinsried, Germany)
Institute of Pharmacology (University of Marburg, Germany)
Oxford Optronics (Oxford, United Kingdom)

Licor electrode

For cell isolation, culture and staining:

Cell culture incubator

Flow Laboratories (Meckenheim, Germany)

Centrifuge Rotina
Cover slips (24x50 mm)
Falcon tubes

Hettich (Tuttlingen, Germany)
Menzel-Gläser (Braunschweig, Germany)
Greiner bio-one (Frickenhausen, Germany)

Fluorescence microscope (Leica CTR MIC)
Freezer -20 °C
Fridge +4 °C
Glass bottles, 250, 500, 1000 ml
Light microscope
Magnet concentrator
Pipetboy
Tissue culture flask T75

Leica (Wetzlar, Germany)
Bosch (Stuttgart, Germany)
Bosch (Stuttgart, Germany)
Fisher (Schwerte, Germany)
Leica (Wetzlar, Germany)
Dynal A.S (Oslo, Norwegen)
Eppendorf (Hamburg, Germany)
Greiner Bio-One (Frickenhausen, Germany)
Dispomed Witt (Gelnhausen, Germany)
HMD Healthcare LTD. (Horsham, UK)
Nunc GmbH & Co. KG (Wiesbaden, Germany)

15G cannula

18G cannula

8er permanox chamber slides

2.1.3 Chemicals and reagents

For isolated lung experiments:

Aqua destillata.
Krebs Henseleit buffer
Ketamine (Ketavet)
Narcoren
Natriumhydrogencarbonat (NaHCO₃) 1 M 8.4%
Thromboxane analogon U-46619
Heparin
Xylazine (Rompun) 2%

Xylocain 2%

Baxter S.A. (Lessines, Belgien)
Serag-Wiessner (Naila, Germany)
Pharmacia GmbH (Erlangen, Germany)
Merial AG (Hallbergmoss, Germany)
Serag-Wiessner (Naila, Germany)
Sigma-Aldrich (St. Louis, USA)
Roche (Basel, Switzerland)
Bayer Vital GmbH (Leverkusen, Germany)
AstraZeneca GmbH (Wedel, Germany)

For spectrophotometry/respirometry:

Antimycin A

Sigma-Aldrich (St. Louis, USA)

Cytochrome c	Sigma-Aldrich (St. Louis, USA)
Medium 199, colorless	Invitrogen (Carlsbad, USA)
Potassium cyanide	Sigma-Aldrich (St. Louis, USA)
Sodium dithionite (SDT)	Sigma-Aldrich (St. Louis, USA)
<i>For fluorescence measurements:</i>	
5,5',6,6'-tetrachloro-1,1',3,3'-tetraethylbenzimidazolcarbocyanine iodide (JC-1)	Invitrogen (Carlsbad, USA)
MitoSox	Invitrogen (Carlsbad, USA)
Fura-2	Invitrogen (Carlsbad, USA)
<i>For cell isolation, culture and media:</i>	
Albumin	Sigma-Aldrich (St. Louis, USA)
Agarose with low melting point	Sigma-Aldrich (St. Louis, USA)
Calcium chloride (CaCl ₂)	Merck (Darmstadt, Germany)
Collagenase type IV	Sigma-Aldrich (St. Louis, USA)
Dulbecco's Phosphate-Buffered Saline (DPBS)	PAN Biotech (Aidenbach, Germany)
Dimethyl sulfoxide (DMSO)	Sigma-Aldrich (St. Louis, USA)
Dithiothreitol	Sigma-Aldrich (St. Louis, USA)
Ethanol absolute	Riedel-de Haen (Seelze, Germany)
Fetal calf serum (FCS)	PAA Laboratories (Cölbe, Germany)
Glucose	Sigma-Aldrich (St. Louis, USA)
Hyaluronidase	Sigma-Aldrich (St. Louis, USA)
Iron oxide	Sigma-Aldrich (St. Louis, USA)
Magnesium chloride (MgCl ₂ x 6 H ₂ O)	Sigma-Aldrich (St. Louis, USA)
Medium 199	Invitrogen (Carlsbad, USA)
Papain	Worthington (St. Katharinen, Germany)
Penicillin/Streptomycin (P/S)	PAN Biotech (Aidenbach, Germany)
Potassium chloride (KCl)	Merck (Darmstadt, Germany)
Sodium chloride (NaCl)	Roth (Karlsruhe, Germany)
Trypsin/ ethylenediaminetetraacetic acid (EDTA)	PAN Biotech (Aidenbach, Germany)
2-(-4-2-hydroxyethyl)-piperazinyl-1-ethansulfonate (HEPES)	Merck (Darmstadt, Germany)
<i>For cell staining:</i>	
Acetone	Sigma-Aldrich (St. Louis, USA)
Collagen solution 0.01 % (collagen type I)	Sigma-Aldrich (St. Louis, USA)
Bovine serum albumin 0.1 % (BSA)	PAA Laboratories GmbH (Pasching, Germany)
Dako Fluorescent Mounting Medium	Dako cytometry (Hamburg, Germany)
Methanol	Sigma-Aldrich (St. Louis, USA)
Potassium dihydrogen phosphate (KH ₂ PO ₄)	Merck (Darmstadt, Germany)
Sodium hydrogen phosphate (Na ₂ HPO ₄ x 2H ₂ O)	Merck (Darmstadt, Germany)
4',6-Diamidino-2-phenylindole (DAPI)	Sigma-Aldrich (St. Louis, USA)

2.1.4 Antibodies

anti- α -smooth muscle actin, Clone 1A4, monoclonal, mouse anti-human, Sigma-Aldrich, Steinheim, Germany

anti-cytokeratin, Clone MNF116, monoclonal, mouse anti-human, Dako Cytometry, Hamburg, Germany

anti-collagen I, rabbit anti-human, Alexa Fluor 488, Invitrogen, Karlsruhe, Germany

anti-von Willebrand factor, rabbit anti-human, Dako Diagnostika, Hamburg, Germany
antibody Alexa Fluor 488, goat anti-mouse IgG, Invitrogen, Karlsruhe, Germany
antibody Alexa Fluor 488, goat anti-rabbit IgG, Invitrogen, Karlsruhe, Germany

2.2 Methods

2.2.1 Isolated lung models

2.2.1.1 Isolated perfused and ventilated rabbit lung

The model of isolated perfused rabbit lungs has been described previously [5]. Pathogen free male rabbits (body weight 2.8-3.8) were deeply anaesthetized with i.v. application of ketamine (30-50 mg/kg) and xylazine (6-10 mg/kg) and anticoagulated with heparin (1500 U/kg body weight). The trachea was cannulated and animals were ventilated with room air (tidal volume 30 ml, frequency 30 strokes/min) by a rodent ventilator (Cat-Rabbit Ventilator). The lungs were excised under deep anesthesia while perfused via the pulmonary artery with Krebs Henseleit buffer (125.0 mmol/liter NaCl, 4.3 mmol/liter KCl, 1.1 mmol/liter KH_2PO_4 , 2.4 mmol/liter CaCl_2 , 1.3 mmol/liter MgCl_2 and 275 mg glucose/100 ml); NaHCO_3 was adjusted to result in a constant pH of 7.37–7.40. In parallel with the onset of artificial perfusion, ventilation was changed from room air to a normoxic gas mixture (5% CO_2 , 21% O_2 , balanced with N_2). A positive end expiratory pressure of 2 cm H_2O was chosen for prevention of regional alveolar collapse. After the lungs were rinsed for 45 min with 6 liter of buffer fluid for washout of the blood, the perfusion circuit was closed for recirculation by a peristaltic pump (BP 742 Fresenius Roller Pump) connected to arterial and venous parts of tubing cannula. The total system volume was 250 ml, the buffer flow rate was 150 ml/min, and left atrial pressure was set at 2.0 mmHg to ensure zone III condition throughout the lung at end-expiration. Because the perfusion rate is constant, changes in pulmonary artery pressure directly reflect changes in the pulmonary vascular resistance. The isolated lungs were freely suspended from a force transducer for continuous monitoring of organ weight. The entire system was heated to 38.5 °C. Pressures in the pulmonary artery, the left atrium, and the trachea were continuously registered. For hypoxic maneuvers, a gas mixing chamber (KM 60–3/6MESO) was employed for step-wise changes in the ventilator O_2 content.

The lungs included in the study were those that 1) had a homogeneous white appearance with no signs of hemostasis, edema, or atelectasis; 2) revealed a constant mean PAP and peak ventilation pressure in the normal range; and 3) were isogravimetric during an initial steady state period of at least 20 min.

2.2.1.2 Isolated perfused and ventilated mouse lung

Changes in pulmonary perfusion pressure were assessed in the isolated buffer-perfused mouse lung similar to the rabbit lung, as described. Briefly, mice were anesthetized with intraperitoneal (i.p.) injection of 80 mg/kg pentobarbital and anticoagulated with 1000 U/kg heparin. Catheters were inserted into the pulmonary artery and left atrium, and buffer perfusion via the pulmonary artery was initiated at a flow of 0.2 ml/min. Ventilation was then changed from room air to a premixed gas (21% O₂, 5% CO₂, balanced with N₂), left atrial pressure was set to 2.0 mmHg, and flow was slowly increased from 0.2 to 2 ml/min. Positive pressure ventilation was performed with a tidal volume of 250 µl, 90 breaths/min, and 2 cm H₂O positive end-expiratory pressure. For hypoxic maneuvers, a gas mixing chamber (KM 60–3/6MESO) was employed for step-wise changes in the ventilator O₂ content. Ten-minute periods of hypoxic ventilation were alternated with 15 min of normoxia. Gas mixtures contained carbon monoxide were premixed and applied via an air tight vessel.

For perfusion Krebs-Henseleit buffer, containing 120 mmol/liter NaCl, 4.3 mmol/liter KCl, 1.1 mmol/liter KH₂PO₄, 2.4 mmol/liter CaCl₂, 1.3 mmol/liter MgCl₂, and 13.32 mmol/liter glucose as well as 5% (wt/vol) hydroxyethylamylopectin (molecular weight 200,000) was employed. The total system volume was 15 ml.

2.2.2 Isolated cell experiments

2.2.2.1 Isolation of pulmonary and renal arterial smooth muscle cells

Smooth muscle cells were isolated from pulmonary precapillary arteries and cultured as described previously [58, 196, 197]. The pulmonary artery of rabbit lungs was cannulated as described for isolated lung experiments. Lungs were slowly washed with 50 ml DPBS via a syringe. Afterwards lungs were perfused with 50 ml iron containing medium (medium 199, 1% P/S, 0.5% agarose with low melting point, 0.5% iron oxide particles, 40°C). Iron particles got fixed in the precapillary vessels [197] and homogenous distribution was controlled visually. Afterwards lung tissue was fixed by tracheal infusion of medium 199, with 1% P/S and 1% agarose at 40°C. Lungs were removed and put in ice-cold DPBS for hardening of agarose. A similar isolation procedure was used for renal precapillary arteries. After cannulation of the renal artery, kidneys were washed and perfused with iron containing medium as described above.

Afterwards lungs or kidneys were cut with scissors for 15 minutes to very small pieces and solved in 30-35 ml DPBS per falcon tube. Iron loaded tissue pieces were collected by external application of a magnet to the falcon tubes. Supernatant consisting of buffer and non iron loaded tissue was removed by suction. Iron loaded tissue was washed by this procedure

three times. Afterwards tissue pieces were incubated at 37°C for 55 minutes with 80 U/ml collagenase type IV (dissolved in medium 199 und 1% P/S) for removal of fibroblasts, and subsequently pulled several times through a 15G cannula and 18G cannular for dissection. Iron containing tissue pieces were washed again three times with medium 199 (containing 1% P/S and 10% FCS) according to the procedure described above including the use of a magnet. Tissue pieces were transferred in T75 flasks for culture.

2.2.2.2 Isolation of aortal smooth muscle cells

The ASMC were dissected from isolated rabbit aortas after removal of the endothelial and adventitial cell layer. For this procedure isolated aortas were transferred into an isolating solution (127.0 mM NaCl, 5.9 mM KCl, 1.2 mM MgCl₂ x 6 H₂O, 11.8 mM glucose, 10.0 mM HEPES, 2.4 mM CaCl₂), adventitia was removed manually, the aorta cut open longitudinally and washed in calcium free isolating solution. Afterwards aortal tissue pieces were first incubated in 5 ml enzyme solution (0.1% albumin 0.07% papaine, 0.5% dithiothreitol in calcium free isolating solution) for 30 minutes at 37°C and 25 rpm and then digested in a second enzyme solution (0.1% albumin, 0.1% collagenase, 0.1% hyaluronidase in isolating solution with 50 µM calcium) for 10 minutes at 37°C and 25 rpm. Aortal tissue pieces solved in 0.5-1.0 ml isolating solution were resuspended with a pasteur pipette for dissolution and seeded on cover slips (24 mm diameter) for culture.

2.2.2.3 Cell culture and preparation for respirometric measurement

All cell types were cultured in a normoxic atmosphere (21% O₂ ~ pO₂ 158 mmHg, 5.3% CO₂ ~ pCO₂ 40 mmHg, balanced with N₂) in medium 199 with 10% FCS (PASMC and RASMC) or 20% FCS (ASMC) and 1% P/S. The cells were characterized by immunoreactivity with α-actin antibodies. The absence of endothelial cells was confirmed by staining for von Willebrand (vWF) factor, staining for cytokeratin was performed to exclude presence of epithelial cells, and staining for collagen I to exclude presence of fibroblasts. Cells were prepared for measurement by washing once with phosphate buffer saline (PBS: 0.8 % NaCl, 0.02 % KCl, 0.115 % Na₂HPO₄ x 2H₂O, 0.02 % KH₂PO₄, pH 7.4) and incubating with trypsin solution (0.25% (m/v)) for 2-5 minutes. The detached cells were then centrifuged 5 minutes at 5000 g. Afterwards they were washed two times with colorless medium 199 with 10% HEPES and resuspended to 2.5 ml for measurement in the O2k measurement chamber. Only cells from first and second passage were used.

2.2.2.4 Immunofluorescence staining

PASMC, ASMC and RASMC were seeded onto eight-well chamber slides at 1500 cells per well. Cells were then washed with cold DPBS with 0.1% BSA and fixed and permeabilized with an ice-cold mixture of acetone and methanol for 5 min at -20°C. After washing 5 times with PBS with 0.1% BSA, slides were incubated in blocking buffer (3% BSA in PBS) for 15-30 min at room temperature, followed by an 1 h incubation with the primary antibodies (SM- α -actin 1:450, Cytokeratin 1:50, vWF 1:500 and Collagen I 1:5) at room temperature. Washing was followed by incubation with fluorescein isothiocyanate (FITC)-labeled secondary antibodies (1:100 in PBS with 0.1% BSA). As secondary antibody goat anti-mouse was used for SM- α -actin und Cytokeratin (Alexa Fluor 488, goat anti-mouse IgG) staining and goat anti-rabbit (Alexa Fluor 488, goat anti-rabbit IgG) for vWF and collagen I. Nuclei were visualized by 4,6-diamidino-2-phenylindole (DAPI, 1:5000 in 0,1 % BSA) staining. Cells were washed 5 x with PBS, slides were covered with mounting medium and a cover slide and analyzed by fluorescence microscopy using the Leica CTR-MIC.

2.2.3 Remission spectrophotometry

2.2.3.1 Principle of spectral measurements

Remission spectrophotometry can be used for determination of redox state of mitochondrial cytochromes. The method is based on the fact that certain cell pigments (cytochromes: cyto=cell, chrôma=color; greek) absorb light of specific wavelengths depending on their redox state. These cytochromes include heme proteins of red blood cells, mitochondria and other different enzymes. The absorption at specific wavelengths can be depicted as wavelength-to-intensity diagram (i.e. spectrum). If mitochondrial cytochromes cannot transfer electrons ("reduction"), they will exhibit different absorption characteristics ("reduced spectrum", Figure 2.1) compared to the condition when they can release an electron ("oxidized spectrum", Figure 2.2). The change in reduction and oxidation (redox state) can be evaluated (Figure 2.3) by comparing both spectra, which is accomplished by calculating reduced minus oxidized spectrum ("difference spectrum").

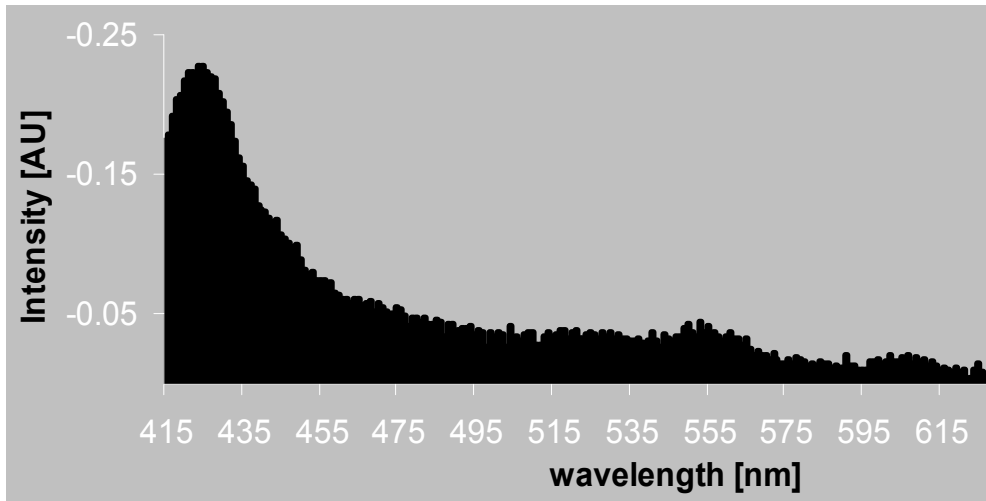


Figure 2.1 Spectrum of reduced mitochondria

Negative intensity represents absorption (y-axis) at specific wavelengths (x-axis). The wavelength-to-intensity/absorption curve (=spectrum) depicts the sum spectrum of single cytochromes.

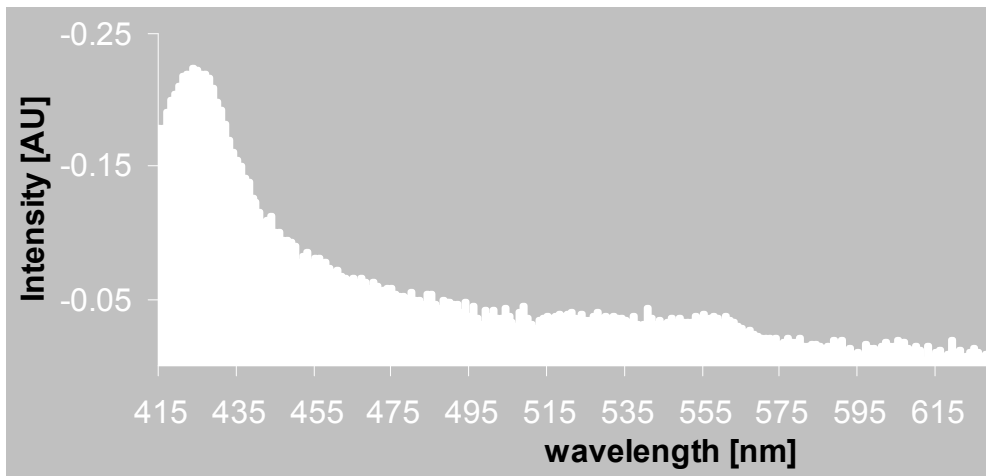


Figure 2.2 Spectrum of oxidized mitochondria

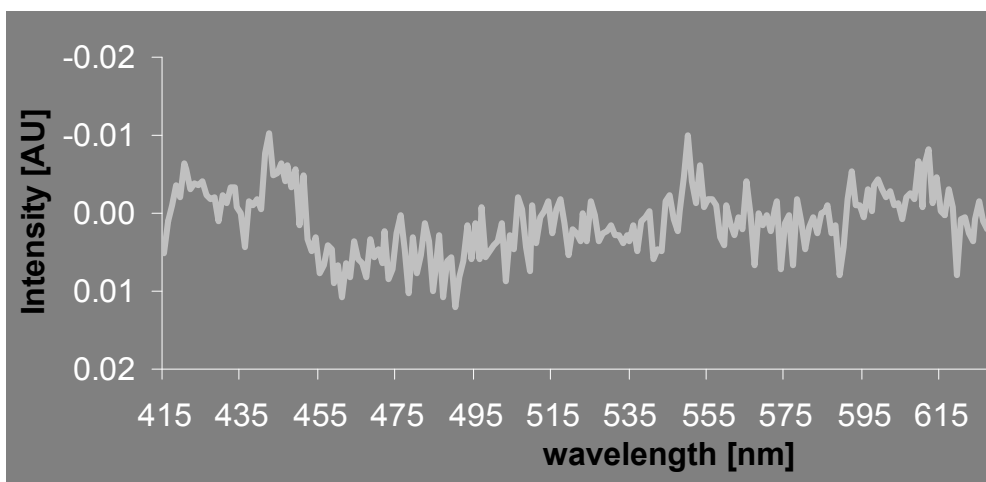


Figure 2.3 Difference spectrum of reduced minus oxidized mitochondria

Calculated by subtraction of reduced minus oxidized spectrum.

The spectra of figure 2.1 to 2.3 were derived by measurements in PSMC.

Inhibition of electron transfer (e.g. by removal of the terminal electron acceptor O_2), will result in an electron retention ("reduction"), whereas release of electrons to O_2 to form superoxide or water will result in "oxidation" (Figure 2.4). Therefore, inhibition of the mitochondrial respiratory chain by anoxia will result in a reduced difference spectrum as shown in Figure 2.3.

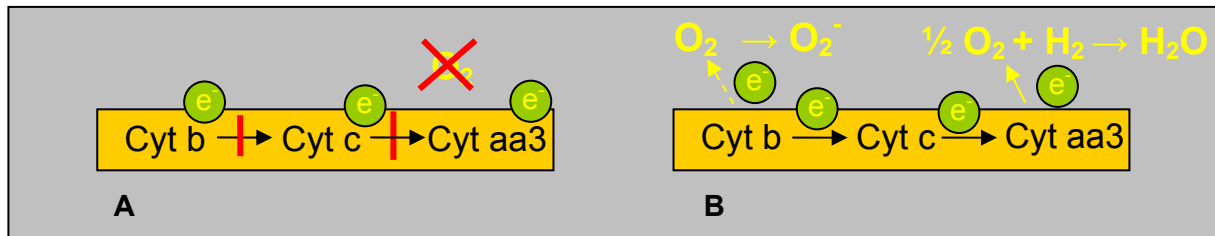


Figure 2.4 Reduction and oxidation of mitochondrial cytochromes

If the final electron acceptor O_2 is not available, electrons cannot be passed along the mitochondrial respiratory system and the cytochromes are reduced (A). Under conditions of O_2 availability the electrons can be passed to O_2 to produce superoxide or water, the cytochromes are oxidized (B).

2.2.3.2 Measurement of redox state in isolated rabbit and mouse lungs

2.2.3.2.1 Setup for measurement in isolated lungs

In order to analyze absorption properties of the mitochondria, the wavelength dependent change of light irradiated into tissue ("broadband spectrum") compared to backscattered (i.e. remitted) light from tissue ("remission spectrum") is detected. Afterwards, the difference spectrum of remission spectrum under condition A (e.g. during hypoxia) minus remission spectrum under condition B (e.g. normoxia) can be calculated. The measurement depth will depend on the distance between the illuminating light spot and the collected backscattered light (Figure 2.5).

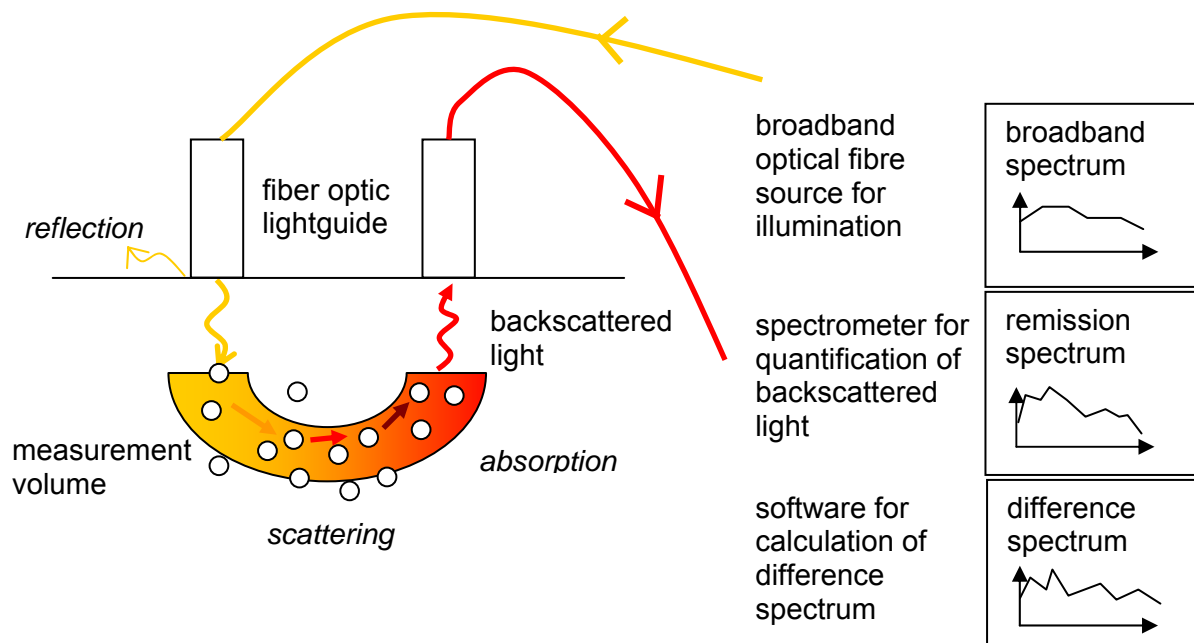


Figure 2.5 Schematic setup for measurement of remission difference spectra

Light of a known spectrum (broadband spectrum) is sent into tissue, where it interacts with boundary layers (reflection), small particles (scattering) and cytochromes (absorption). On its way through tissue it is therefore changed in its spectrum. The backscattered part of the altered light is collected at the tissue surface by a fiber optic lightguide and forwarded to the spectrometer for quantification of the intensity at the different wavelengths (remission spectrum). Remission spectra at different conditions can be compared and are depicted as difference spectra.

Measurement of remission difference spectra were performed by a spectrophotometric system using a CytoSPEC II (Figure 2.6). This consists of a temperature- and current-controlled broadband optical fiber source (395-670 nm) for illumination, and a temperature-controlled spectrophotometer with an asymmetric crossed Czerny-Turner design (detection range of 390-650 nm; optical resolution of 1.5 nm) for detection and quantification of light. Spectra were acquired at a rate of 3 – 800 ms, depending on the optical properties of the sample, and averaged over a period of 2 s up to 10 s. Calculation of difference spectra was performed by the CytoSPEC II software. A newly developed fiber-optic light guide (LEA flat probe for rabbit, LEA endoscopic probe for mouse) fixed at the surface of the lung (Figure 2.7) was used for collection of spectra.

For measurements in the rabbit lung, the separation of illuminating and sampling spot was set at 4 mm in order to maximize measured tissue volume.



Figure 2.6 CytoSPEC II

CytoSPEC II consists of the broadband optical fiber source, the spectrometer for analysis of backscattered light and the software for calculation of difference spectra. The fiber optic lightguide is connected to the optical fiber source and spectrometer.

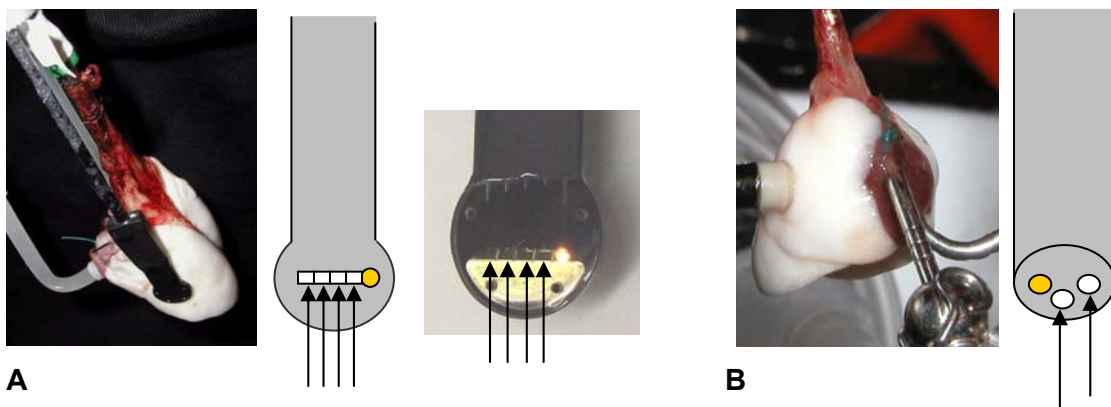


Figure 2.7 LEA flat and endoscopic probe

LEA flat probe (A) or LEA endoscopic probe (B) are fixed at the surface of isolated rabbit or mouse lungs, respectively. The probes consist of separated illuminating (yellow) and detecting (arrow) fibers with a different distance between the fibers to set the depth of the measurement sample.

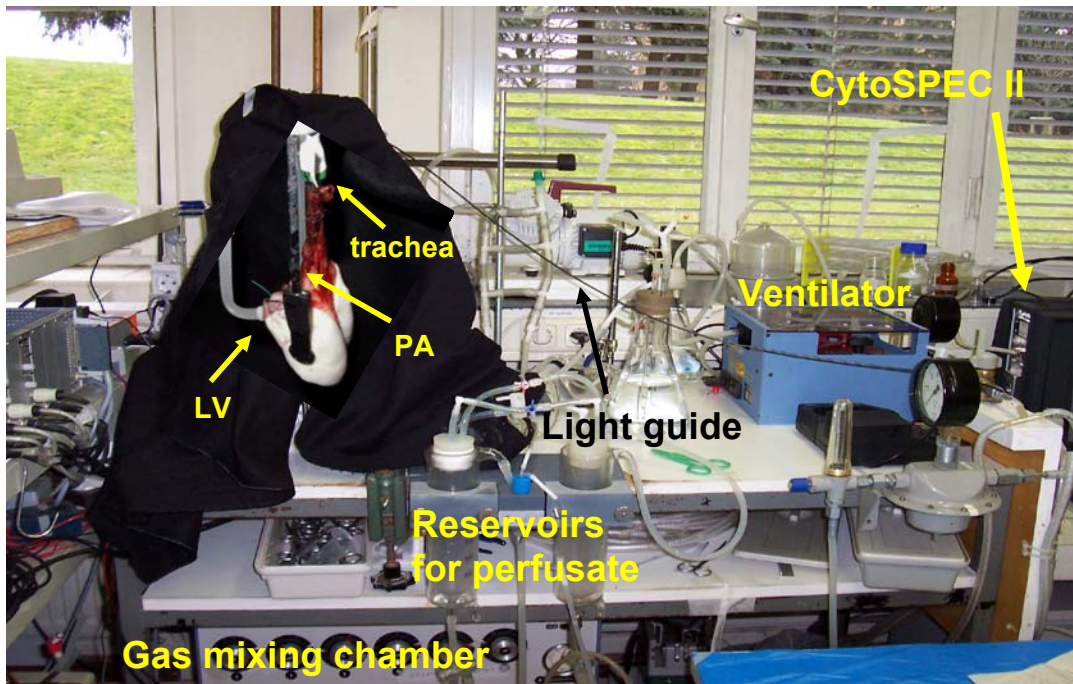


Figure 2.8 Setup for measurement in isolated lungs

The isolated lung is ventilated via the trachea and perfused via the pulmonary artery (PA). Perfusate from the lung is collected in the left ventricle (LV). The lung is freely suspended from a weight transducer. The flexible fiber optic light guide is softly attached to the lung surface, allowing it to follow the movement of the ventilatory excursion of the lung. The whole lung is covered by a black tissue to avoid artefactual light incidence (here uncovered for demonstration purposes).

2.2.3.2.2 Experimental procedure

In isolated rabbit and mouse lungs periods of 15 minutes normoxic ventilation were alternated with 10 minutes of hypoxic ventilation. Hypoxia was applied by ventilation with gas mixtures of 0% (0 mmHg), 1% (8 mmHg), 3% (23 mmHg), 5% (38 mmHg), 7% (53 mmHg), 10% (75 mmHg) and 15% (158 mmHg) O₂ (pO₂) with 5% (38 mmHg) CO₂ (pCO₂, balanced with N₂) chosen in a random order. Pulmonary arterial pressure, pulmonary venous pressure, ventilation pressure, lung weight and cytochrome spectra were recorded continuously. Cytochrome difference spectra were calculated as follows: Remission spectra were recorded every second and averaged over one minute. The averaged spectra of the minute before switching to hypoxia (spectrum 1), the fifth minute after switching to hypoxia (spectrum 2), the minute before switching to normoxia (spectrum 3) and the fifth minute after switching to normoxia (spectrum 4) were used for calculation of two difference spectra by subtraction of spectrum 1 from spectrum 2 and spectrum 4 from spectrum 3. Both difference spectra were averaged to achieve the final difference spectrum at a specific hypoxic condition. This procedure allows for correction of potential time dependent spectral alterations, as the normoxic spectrum once taken before hypoxia (spectrum 1) and once taken after hypoxia (spectrum 4) is subtracted from the hypoxic spectrum.

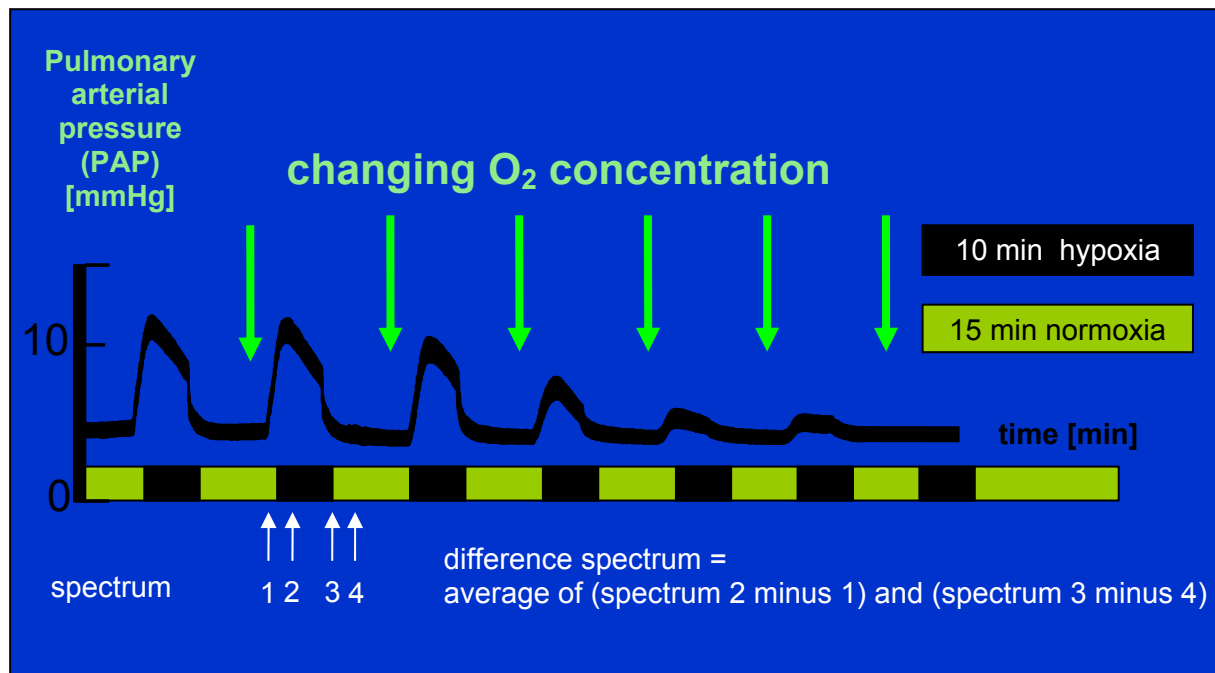


Figure 2.9 Experimental procedure for redox measurements in isolated lungs

2.2.3.3 Measurement in cell suspensions

2.2.3.3.1 Experimental setup

Measurements in cell suspension were based on the same principle as described for light interaction with tissue in the isolated lung (see Figure 2.5). Measurements were performed in a closed chamber of the Oxygraph-2k (O2k, OROBOROS, Innsbruck, Austria) with integrated fiber-optic light guides from the CytoSPEC II. Light of the broadband optical fiber source (395-670 nm) illuminated the cell suspension via glass fiber probes integrated into the stopper of the measurement chamber (Figure 2.10 and 2.11). The light interacted with the cells and was collected by the glass fiber probe for spectrometer analysis (Figure 2.10).

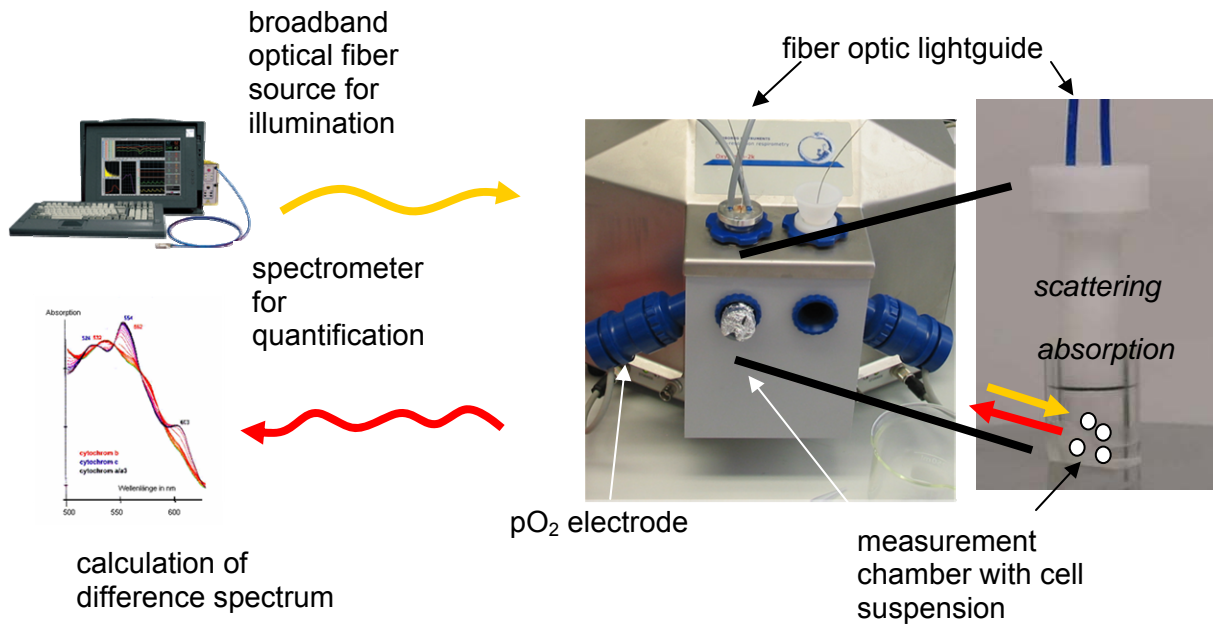


Figure 2.10 Schematic setup for measurement in cell suspensions

Light of a known spectrum (broadband spectrum) is irradiated into the cell suspension via a fiber optic light guide. There it interacts with small particles, like mitochondria and cells (scattering) and cytochromes (absorption). On its way through the cell suspension it is therefore changed in its spectral characteristics. The backscattered part of the altered light is collected by the fiber optic lightguide and sent into the spectrometer for quantification and calculation of difference spectra.

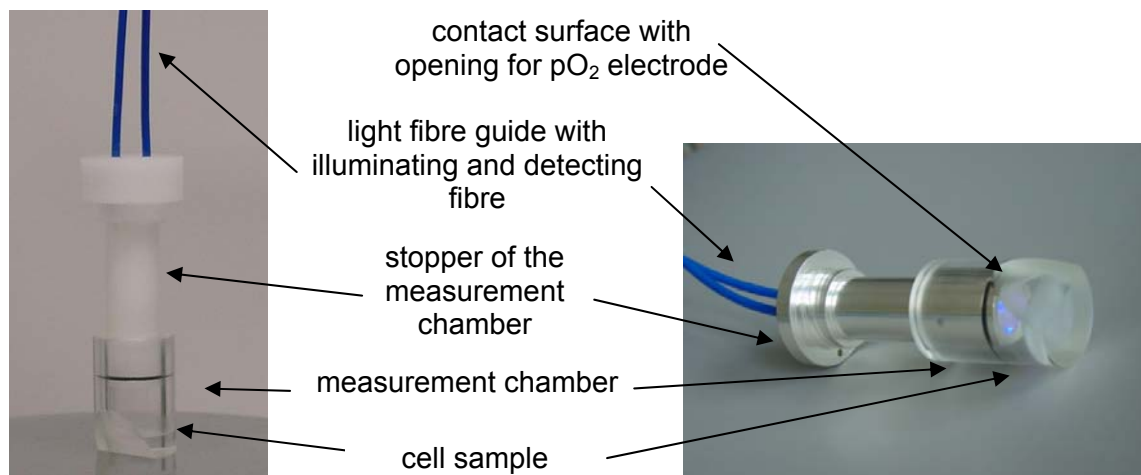


Figure 2.11: Light fiber probe for Oxygraph-2k (O2k) chamber

Light fiber probe (blue) integrated into stopper (white) of the measurement chamber

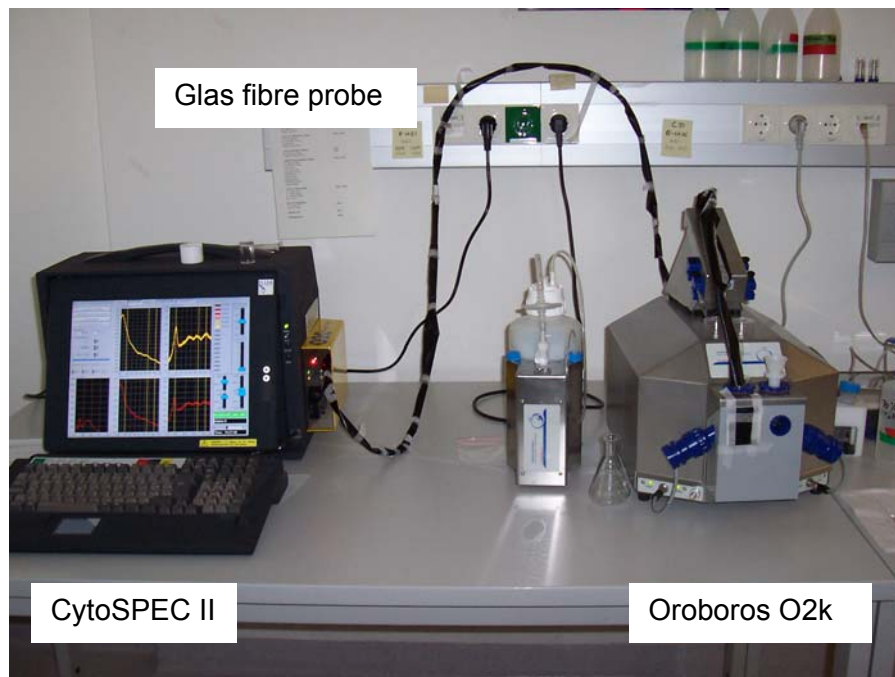


Figure 2.12 Setup of redox measurement in cell suspension

2.2.3.3.2 Experimental procedure

2.5 ml of cell suspension (2.5-5 million cells/ml) prepared as described above were filled into the measurement chamber of the O2k. After ten minutes of equilibration with room air, the chamber was sealed air-tight with the glass fiber integrated stopper and spectra were recorded continuously. O_2 concentrations decreased according to mitochondrial respiration. After reaching anoxia, the chamber was opened and the cell suspension reoxygenated. O_2 partial pressure was calibrated by a two-point calibration procedure with defined O_2 concentrations of room air (21% O_2 ~ pO_2 158 mmHg) and anoxia (0% O_2 , pO_2 0 mmHg) (see methods 2.2.4). Remission spectra recorded at specific O_2 concentrations were subtracted from recorded normoxic spectra (18% O_2 , pO_2 137 mmHg) to calculate hypoxic difference spectra.

2.2.4 High-resolution respirometry and O_2 kinetics

Mitochondrial respiration was determined at 37 °C by high-resolution respirometry using an Oxygraph-2k (Figure 2.13). Due to the high sensitivity of the pO_2 sensor (O_2 consumption <2 $\text{pmol} \cdot \text{s}^{-1} \cdot \text{cm}^{-3}$, signal-to-noise ± 0.02 mmHg [0.00 % O_2]) and high temporal resolution, this system allows analysis of the O_2 kinetics of cellular respiration. Cellular O_2 consumption (J_{O_2}) was calculated from the time derivative of O_2 concentration (2 s time-intervals) and corrected for the background of the instrumentation and the response time of the O_2 sensor (2-3.5 s). A

two-point calibration was performed for all experiments by equilibration with 21% O₂ adjusted to air pressure (pO₂ ~ 158 mmHg) and sodium dithionate (SDT) (zero O₂). The O₂ consumption compared to pO₂ exhibited biphasic kinetics. A typical recording is illustrated in Figure 2.14. The linear part at high O₂ concentrations can partially be attributed to decreased mitochondrial respiration, due to loss of function, and non-mitochondrial respiration, which illustrates that O₂ consumption measurement alone does not allow for a complete description of the reaction of the mitochondrial respiratory system to hypoxia [186]. Therefore, the O₂ affinity of the cells was studied in transition from aerobic to anoxic states. Below a pO₂ of 1.1% O₂ (pO₂ 8.3 mmHg) a hyperbolic fit of the O₂-dependent respiration allows determination of p50 of mitochondrial respiration [117, 186]. p50 is the O₂ concentration at which the cellular respiratory rate is half-maximal. This parameter was calculated plotting O₂ consumption at specific O₂ concentration (J_{O₂}) as a function of O₂ concentration (pO₂) and fitting the hyperbolic function $J_{O_2} = (J_{max} \cdot pO_2) / (p50 + pO_2)$ for the pO₂ range of 0 – 1.1% O₂ (pO₂ 8.3 mmHg), where J_{max} is the maximal O₂ consumption (Figure 2.15). All calculations were performed with Matlab software (OROBOROS, Innsbruck, Austria) as described [198-200]. All measurements in cell suspensions were performed in intact cells in medium 199. As determination of p50 is adjusted to the currently measured air pressure, O₂ concentrations for p50 value are given as pO₂ in mmHg and for comparison in % O₂ in brackets (assuming air pressure of 750 mmHg).



Figure 2.13 Oxygraph-2k (O2k) from Oroboros for high-resolution respirometry

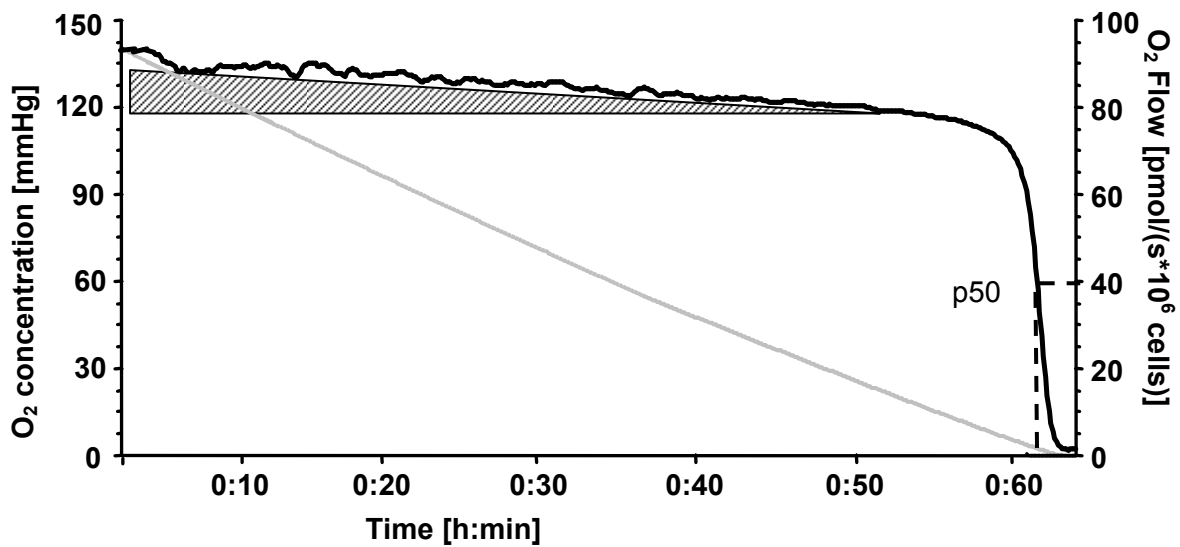


Figure 2.14 Mitochondrial and non-mitochondrial respiration

The O_2 consumption in pulmonary arterial smooth muscle cells (PASMC) (black line) was calculated by the first derivative of O_2 concentration (grey line). The decrease in O_2 consumption due to non-mitochondrial O_2 consumption and cell damage is depicted by the hatched area.

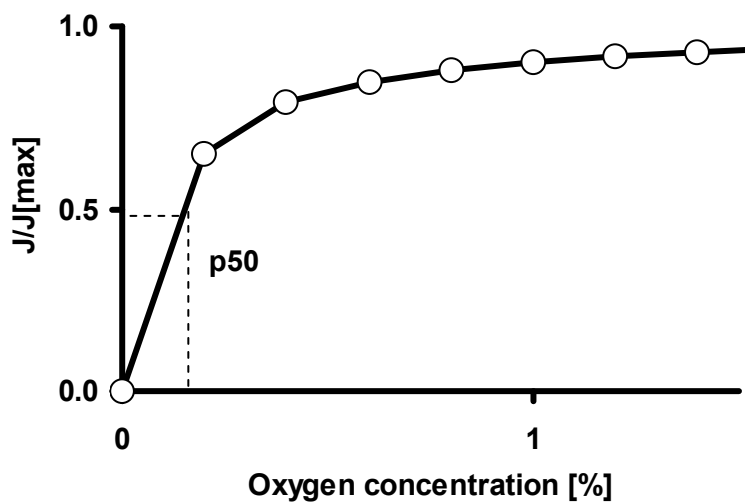


Figure 2.15 Determination of O_2 affinity (p50)

p50 was calculated plotting O_2 consumption (J_{O_2}) as a function of O_2 concentration and fitting the hyperbolic function $J_{O_2} = (J_{max} \cdot pO_2) / (p50 + pO_2)$ for the pO_2 range of 0 – 8.3 mmHg (1.1% O_2), where J_{max} is maximal O_2 consumption.

2.2.5 Mitochondrial membrane potential and mitochondrial matrix superoxide measurement

Mitochondrial membrane potential was measured in a flow-through system in isolated cells using JC-1 as a ratiometric indicator dye. Mitochondrial ROS production was measured with MitoSox.

For measurements with JC-1 cells plated on coverslips were incubated for 20 minutes at 37 °C in medium 199 containing 1 µg/ml JC-1. MitoSox measurements were performed after incubation with 5µM MitoSox for 20 min in PBS. For microscopic analysis coverslips were then placed in a 0.5 ml volume glass-covered perfusion chamber, perfused (2 ml/min) with HEPES-Ringer-Buffer (HRB: 5.6 mM KCl, 136.4 mM NaCl, 1.0 mM MgCl₂, 2.2 mM CaCl₂, 11.0 mM Glucose, 10 mM HEPES, pH 7.4) saturated with O₂ (21% O₂, pO₂ 158 mmHg) and maintained at 32.0 ± 0.2°C by heating both the HRB and the chamber. Hypoxia was induced by switching the perfusing medium from normoxic medium to medium of different levels of hypoxia (bubbled with N₂). For JC-1 measurements the excitation wavelength was set at 480 nm, and emitted light was collected with a CCD camera at 530 and 590 nm. Membrane hyperpolarization leads to a reversible change in fluorescence emission from green (530 nm) to red (590 nm) when JC-1 is excited at 480 nm [201]. MitoSox measurements were performed at 510 nm for excitation and 580 nm for emission [201, 202].

2.2.6 Statistics

Results are presented as means ± SEM. One-way ANOVA with Dunnett's *post hoc* test was performed for comparison of respiration at different O₂ concentrations with respiration at a pO₂ of 137 mmHg serving as control group. A one-way-ANOVA with the Student-Newman-Keuls *post hoc* test was performed for the comparison of redox states of different cytochromes, strength of HPV, mitochondrial membrane potential and ROS measurements. A Student's t-test was used for the comparison of two groups.

3 Results

3.1 Remission spectrophotometry in isolated lungs and cell suspensions

3.1.1 Evaluation of tissue cytochrome spectra

Mitochondrial cytochromes were identified in the isolated lung by addition of cyanide for complete reduction of all mitochondrial cytochromes (Figure 3.1) and by comparison with mitochondrial cytochrome reference spectra derived from literature (see appendix). The spectral alterations in the lung at 0% O₂ (pO₂ 0 mmHg) were only partially congruent to the mitochondrial spectra. For comparison of cytochromes that might contribute to the hypoxia-induced sum spectrum, the spectra of non-mitochondrial cytochromes are depicted in Figure 3.1. Cytochrome *b*₅₅₈ was reduced by SDT during anoxic ventilation (see 3.3.1), and cytochrome P450 by ventilation with carbon monoxide (see 3.3.2). Hemoglobin was identified by addition of blood (see 3.3.5). These cytochromes could partially contribute to the spectrum derived during ventilation with anoxic gas ("0% O₂").

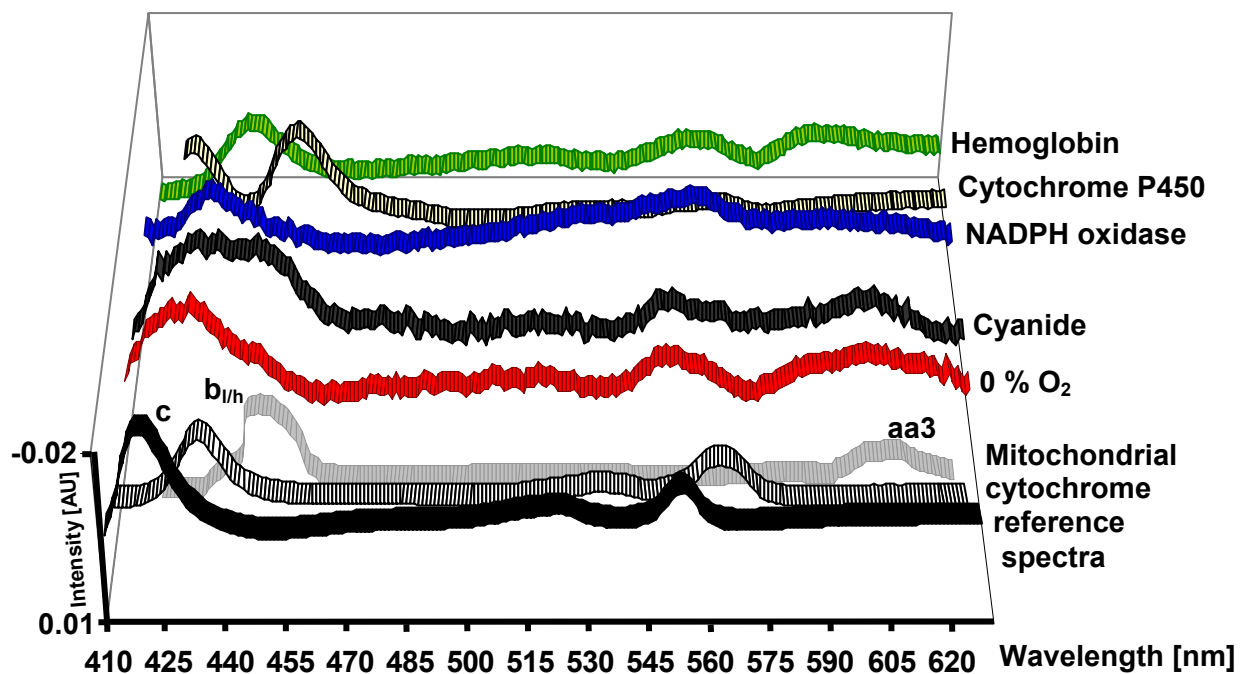


Figure 3.1 Cytochrome spectra in the isolated lung

Difference spectra of hemoglobin, cytochrome P450 and NADPH oxidase were acquired in isolated lungs as described above. Data are from $n=3$ different lung preparations for each cytochrome. Mitochondrial cytochrome reference spectra are derived from literature (see appendix). Spectral alterations during ventilation with 0% O₂, as well as after application of cyanide for demonstration of mitochondrial cytochromes are given for comparison ($n=5$ lung preparations).

3.1.2 Evaluation of scattering, reflection and water content in tissue

In tissue remission spectrophotometry the spectrum is not only altered by absorption of light, but also by wavelength dependent scattering and reflection (see Figure 2.5). Scattering phenomenon was illustrated in milk as a scattering medium, where light is backscattered by lipid droplets. Light of the same intensity at every wavelength was irradiated into milk and the backscattered light exhibited a spectrum shown in Figure 3.2. The backscattering phenomenon resulted in higher intensities of detected light at high wavelengths.

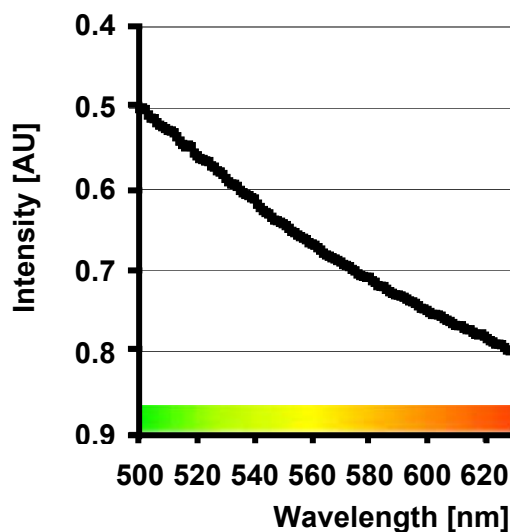


Figure 3.2 Spectrum of white light backscattered by milk

Intensity of light at low wavelengths was lower compared to that at high wavelengths, indicating that light at lower wavelengths is less backscattered. Spectrum is shown from one representative measurement.

In tissue the light is additionally influenced by reflection at boundary layers, e.g. when crossing compartments of high and low water content, and by alterations in density of tissue due to ventilatory excursion or edema development. To evaluate the influence of tissue water content, it was increased by increasing pulmonary venous pressure or decreased by non-hypoxia-induced vasoconstriction with the thromboxane mimetic U-46619 (Figure 3.3). The resulting spectra are given in Figure 3.3. and resembled lung remission spectra as detected by measurement of light backscattered from lung tissue during normoxic ventilation.

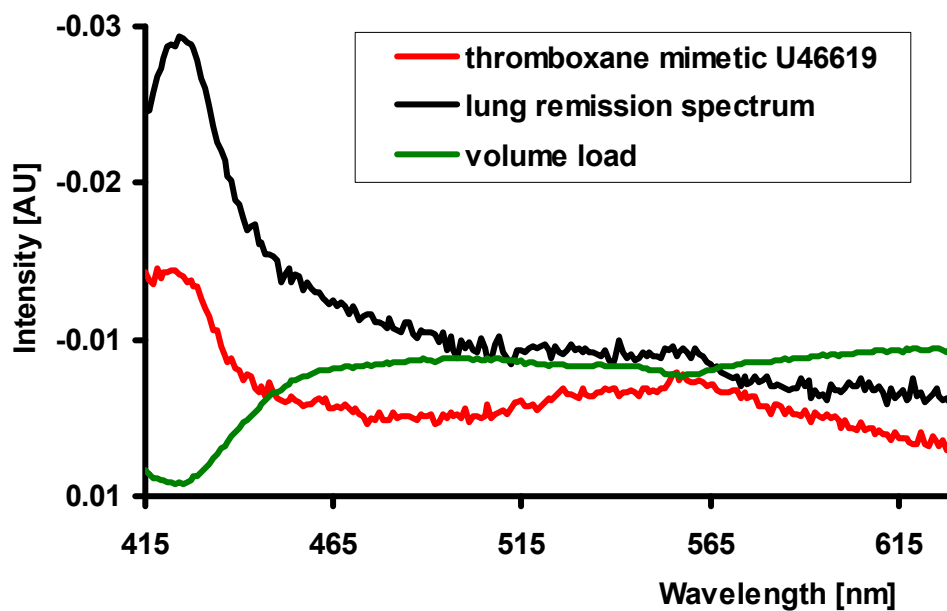


Figure 3.3 Influence of tissue water content on difference spectra

Decreased absorption (volume load, $n=3$ lung preparations) or increased absorption (vasoconstriction by thromboxane mimetic U46619, $n=5$ lung preparations) was the result of lower or higher density, respectively, of absorption particles (=tissue) in the measurement volume and/or result of increased reflection.

3.1.3 Evaluation of cellular cytochrome spectra

As basis for the identification of measured difference spectra in isolated cells previously reported mitochondrial cytochrome difference spectra were used (Figure 3.4 and appendix). Additionally, reference absorption spectra for single cytochromes were determined in the closed chamber system. As a reference spectrum of cytochrome *c*, difference spectra were acquired from purified bovine cytochrome *c*. The reference spectrum for cytochrome $b_{1/h}$ of complex III was measured by reducing cytochrome $b_{1/h}$ in isolated PASMCM with antimycin A. This provides difference spectra for cytochrome b_h (b562) and b_l (b566). Subsequently, cytochrome *aa3* difference spectra were calculated from maximally-reduced PASMCM spectra minus cytochrome $b_{1/h}$ and cytochrome *c*. Cytochromes *a* and *a3* could not be distinguished, as determined by differential reduction of cytochrome *a* with cyanide. Cytochrome c_1 and b_{560} of complex II was also not visible. Results of measured reference spectra are provided in Figure 3.4 and the appendix.

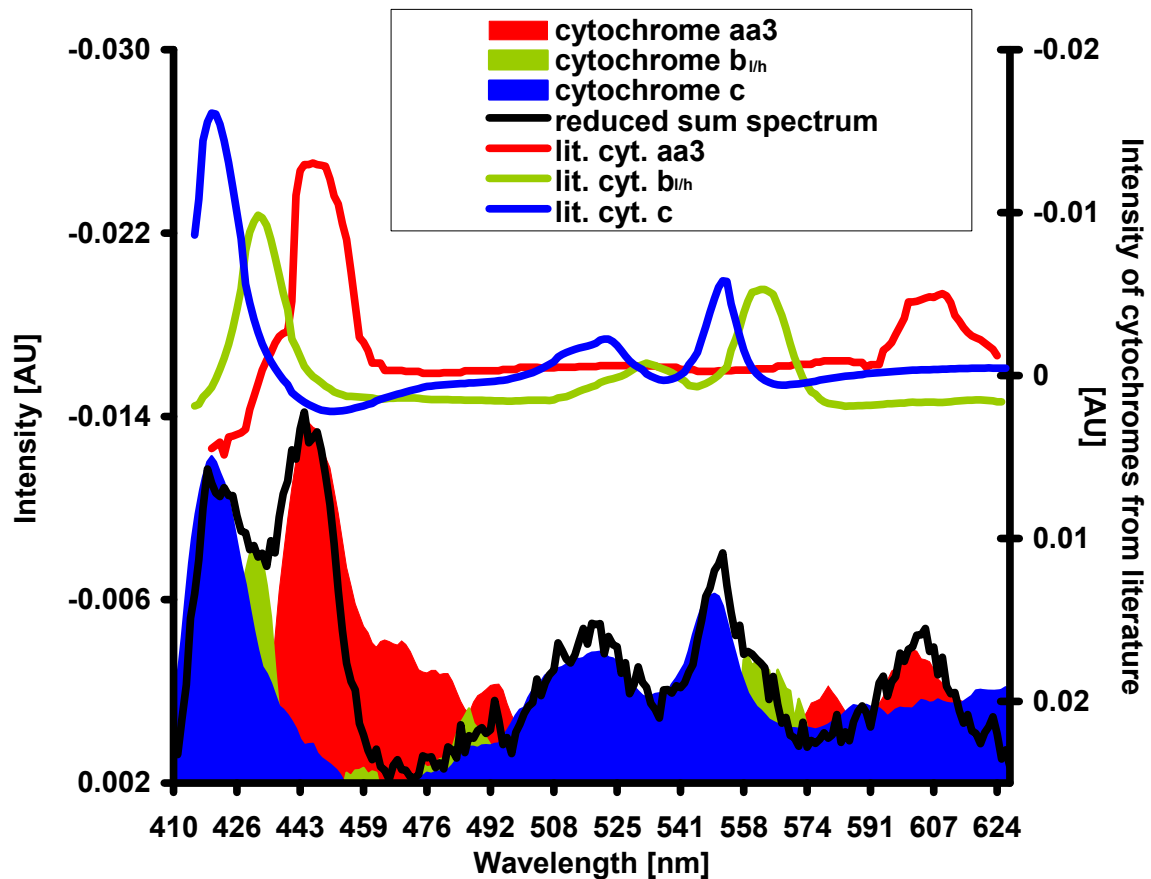


Figure 3.4 Reference spectra and anoxic difference spectrum

Reference spectra for cytochrome *aa3*, *b_{LH}* and *c* were derived as described above and are depicted as red, green and blue areas, respectively. For comparison a measured reduced sum spectrum (black line), acquired by calculation of the difference spectrum of anoxic minus normoxic spectra of PASM (= anoxic difference spectrum) is displayed. Data are from $n=3$ experiments. Reference spectra taken from literature are shown as red, green and blue lines (lit. cyt. *aa3*, *b_{LH}*, *c*).

The comparison of the measured anoxic difference spectrum with the reference spectra of the single cytochromes suggests that mainly mitochondrial cytochromes contribute to the measured anoxic difference spectrum. To support this hypothesis the spectrum was compared to spectral alterations after application of cyanide which specifically reduces mitochondrial cytochromes. The cyanide reduced spectrum was almost identical with the anoxia derived spectrum (Figure 3.5).

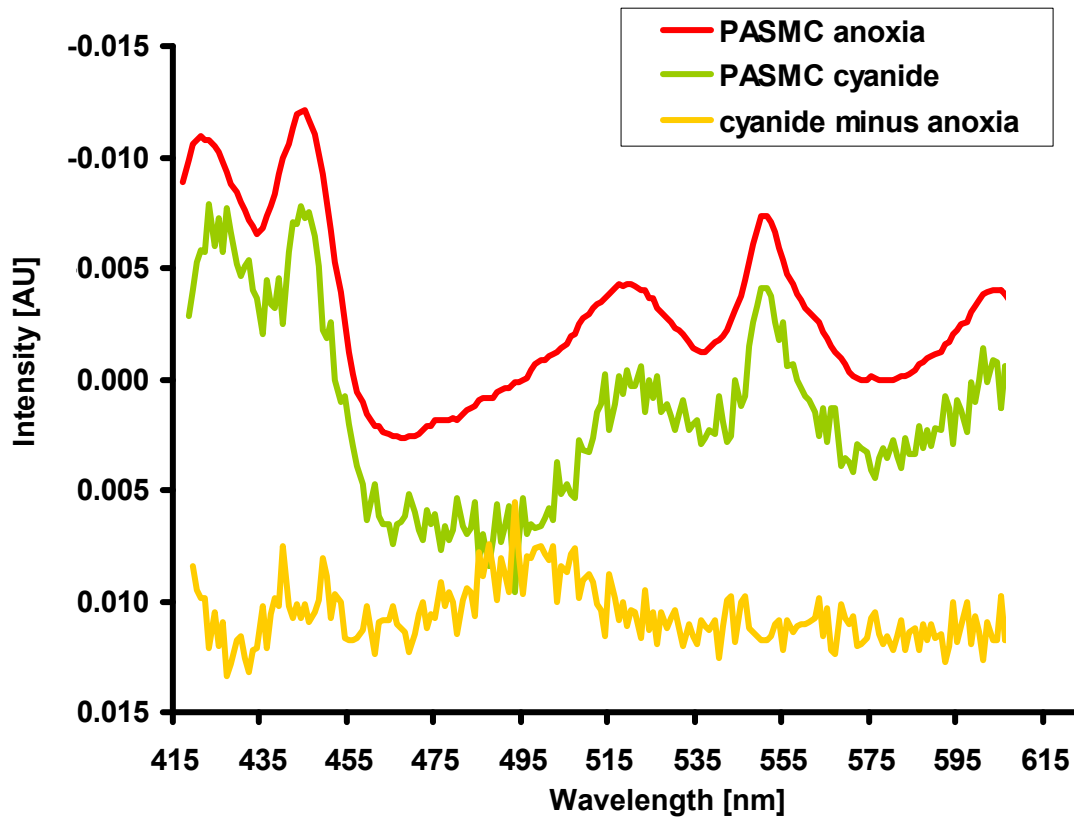


Figure 3.5 Mitochondrial reduction by anoxia and cyanide

Comparison of a fully reduced PASM C spectrum (PASM C anoxia, $n=9$ experiments) with a cyanide-inhibited PASM C spectrum (PASM C cyanide, $n=4$ experiments). The difference spectrum of anoxia minus cyanide spectrum illustrates congruence of both spectra.

3.1.4 Evaluation of scattering interference in cell suspensions

In cell suspension scattering properties are dependent on mitochondrial and cellular shape, as well as on their size. To simulate scattering changes cells were permeabilized by digitonin (Figure 3.6) and typical scattering alterations could be detected (please compare to Figure 3.2). In contrast, dilution of cell suspension by addition of medium resulted in higher intensities of the spectral light due to less absorption in the measurement volume (Figure 3.6), similar to the pattern provoked by increased tissue water content (Figure 3.3).

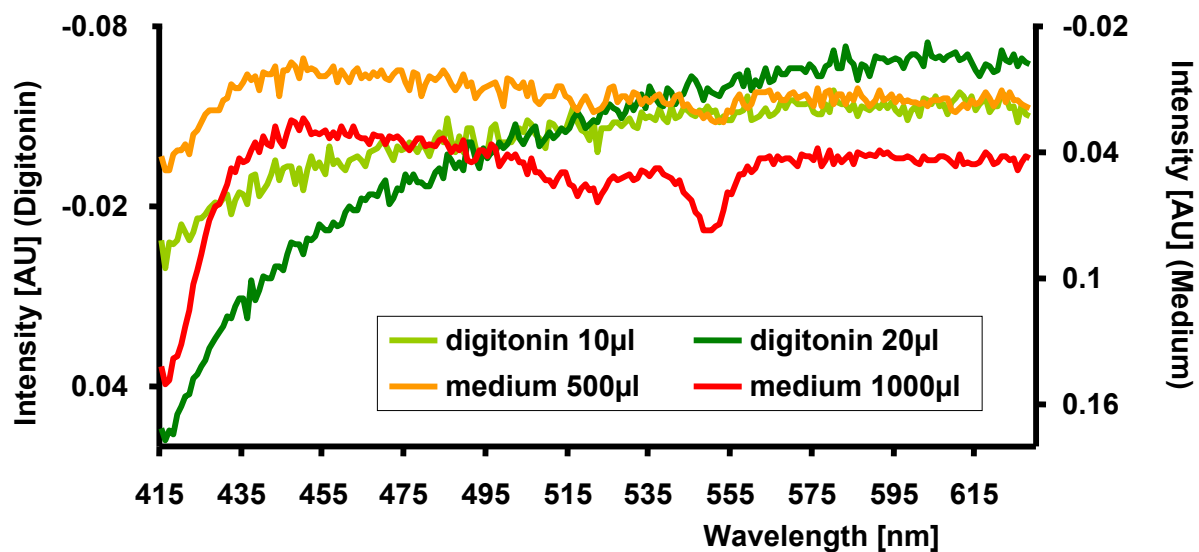


Figure 3.6 Spectral changes induced by addition of digitonin or medium

Increasing concentrations of digitonin resulted in decreased scattering due to destruction of cells and mitochondria. The typical wavelength dependent change in intensity can be seen. Dilution of the cell suspension with medium resulted in increased intensities (=decreased absorption), as the concentration of absorbing particles in the measurement volume decreased. Data are from $n=3$ experiments.

Scattering in cell suspension can influence the quantitative evaluation of absorption changes, as it leads to the effect that the relationship between intensity of backscattered light and absorption is not linear. The concentration of an absorbing protein (cytochrome c) was compared with the intensity of the backscattered light. A linear correlation between the concentration of cytochrome c and the backscattered light intensity at 550 nm and 415 nm was found (Figure 3.7). Therefore, if scattering is constant, changes of light intensity of backscattered light correlate linearly to absorption changes.

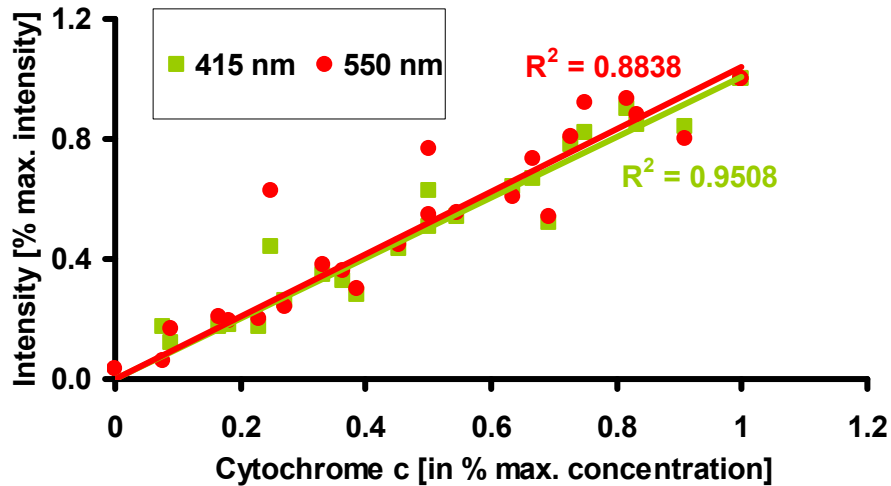


Figure 3.7 Cytochrome c concentration in comparison to light attenuation

Light attenuation at 415 nm and 550 nm (see spectrum cytochrome c in appendix) and linear correlation between measured light intensity and cytochrome c concentration is depicted. Measurements are performed with HL60 cells (6-7 Mio cells/ml, Cytochrome c concentration was 0.2-13.0 μ l, $n=25$ of 4 separate experiments).

However, scattering changes cannot be excluded to occur during hypoxia. As scattering alterations would have non linear impact on measured intensities depending on wavelength (see Figure 3.2), the scattering alterations should be reflected by different results, when analyzing the redox state at low or high wavelength ranges. This was excluded by measurements in the low O_2 range, showing similar redox alterations, when analyzed in the low and high wavelength range (Figure 3.8).

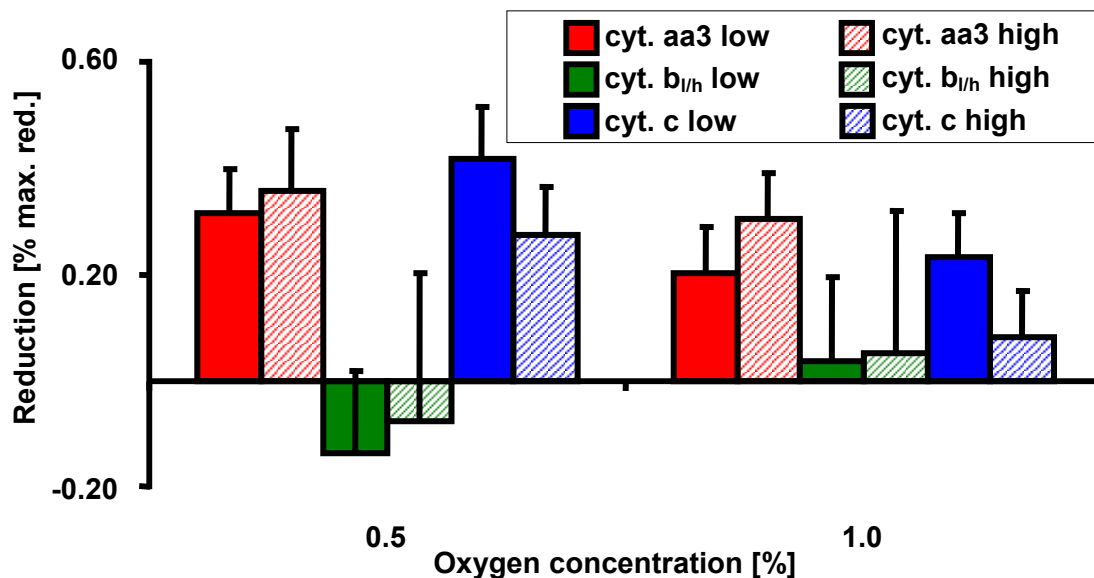


Figure 3.8 Analysis of redox state at different wavelength ranges

Least square fitting, as described below, was performed in the low (415-460 nm, full bars) and high (500 -620 nm, hatched bars) wavelength range and calculated reduction levels of the different wavelength ranges were compared to each other (depicted as relative reduction referred to maximal reduction measured at anoxia). No significant differences between the wavelength ranges for cytochrome aa3 (red), b_{1/h} (green) or c (blue) could be detected ($n=6$).

3.1.5 Semiquantitative analysis of cytochrome redox state based on difference spectra

Difference spectra were calculated by subtraction of normoxic spectra from hypoxic spectra (normoxia: in the isolated lung 21% O₂ [pO₂ 158 mmHg], in cell suspensions 18 % O₂ [pO₂ 135 mmHg] reached after equilibration), as described above.

Difference spectra were used to calculate changes in cytochrome redox states. Reference spectra of single cytochromes were fit in the measured sum difference spectrum by multi-wavelength least-square fitting (TechPlot, Sftek, Braunschweig, Germany). As shown in Figure 3.9, the measured sum difference spectrum (= measured reduced spectrum, open circles) was almost identical with the sum difference spectrum that was recalculated on the basis of the single reference spectra (= fitted spectrum, black line).

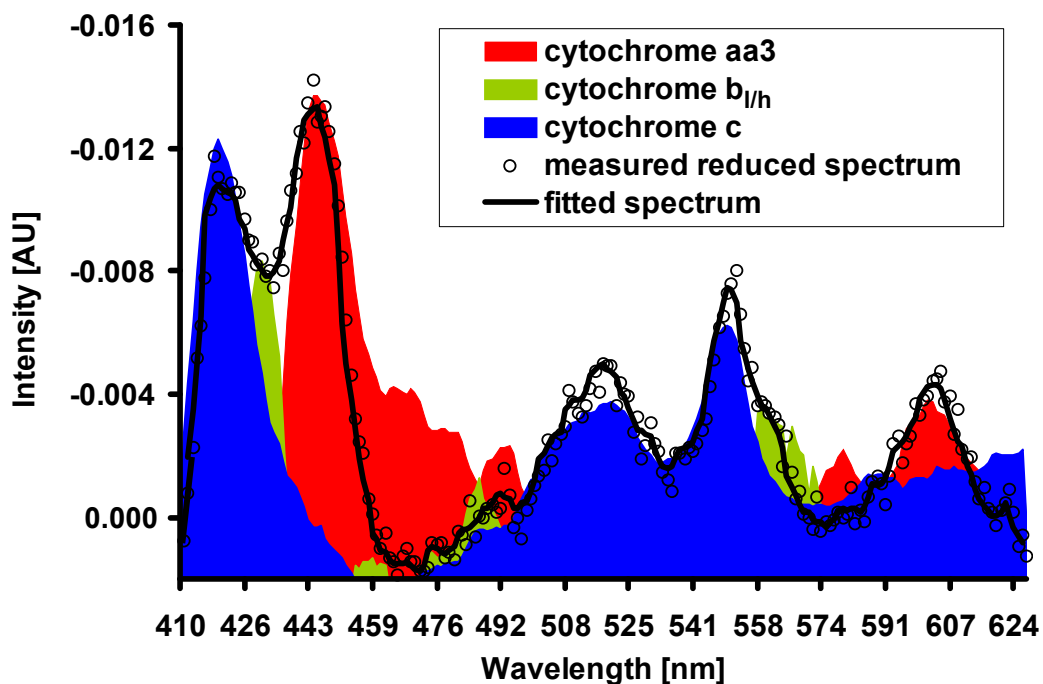


Figure 3.9 Fitting of mitochondrial spectra

Fitting of single mitochondrial spectra into anoxic difference spectra of isolated pulmonary arterial smooth muscle cells (PASMC). Data are from $n=3$ experiments.

3.2 Mitochondria as oxygen sensors

3.2.1 Mitochondrial complex IV in oxygen sensing of HPV

3.2.1.1 Hypoxia-induced inhibition of the mitochondrial electron transport system and HPV in the isolated lung

Isolated blood-free perfused lungs were ventilated with different O₂ concentrations, resulting in alveolar O₂ concentrations (PAO₂) of 0-15% O₂ (pO₂ 0-113 mmHg) for 10 minute periods, alternating with 15 minute periods of normoxic ventilation (21% O₂, pO₂ 158 mmHg). The different O₂ concentrations were applied in each lung preparation in random order. Increases in pulmonary arterial pressure (Δ PAP) during hypoxic ventilation were detected at a PAO₂ of \leq 10% O₂ (pO₂ \leq 75 mmHg) (Figure 3.10).

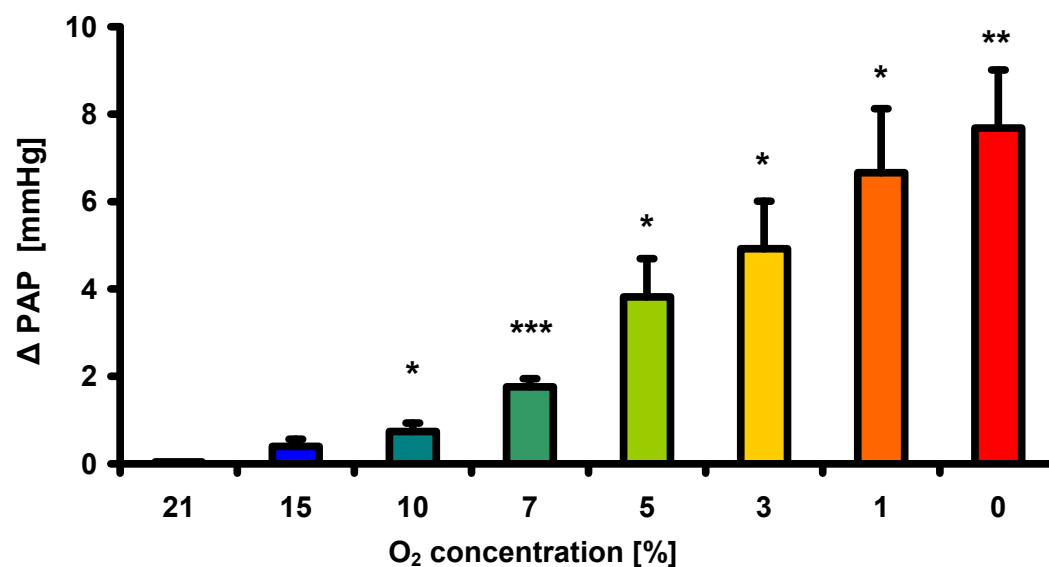


Figure 3.10 O₂ dependency of HPV

The strength of HPV is given as the maximum increase in pulmonary arterial pressure (Δ PAP) during 10 minute periods of hypoxic ventilation for the depicted O₂ concentrations. Data are from $n=5$ lung preparations. * indicates significant differences compared to normoxic ventilation (21% O₂, pO₂ 158 mmHg). * $p < 0.05$, ** $p < 0.005$, *** $p < 0.001$.

Parallel determination of difference spectra by remission spectrophotometry showed first detectable changes at a PAO₂ of 10% O₂ (pO₂ 75 mmHg). Further spectral alterations were observable at a PAO₂ of \leq 5 % O₂ (pO₂ \leq 38 mmHg) in the range of 520-590 nm and at a PAO₂ of 0 % O₂ (pO₂ 0 mmHg) in the ranges of 410-460 nm and 500-630 nm (Figure 3.11). As reference, a difference spectrum after total reduction of mitochondrial cytochromes with cyanide, as well as reference spectra for cytochrome *c* (420/550 nm), *b_{lh}* (430/563 nm), and *aa3* (445/603/605 nm) are provided.

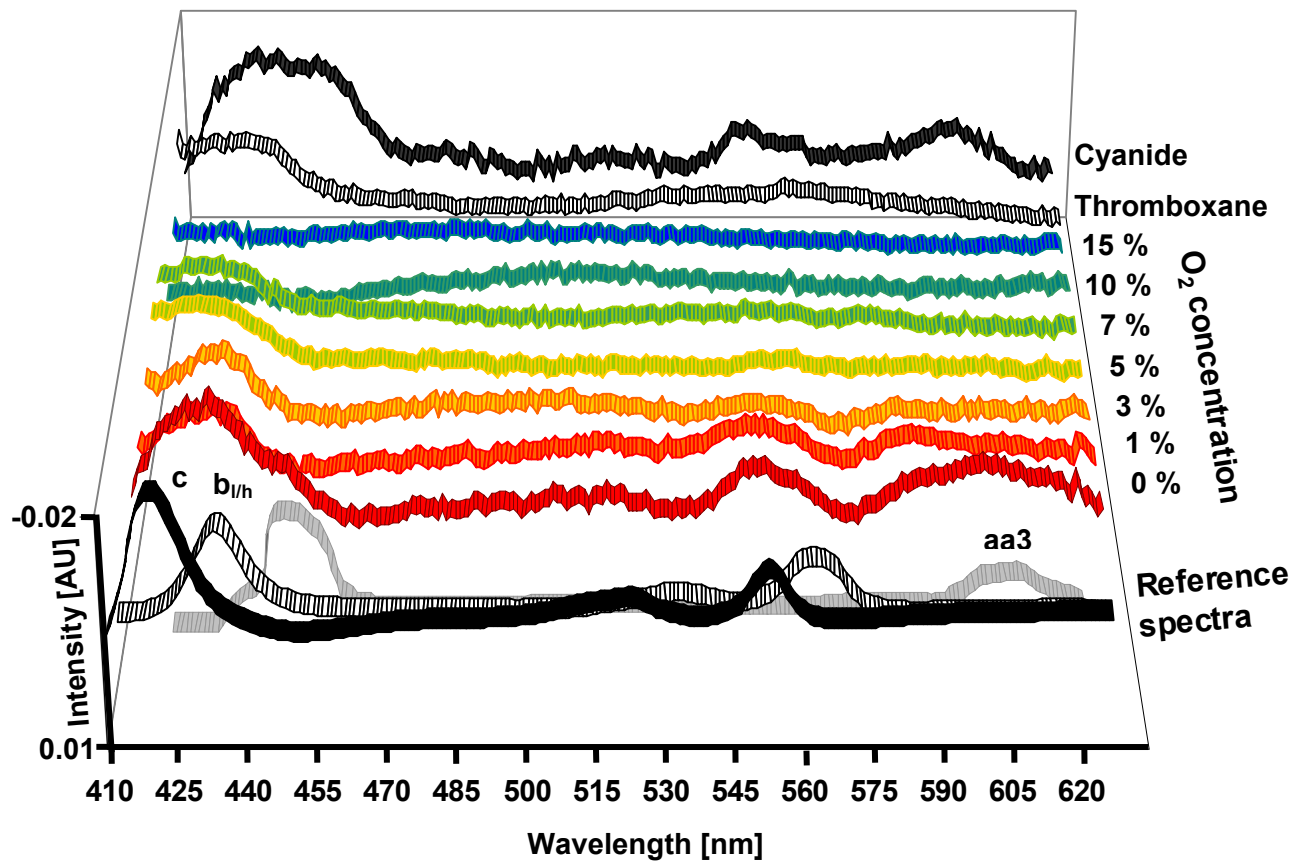


Figure 3.11 Hypoxia-dependent alterations of remission spectra

Difference spectra were assessed by subtraction of normoxic from hypoxic spectra for repetitive hypoxic ventilation maneuvers corresponding to Figure 3.10. Spectra in the presence of cyanide (80 μM) and bolus of thromboxane mimetic U46619 (0.5 nM) were recorded at the end of each experiment. Reference spectra for single cytochromes are depicted for comparison. Data are from $n=5$ lungs.

When comparing the reference mitochondrial and non-mitochondrial spectra (Figure 3.1 and 3.11) to the hypoxia-induced spectral alterations, only the spectral alterations in the wavelength range of 600 - 610 nm could be clearly assigned to reduction of cytochrome aa3 correlating to an inhibition of complex IV. The other hypoxia-induced spectral alterations showed overlapping features of mitochondrial cytochromes, non-mitochondrial cytochromes and spectral alterations caused by scattering changes in consequence of vasoconstriction (see thromboxane spectrum Figure 3.3 and Figure 3.1). The reduction of mitochondrial cytochrome aa3, peaking at 445 nm and 603/605 nm could only be detected at a PAO_2 of 0% O_2 (pO_2 0 mmHg), so that at higher O_2 ranges, mitochondrial respiration seemed to be largely unrestricted.

3.2.1.2 Hypoxia-induced inhibition of the mitochondrial electron transport system and HPV in isolated PASMC

3.2.1.2.1 Redox changes in isolated PASMC

As remission spectroscopy in intact lungs is limited by the fact that the sum spectra of all pulmonary cells is detected, but PASMC are thought to be the sensor cells of at least acute HPV (lasting seconds to minutes), cytochrome redox alterations in isolated PASMC were measured by combination of respirometry and spectrophotometry and compared with the strength of HPV. Difference spectra from PASMC under different O_2 concentrations showed similar alterations as observed in isolated lungs at anoxic ventilation (Figure 3.12).

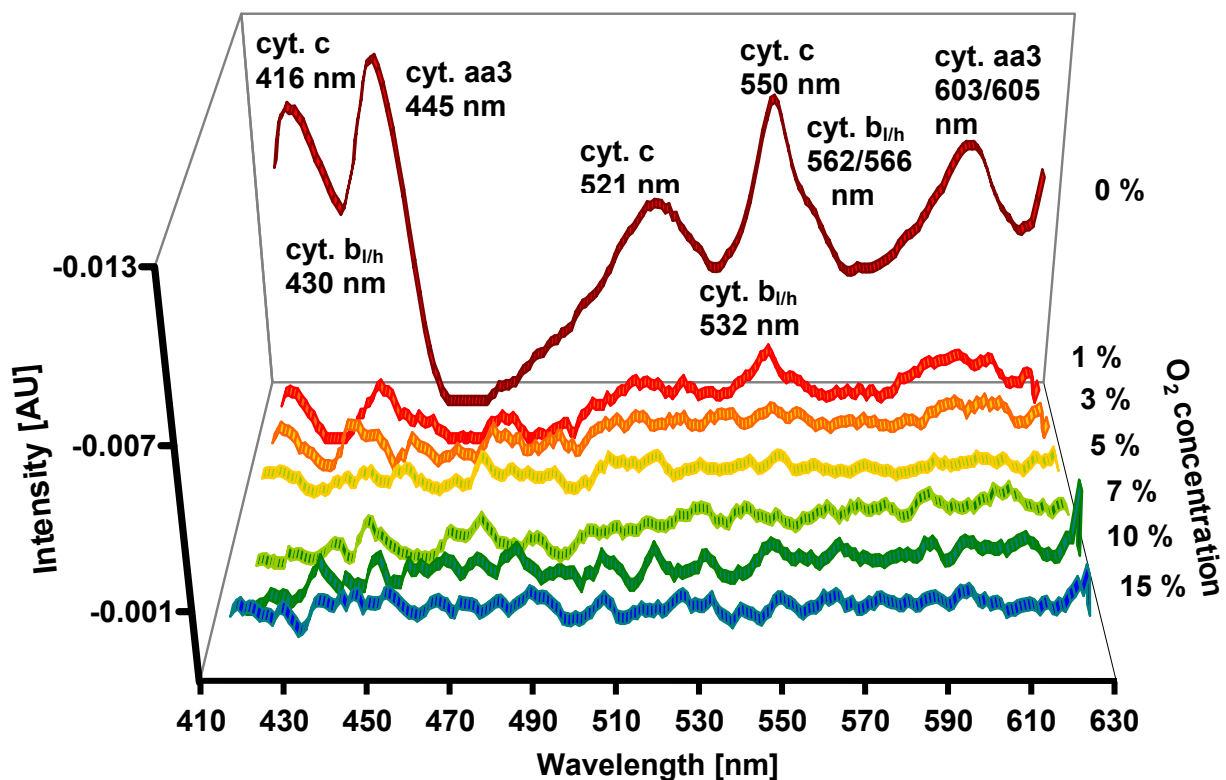


Figure 3.12 O_2 -dependent alterations of remission difference spectra in PASMC

Hypoxic difference spectra of pulmonary arterial smooth muscle cells (PASMC) were assessed by subtraction of normoxic from hypoxic spectral values. Negative intensity represent absorption peaks at specific wavelengths for single cytochromes (cytochrome *c* [420/550 nm], *b_{1/h}* [430/563 nm], and *aa3* [445/603/605 nm]). Fitting of single cytochromes to quantify absorption is shown in Figure 3.13. Data are from $n=9$ experiments (from $n=6$ independent cell preparations).

At 0 % O₂ (pO₂ 0 mmHg) clear alterations of mitochondrial cytochromes, congruent with alterations induced by cyanide (see Figure 3.5) could be detected. At higher O₂ concentrations far smaller redox changes, exceeding the level of signal-to-noise ratio at about 5 % O₂ (pO₂ 38 mmHg) could be seen. Compared to spectral alterations in the isolated lung, no changes in the wavelength range of 410-440 nm could be detected at mild hypoxia. Fitting of mitochondrial cytochromes into measured remission difference spectra was performed for each O₂ concentration. While a reduction of cytochrome *b*_{1/h} was only detectable at O₂ concentrations of ≤ 1% O₂ (pO₂ ≤ 8 mmHg), cytochrome *c* was already reduced at 5% O₂ (pO₂ 38 mmHg) in PASMC. For cytochrome *aa*₃, reduction was observed at ≤ 3% O₂ (pO₂ ≤ 23 mmHg) (Figure 3.13). The O₂ dependency of redox alterations paralleled respiration determined by high-resolution respirometry (Figure 3.13).

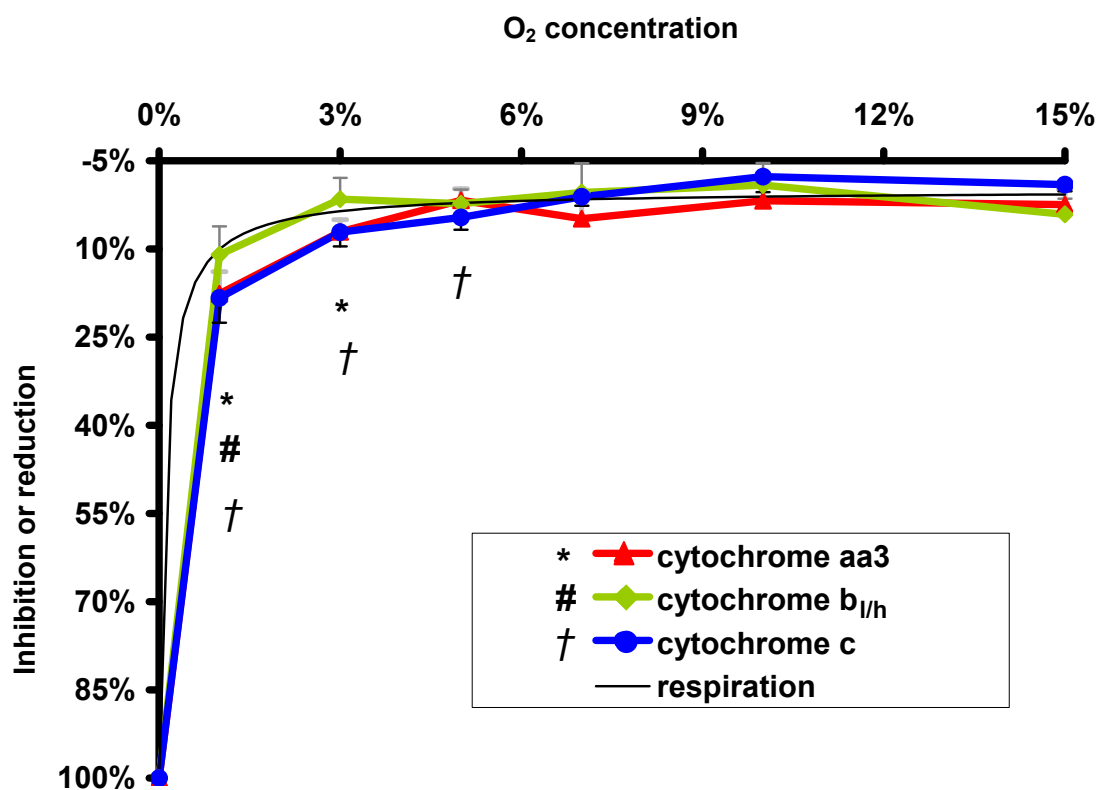


Figure 3.13 O₂ dependency of cytochrome redox alterations in PASMC

Reduction of cytochromes *aa*₃, *b*_{1/h}, *c* in pulmonary arterial smooth muscle cells (PASMC) between 15-0% O₂ (pO₂ 113-0 mmHg). For comparison, the reduction in respiration from Figure 3.14 is depicted. Data are from *n*=16 experiments from *n*=8 independent cell preparations. *, #, † indicate significant differences of cytochrome *aa*₃, *b*_{1/h}, and *c* compared to normoxia (*p*<0.05).

Taking into account the higher sensitivity of redox measurements in isolated PASMC due to lower interference by scattering and cytochromes of other cell types, the results are comparable to alterations of mitochondrial cytochromes in isolated lungs. Substantial

inhibition of mitochondrial respiratory chain could be detected in both experimental setups at 0% O₂ (pO₂ 0 mmHg). However, in PASMC small reduction of cytochromes was also detected at O₂ concentrations of 5 and 3% O₂ (pO₂ 38 mmHg and 23 mmHg) resembling hyperbolic inhibition kinetics similar to respiration. Redox changes at higher O₂ concentrations are beyond sensitivity of the method and obscured by signal-to-noise ratio.

3.2.1.2.2 Respiration in isolated PASMC

Another very sensitive measure for the activity of the mitochondrial respiratory chain is the determination of respiration. High resolution respirometry allows measurement of respiration at very low O₂ concentrations and thus determination of O₂ concentration at half-maximal respiration (please see 2.2.4).

O₂ concentration at half-maximal respiration (p50) for PASMC was calculated to be a pO₂ of 0.8 ± 0.0 mmHg (0.1 % O₂). From these values respiration at any O₂ concentration can be calculated and compared to maximal respiration at normoxia (21% O₂, 158 mmHg). Hence the first significant inhibition of respiration was found at pO₂ levels of ≤ 105 mmHg ($\leq 14\%$ O₂) in PASMC (Figure 3.14). Thus inhibition of respiration occurs in an O₂ range, when HPV occurs.

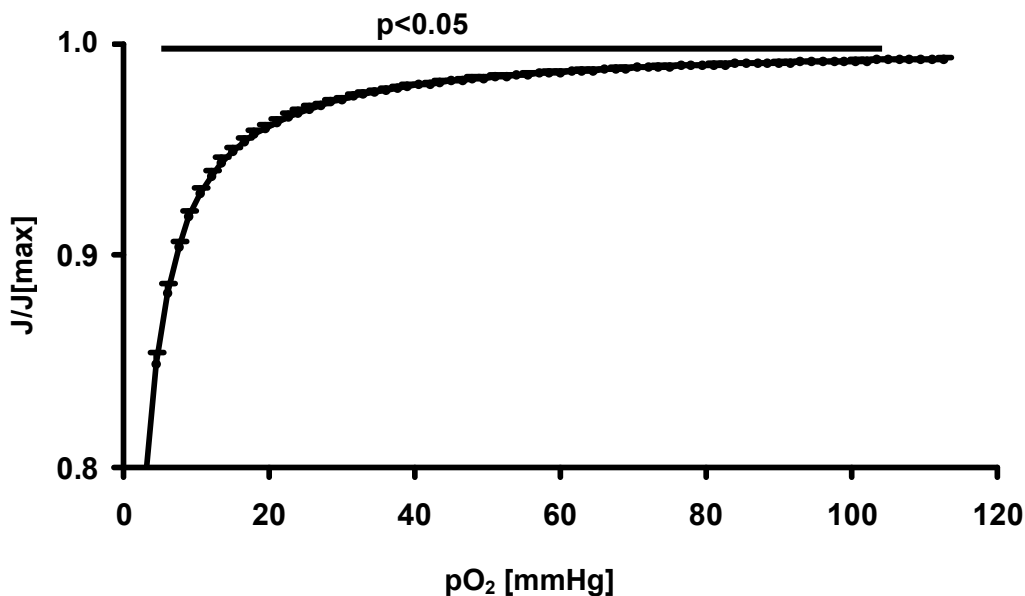


Figure 3.14 O₂ dependency of respiration in PASMC

Mean and SEM of original recording from pulmonary arterial smooth muscle cells (PASMC) ($n=9$). Respiration at different O₂ concentrations, calculated from p50. Bar indicates significant decrease in respiration compared to 21% O₂ (158 mmHg).

3.2.2 Mitochondrial complex III in oxygen sensing of HPV

In the next step measurements focused on the regulation of cytochrome $b_{l/h}$ compared to cytochrome $aa3$ and c during hypoxia. After analysis of hypoxia-induced redox alterations, it became evident, that cytochrome $b_{l/h}$ was reduced only at O_2 concentrations $\leq 1\%$ O_2 ($pO_2 \leq 8$ mmHg), whereas cytochrome $aa3$ and c became already significantly reduced at concentrations $\leq 3\%$ O_2 ($pO_2 \leq 23$ mmHg) and 5% O_2 ($pO_2 38$ mmHg), respectively (Figure 3.13). When comparing the redox state of cytochrome $b_{l/h}$ directly with cytochrome $aa3$ and c , a higher oxidation state of cytochrome $b_{l/h}$ compared to cytochrome $aa3$ and c could be found at 1 and 3% O_2 ($pO_2 8$ and 23 mmHg) (Figure 3.15).

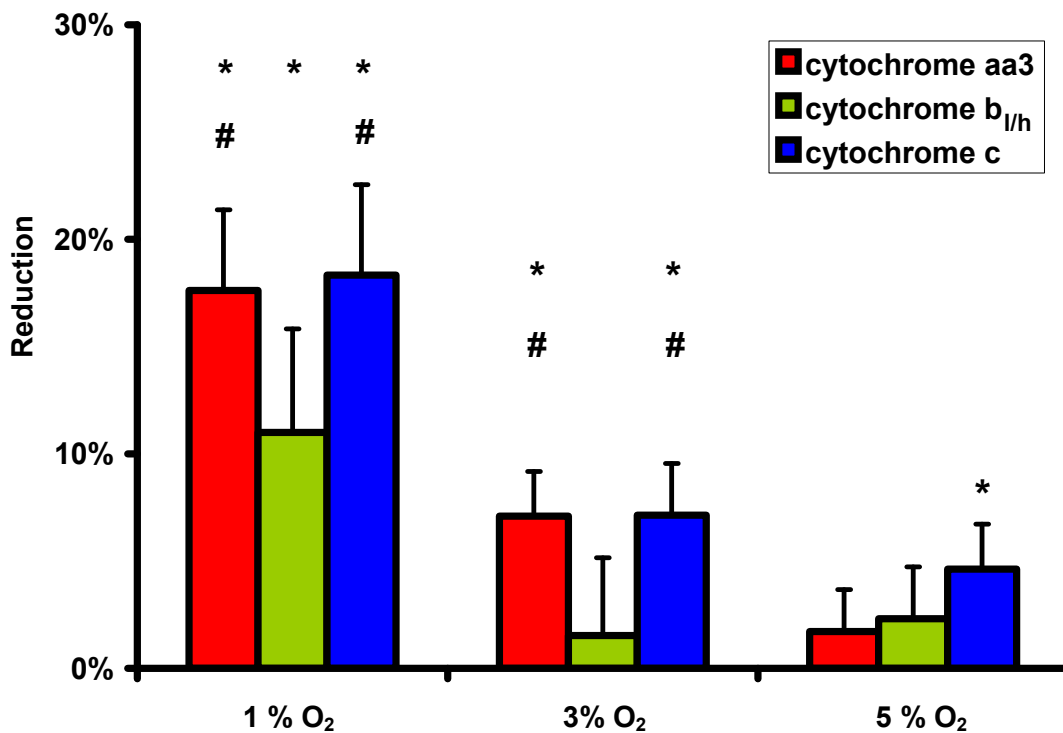


Figure 3.15 Differential regulation of mitochondrial cytochromes in PASMC

Comparison of redox alterations of cytochrome $aa3$, $b_{l/h}$, c in pulmonary arterial smooth muscle cells (PASMC). Data are from $n=16$ individual experiments from at least $n=8$ independent preparations. * indicate significant differences of cytochrome $aa3$, $b_{l/h}$, or c compared to normoxia ($p<0.05$). # indicate significant differences of cytochrome $aa3$ and c , compared to cytochrome $b_{l/h}$ ($p<0.05$).

The higher oxidation state of cytochrome $b_{L/h}$ could indicate an electron leak at complex III. Thus mitochondrial ROS production was measured. These experiments revealed an O_2 -dependent ROS production, correlating with redox state of cytochrome $b_{L/h}$.

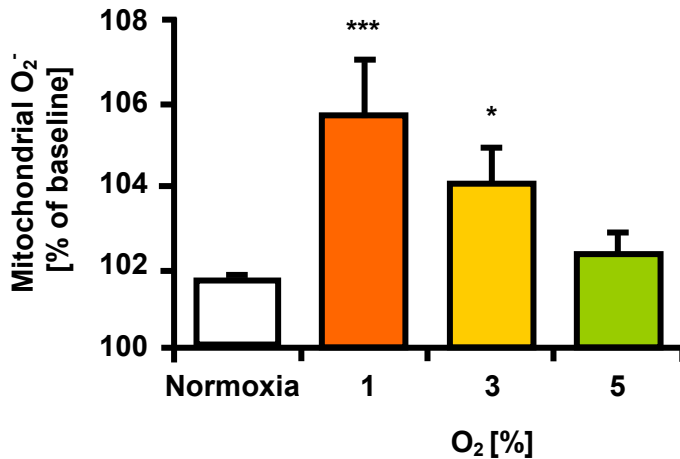


Figure 3.16 Hypoxia-dependent alterations of mitochondrial superoxide concentration in PASMC

Data are from $n=3$ individual experiments.

As mitochondrial membrane hyperpolarization is known to favor ROS production, mitochondrial membrane potential was determined. These experiments revealed an O_2 -dependent increase of mitochondrial membrane potential, correlating with cytochrome redox states.

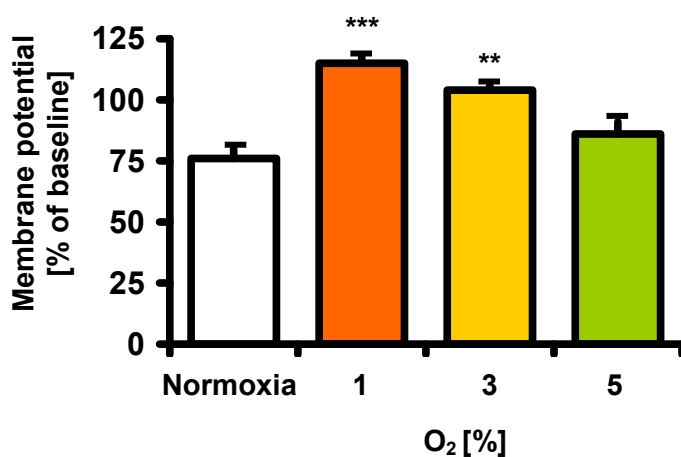


Figure 3.17 Hypoxia-dependent changes of mitochondrial membrane potential in PASMC

Data are from $n=3$ individual experiments.

3.2.3 Comparison of PASMC to arterial smooth muscle cells of the systemic vasculature

When comparing the hypoxia-induced reduction of mitochondrial cytochromes in PASMC with that of ASMC and RASMC, the reduction level of PASMC, ASMC and RASMC did not differ significantly (Figure 3.18).

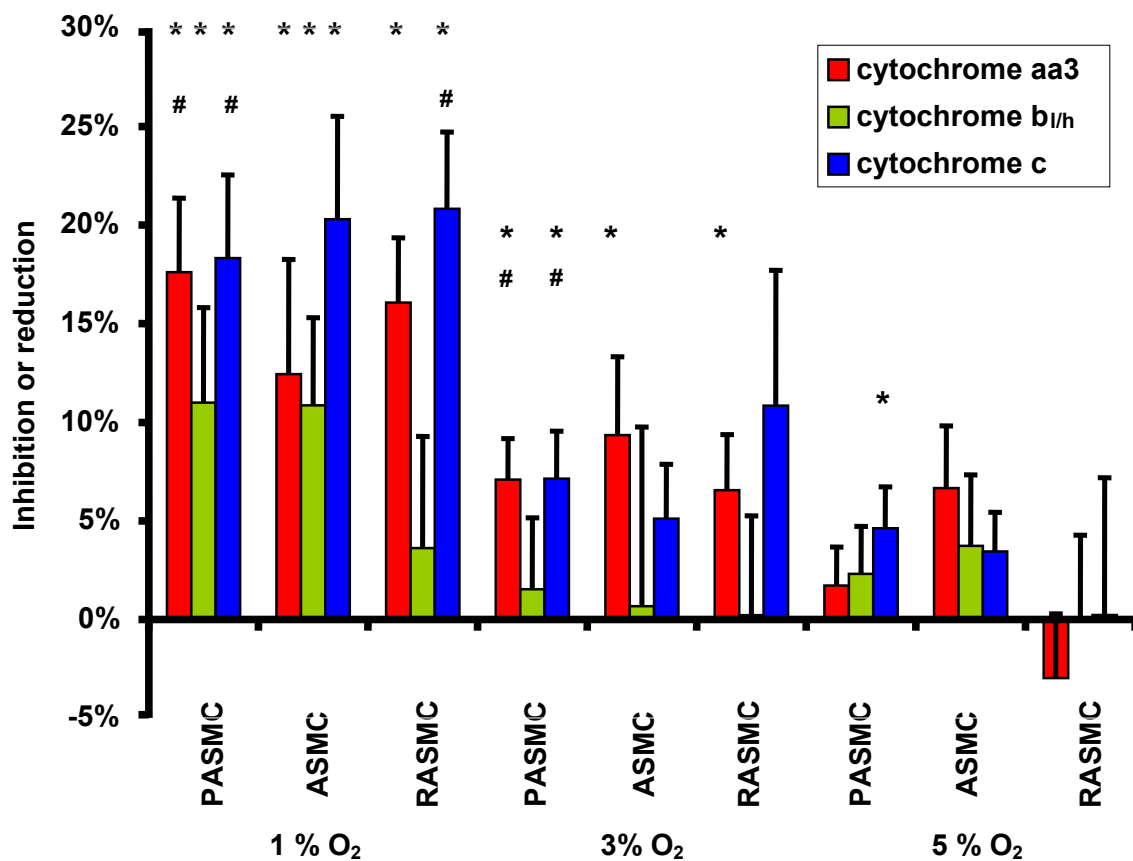


Figure 3.18 Comparison of redox alterations of cytochrome *aa3*, *b_{1/h}*, *c* in PASMC, ASMC and RASMC

Data are from at least $n=7$ individual experiments from at least $n=4$ independent preparations. * indicate significant differences of cytochrome *aa3*, *b_{1/h}*, or *c* compared to normoxia ($p<0.05$). # indicate significant differences of cytochrome *aa3* and *c*, compared to cytochrome *b_{1/h}* ($p<0.05$).

However, hypoxia inhibited respiration less in RASMC compared to PASMC and ASMC, represented by higher pO_2 at half maximal respiration (p_{50}) depicted in Figure 3.19. Half-maximal respiration (p_{50}) for PASMC was calculated to be a pO_2 of 0.8 ± 0.0 mmHg ($0.1 \pm 0.0\%$ O_2), 0.8 ± 0.1 mmHg ($0.1 \pm 0.0\%$ O_2) for ASMC, and 0.6 ± 0.0 mmHg ($0.1 \pm 0.0\%$ O_2) for RASMC (Figure 3.19).

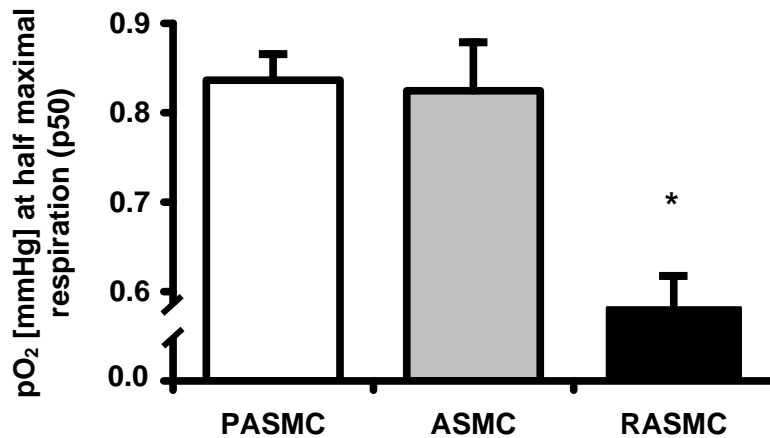


Figure 3.19 O_2 affinity of PASMC, ASMC, and RASMC

Calculated as the O_2 concentration at half maximal respiration (p_{50} ; $n=5-9$ experiments). * indicate significant difference compared to PASMC and ASMC.

As increased ROS production was detected in PASMC during hypoxia, ROS production was next determined in RASMC and ASMC.

Although similar to PASMC cytochrome $b_{1/h}$ was more oxidized in hypoxia compared to cytochrome c in RASMC (Figure 3.18), in contrast to PASMC no increase in ROS production could be detected in RASMC.

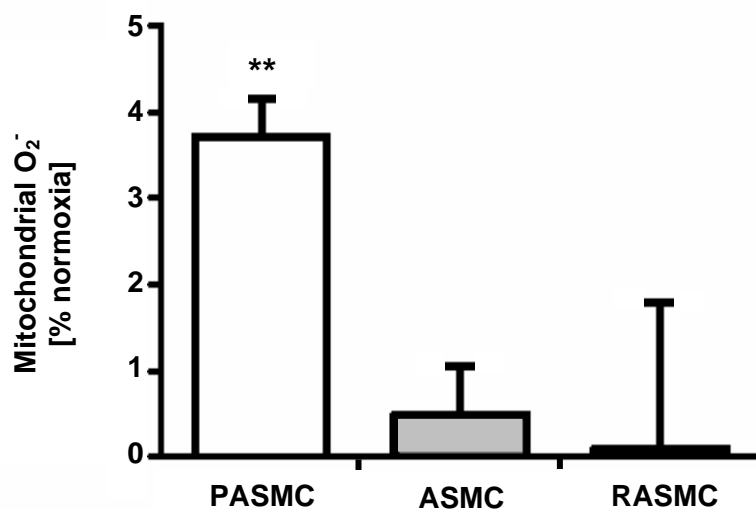


Figure 3.20 Hypoxic mitochondrial superoxide concentration in PASMC, ASMC and RASMC

O_2 concentration was reduced from normoxia to 1% O_2 (pO_2 8 mmHg). * indicates significant difference compared to normoxia (** $p < 0.005$).

As a possible explanation for the different ROS production of PASMC and RASMC the finding may serve, that mitochondrial membrane potential in RASMC was not increased during hypoxia.

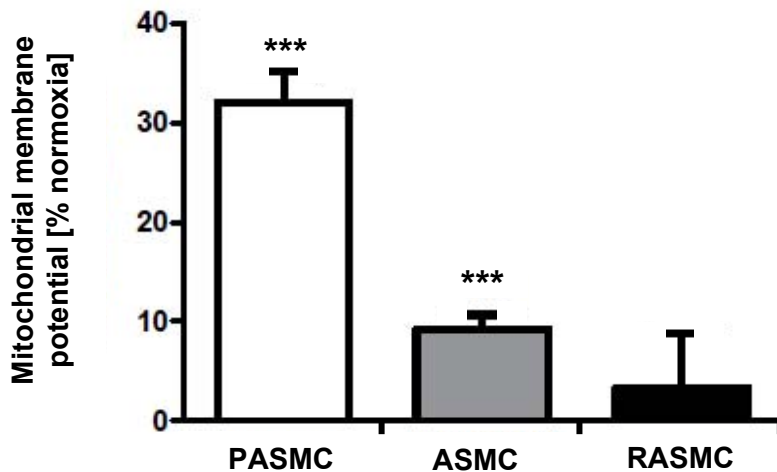


Figure 3.21 Hypoxic mitochondrial membrane potential in PASMC, ASMC and RASMC

O₂ concentration was reduced from normoxia to 1% O₂ (pO₂ 8 mmHg). * indicate significant difference compared to normoxia (***) p<0.001). Data are from n=3 individual experiments.

In summary, in PASMC redox alterations and inhibition of mitochondrial respiration occurred at O₂ concentrations at which hypoxia-induced ROS production and mitochondrial membrane hyperpolarization could be detected. The respiration of RASMC was slightly less inhibited by hypoxia than the respiration of PASMC or ASMC and neither ROS production, nor mitochondrial membrane hyperpolarization could be found in RASMC during hypoxia.

With regard to the isolated lung, mitochondrial respiration was slightly inhibited at O₂ concentrations, at which HPV occurred in isolated lungs. Spectral alterations in the isolated lung that can be attributed to mitochondrial cytochromes were similar to the redox changes measured in PASMC, but multiple spectral alterations that can be assigned to scattering phenomena and non-mitochondrial cytochromes overlapped mitochondrial cytochromes.

Therefore, inhibition of respiration and mitochondrial cytochrome redox alterations could be responsible for hypoxia-induced events in PASMC and for initiation of HPV in isolated lungs.

In order to confirm the findings and to overcome the limitations of hypoxic measurements in the isolated lung, in the next approach HPV was manipulated by mitochondrial inhibitors and correlated to redox changes and respiration under these conditions.

3.2.4 Correlation of HPV to respiration and redox state during application of mitochondrial inhibitors

3.2.4.1 Correlation of HPV with redox state of mitochondrial cytochromes

3.2.4.1.1 Application of cyanide

Inhibition of complex IV by cyanide resulted in a dose-dependent decrease of HPV. In the absence of cyanide, the strength of HPV was 3.0 ± 0.5 mmHg at a PAO_2 of 3 % O_2 (pO_2 23 mmHg) ($n=4$). The decrease of the strength of HPV during application of cyanide paralleled the reduction of mitochondrial cytochromes, particularly of cytochrome *c* (Figure 3.22). Cytochrome *b_{l/h}* was significantly less reduced than cytochrome *aa3* and *c* by cyanide treatment (Figure 3.22). In parallel with inhibition of HPV, cyanide induced a vasoconstriction during normoxic ventilation determined as a PAP increase of 0.8 ± 0.2 mmHg ($n=4$).

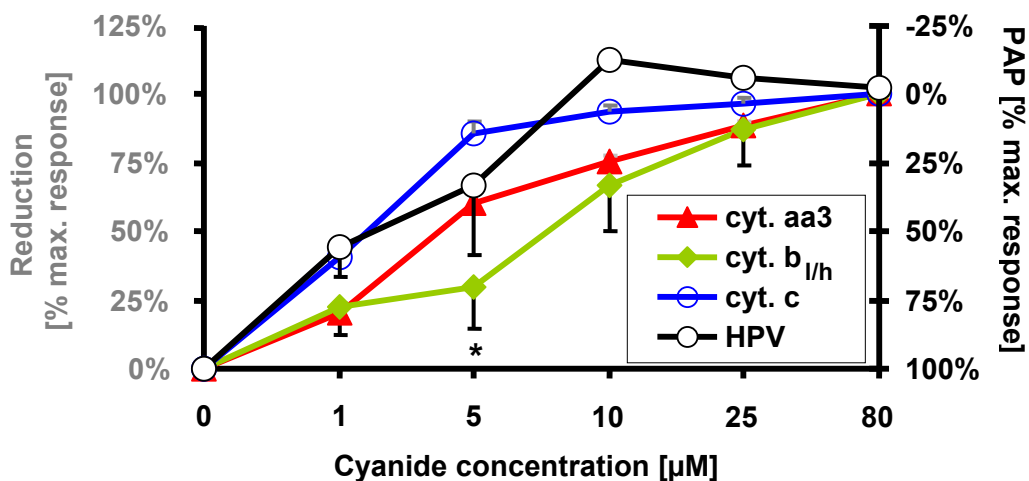


Figure 3.22 HPV and redox state at different cyanide concentrations in the isolated lung

Data are given in percent of maximal reduction or maximum strength of HPV, respectively (% max. response) * significant difference compared to cytochrome *c* ($p < 0.05$).

Similar results were found in isolated PASM. After adding cyanide to the cell suspension the cytochromes became increasingly reduced in normoxia and therefore the difference from normoxia to the fully reduced cytochromes in anoxia was decreased. The maximum response was defined as the reduction between normoxia and anoxia without presence of cyanide. Except for 10 μ M cyanide, cytochrome reduction paralleled HPV.

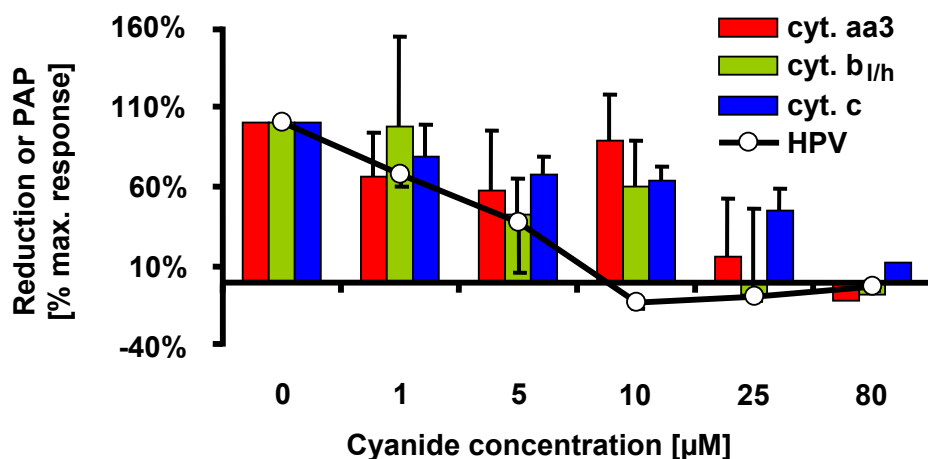


Figure 3.23 HPV and redox state at different cyanide concentrations in PASMC

Inhibition of HPV compared to the maximal reduction of mitochondrial cytochromes at different cyanide concentrations in isolated pulmonary arterial smooth muscle cells (PASMC). Data are from $n=3$ experiments.

3.2.4.1.2 Application of 2-n-heptyl-4-hydroxyquinoline-N-oxide (HQNO)

Interference of electron transfer at the Q_i site of complex III by HQNO resulted also in an inhibition of HPV. In isolated lungs HQNO reduced cytochrome $b_{1/h}$ and oxidized cytochrome c to a similar extent as it inhibited HPV (Figure 3.24). In normoxia no change of PAP could be detected.

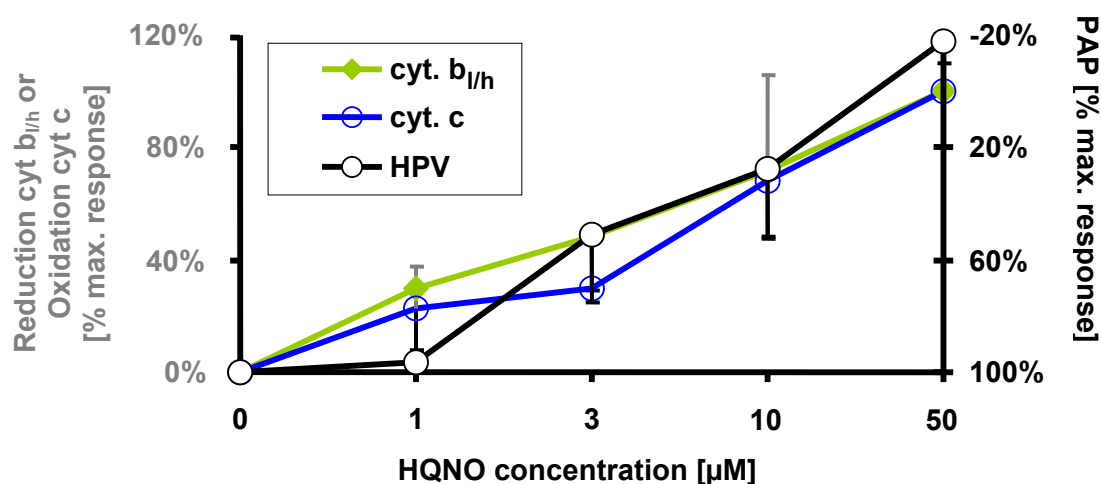


Figure 3.24 HPV and redox state at different HQNO concentrations in the isolated lung

Data are given in percent of maximal reduction or maximum strength of HPV, respectively (% max. response). Data are from $n=4$ isolated lungs.

After application of HQNO in cell suspensions normoxic spectra were taken as reference spectra. The difference of these spectra to maximally reduced anoxic spectra decreased with increasing concentrations of HQNO, as HQNO inhibited electron flow through the respiratory chain. Cytochrome reduction correlated with strength of HPV.

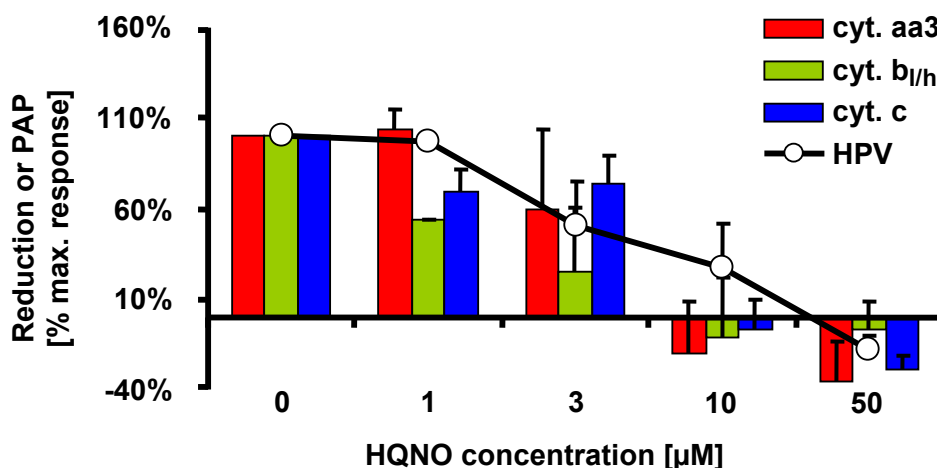


Figure 3.25 HPV and redox state at different HQNO concentrations in PASM

Inhibition of HPV compared to the maximal reduction of mitochondrial cytochromes at different HQNO concentrations in isolated pulmonary arterial smooth muscle cells (PASM). Data are from $n=3$ experiments.

3.2.4.1.3 Application of rotenone

Inhibition of complex I by rotenone inhibited HPV, but resulted in no detectable redox change during normoxia or hypoxia (PAO₂ of 3 % O₂, pO₂ 23 mmHg) in the isolated lung ($n=4$, Figure 3.26). Additionally to the inhibition of HPV, rotenone induced a dose-dependent normoxic decrease in PAP of maximally 0.5 ± 0.2 mmHg at 170 nM ($n=4$).

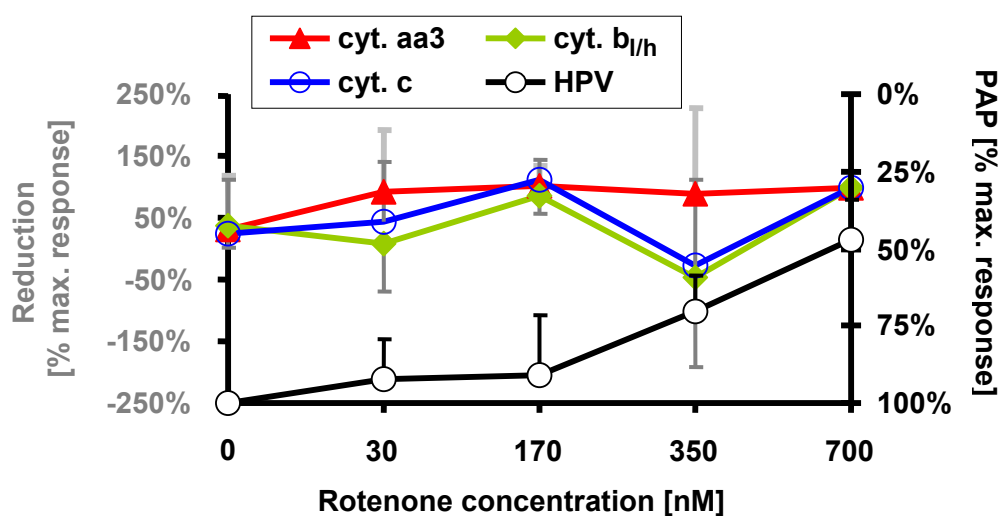


Figure 3.26 HPV and redox state at different rotenone concentrations in the isolated lung

Data are given in percent of maximal reduction or maximum strength of HPV, respectively (% max. response).

However, as rotenone inhibits electron entry into the respiratory chain, effects on redox state would result in increased oxidation, which might only be seen under conditions of reduced cytochromes. In cell suspension, the mitochondrial cytochromes of PASMC could be less reduced in anoxia after application of rotenone than without rotenone. The difference in maximal possible reduction correlated well with the inhibition of HPV in intact lungs (Figure 3.27).

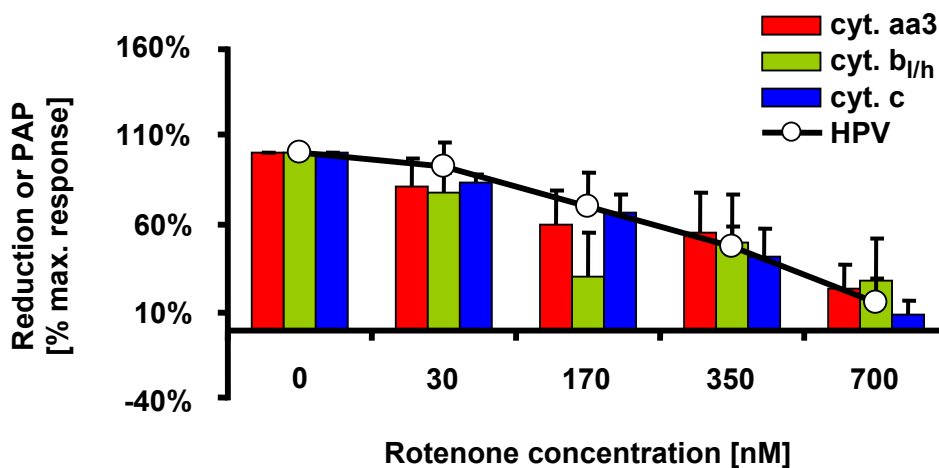


Figure 3.27 HPV and redox state at different rotenone concentrations in PASMC

Inhibition of HPV compared to the maximal reduction of mitochondrial cytochromes at different rotenone concentrations in isolated pulmonary arterial smooth muscle cells (PASMC)
Data are from $n=5$ experiments.

3.2.4.1.4 Application of FCCP

Uncoupling of mitochondrial respiration with FCCP resulted in no detectable alteration of redox state in isolated lungs. In isolated cells difference of normoxia and anoxic reduction increased with 4 μ M FCCP. Regarding HPV and normoxic vasoconstriction, FCCP induced dose-dependent alterations that did not correlate with redox state (Figure 3.28).

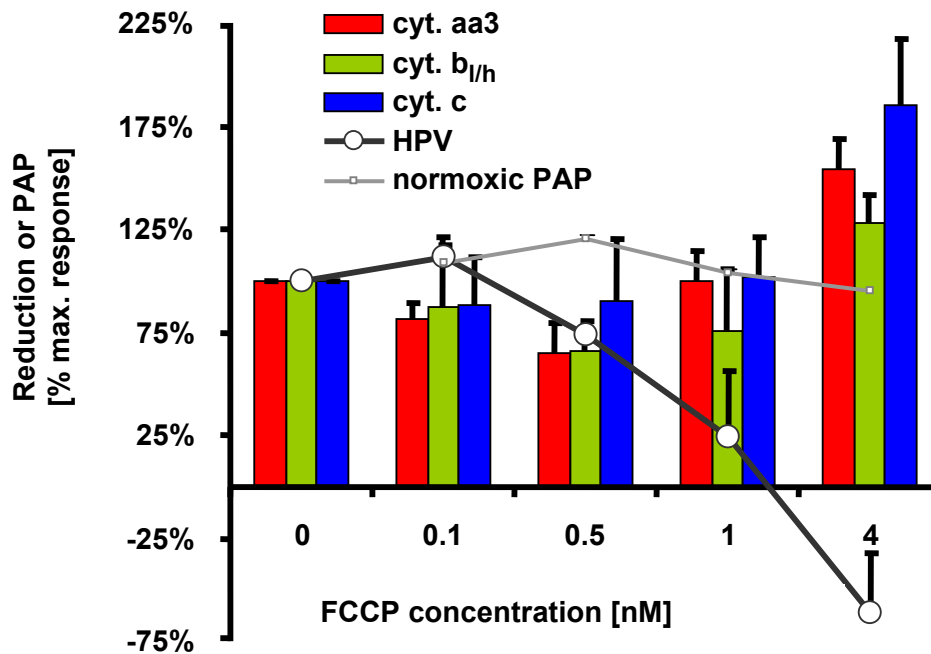


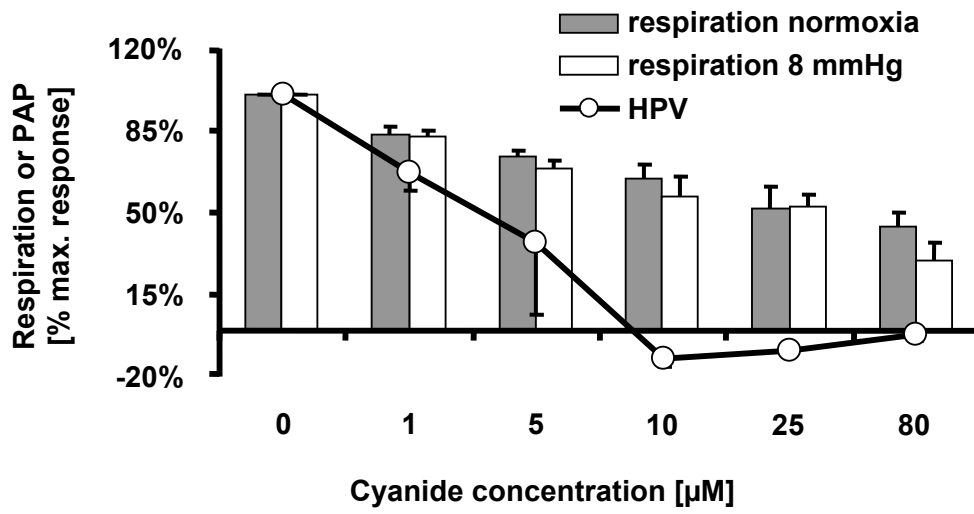
Figure 3.28 HPV and redox state at different FCCP concentrations in PASMC

HPV and normoxic PAP compared to the maximal reduction of mitochondrial cytochromes at different FCCP concentrations in isolated pulmonary arterial smooth muscle cells (PASMC). Data are from $n=4$ experiments.

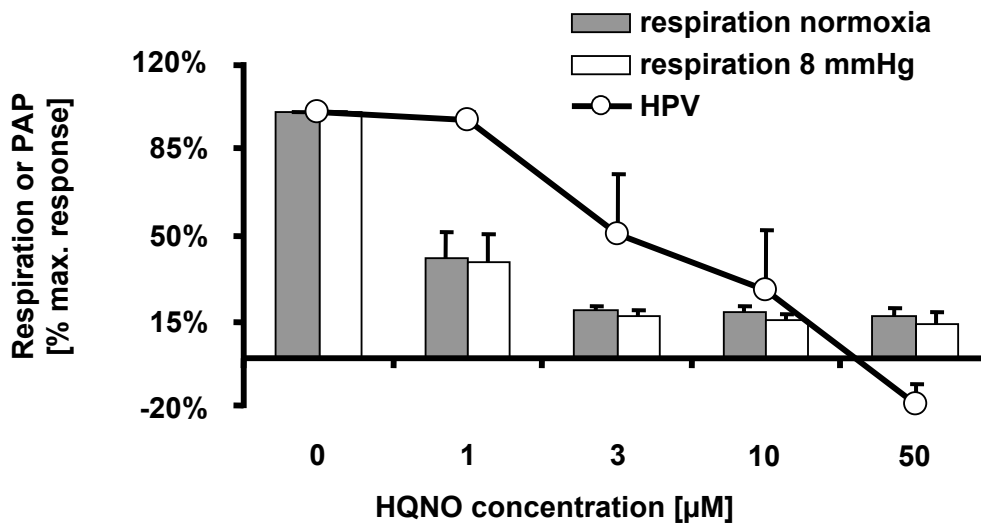
3.2.4.2 Correlation of HPV with mitochondrial respiration during application of cyanide, HQNO, rotenone and FCCP

In contrast to the cytochrome redox state in isolated lungs and cell suspensions of PASMC, inhibition of respiration by cyanide, HQNO and rotenone only partially correlated to alterations of the strength of HPV. During application of cyanide HPV was more decreased than respiration, whereas HQNO and rotenone inhibited respiration more than the strength of HPV. In presence of FCCP both, respiration and HPV initially increased, but their changes did not correlate in the further course of experiments (Figure 3.29, respiration is given during normoxia and at hypoxia [1% O₂, pO₂ 8 mmHg]).

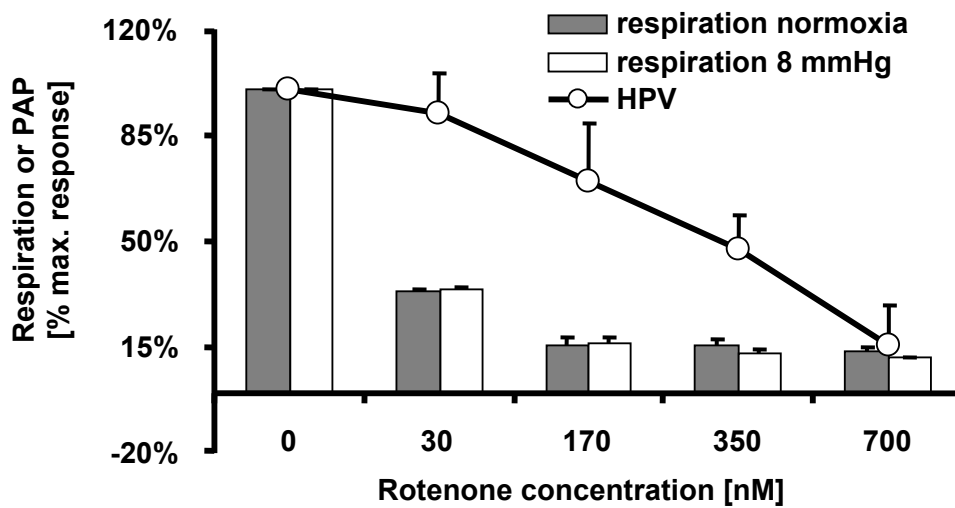
a)



b)



c)



d)

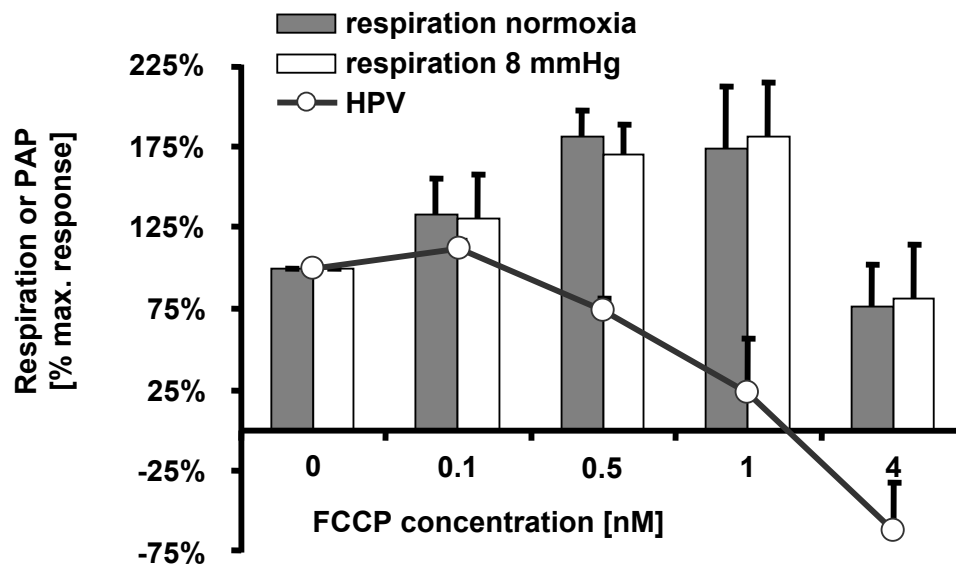


Figure 3.29 HPV and mitochondrial respiration in isolated PASC in presence of mitochondrial inhibitors

Data are from $n=5$ experiments each.

3.3 Identification of non-mitochondrial cytochromes

3.3.1 Cytochrome b_{558} of the NADPH oxidase

Hypoxic difference spectra revealed only redox alterations of cytochromes of the mitochondrial chain, as identified by comparison to cyanide spectra and fitting of single mitochondrial spectra in sum difference spectra (see Figure 3.5 and 3.9). Reduction of cytochrome b_{558} of NADPH oxidase could be induced by addition of SDT to completely anoxic PASC (Figure 3.30). The difference spectra in presence of SDT were in agreement to previously published cytochrome b_{558} spectra [203, 204].

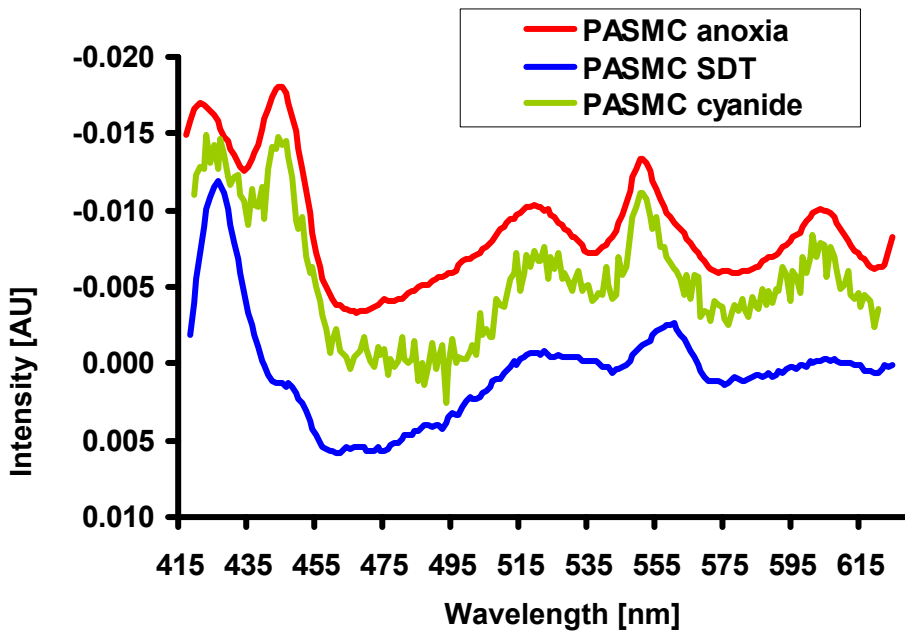


Figure 3.30 Spectrum of cytochrome b_{558} of the NADPH oxidase

Comparison of fully reduced PASM C spectra (PASM C anoxia) with PASM C spectra after application of cyanide (PASM C cyanide) and cytochrome b_{558} (PASM C SDT). Reduction of cytochrome b_{558} was achieved by addition of sodium dithionite (SDT) to fully reduced PASM C (PASM C SDT). Data for SDT are from $n=3$ experiments.

In the isolated lung reduction of cytochrome b_{558} of NADPH oxidase could be induced by perfusion of anoxically ventilated lungs with SDT (Figure 3.31). Mitochondrial cytochromes were pre-reduced with cyanide and do therefore not interfere with cytochrome b_{558} .

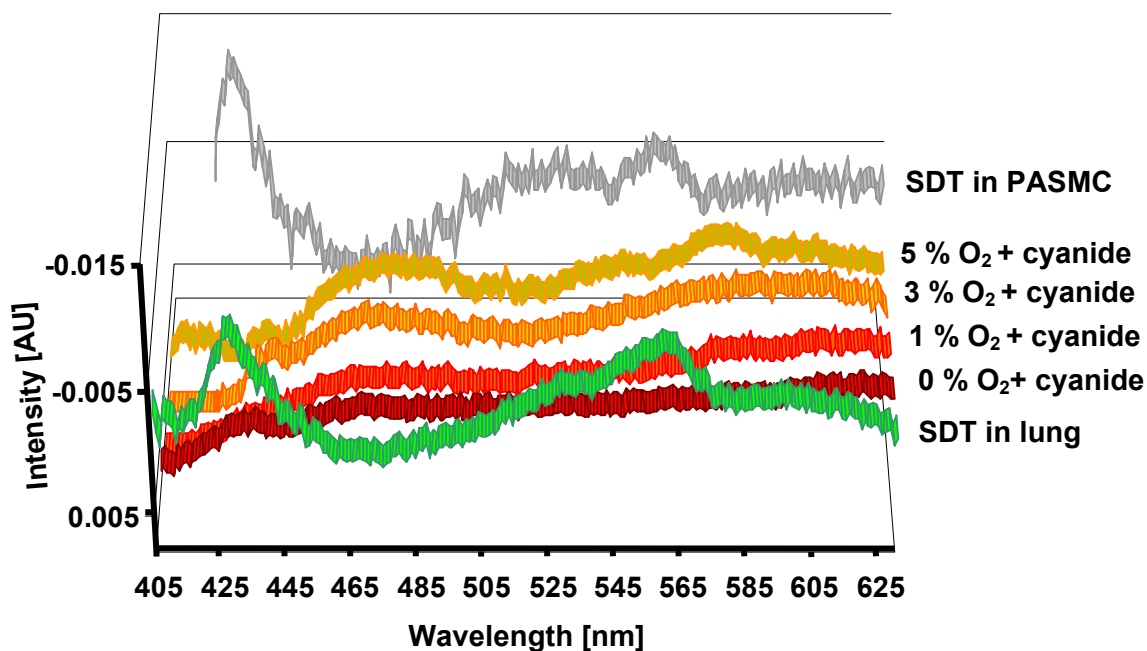


Figure 3.31 Identification of difference spectrum of NADPH oxidase in isolated lungs

Spectra at different O_2 concentrations and with additional perfusion with SDT are given. Mitochondrial cytochromes are inhibited with cyanide. For comparison a spectrum of cytochrome b_{558} , obtained by addition of SDT to anoxic PASM C is depicted. $n=3$.

3.3.2 Cytochrome P450

To limit amount of used CO these experiments were performed in isolated mouse lungs, as less amount of toxic gas was necessary for ventilation. In isolated lungs cytochrome p450 could be identified by addition of CO to the inhaled gas (Figure 3.32). In contrast to isolated lungs, in isolated PASMIC absorption changes of cytochrome P450 could not be illustrated by addition of CO (Figure 3.32).

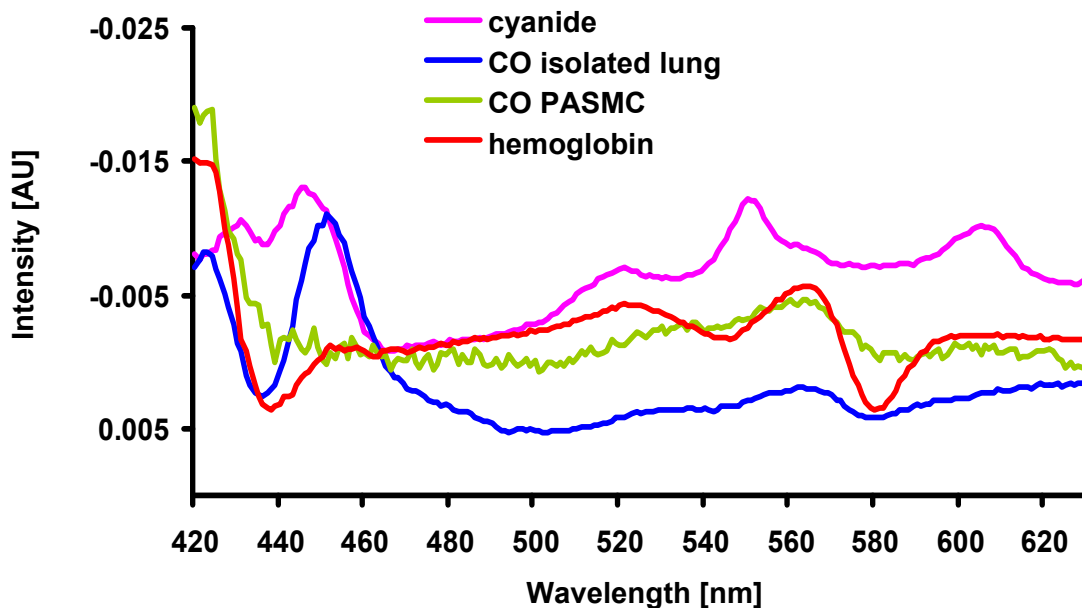


Figure 3.32 Carbon monoxide (CO) in isolated lungs and PASMIC

CO was applied at a concentration of 10% (pCO 75 mmHg) in a gas mixture with 21% O₂ (pO₂ 158 mmHg), balanced with N₂ in PASMIC and additionally 5% CO₂ (pCO₂ 40 mmHg) in isolated lungs. *n*=3. For comparison mitochondrial cytochrome spectra obtained by addition of cyanide to the perfusate of the isolated mouse lung preparation are given, as well as difference spectra of oxygenated hemoglobin added to the perfusate minus oxygenated hemoglobin during ventilation with CO (10%, pCO 75 mmHg).

3.3.3 Soluble guanylate cyclase

In isolated lungs and PASMIC a b-type cytochrome peaking at 423 nm was detected during application of CO (Figure 3.32). It resembles CO difference spectra of hemoglobin (Figure 3.32) or sGC (see Table 3). Therefore in isolated PASMIC the cytochrome peaking at 423 nm might reflect CO binding to sGC, whereas in isolated lungs also residual hemoglobin might contribute to spectral changes.

3.3.4 Myoglobin

Considering published spectra from literature (see Table 3) no myoglobin could be detected in PASM, neither during anoxia, nor during CO application.

3.3.5 Hemoglobin

Spectrophotometric measurements in isolated lungs were obscured by multiple tissue chromophores and scattering alterations. The most prominent cytochrome besides mitochondrial cytochromes was hemoglobin. Even in buffer-perfused lungs residual hemoglobin, which might result in the occurrence of a b-type cytochrome, cannot be excluded. It was possible to fit hemoglobin and mitochondrial cytochromes in sum difference spectra obtained from isolated lungs that showed clear signs of hemoglobin presence. When comparing the fitting result of fitting the hemoglobin spectrum together with that the mitochondrial spectra versus fitting the hemoglobin spectrum or mitochondrial spectra alone, the best fitting result was achieved by addition of all spectra to the fitting algorithm (Figure 3.33).

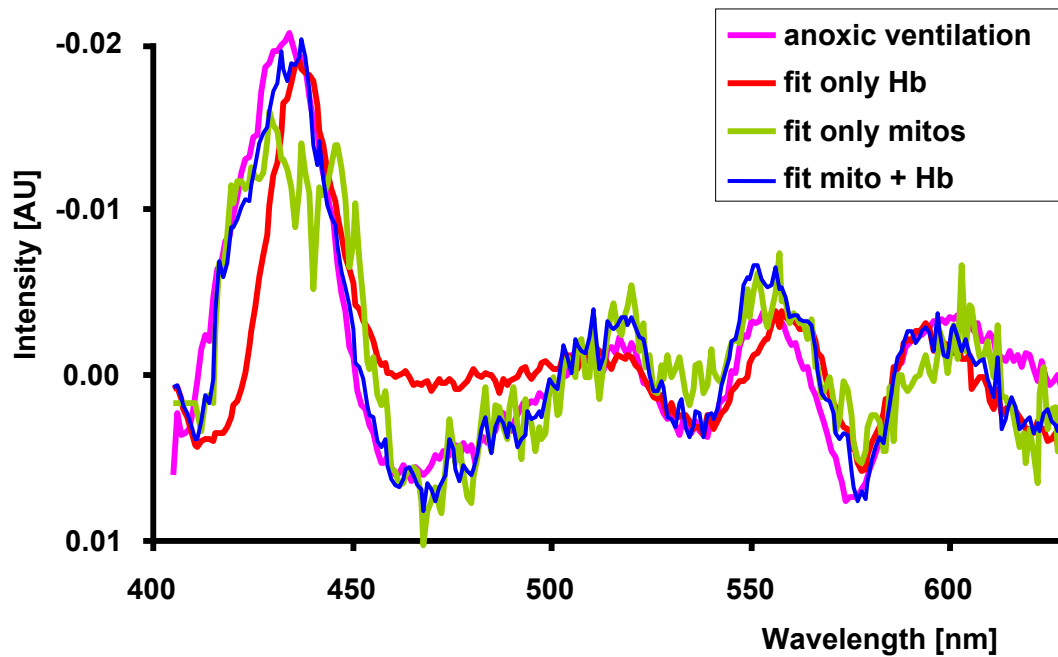


Figure 3.33 Fitting of hemoglobin in isolated lungs

Fitting of mitochondrial cytochromes (fit only mitos) and hemoglobin spectrum (fit only Hb) in sum difference spectrum (anoxic ventilation) of isolated lungs during anoxic ventilation. Fitting of both, mitochondrial and hemoglobin spectra (fit mito + Hb), resulted in best agreement with measured anoxic spectrum. Data are from $n=5$ experiments.

Analysis of the fitting results revealed that the strength of HPV corresponded to the oxygenation of hemoglobin (Figure 3.34) and amount of residual hemoglobin (Figure 3.35).

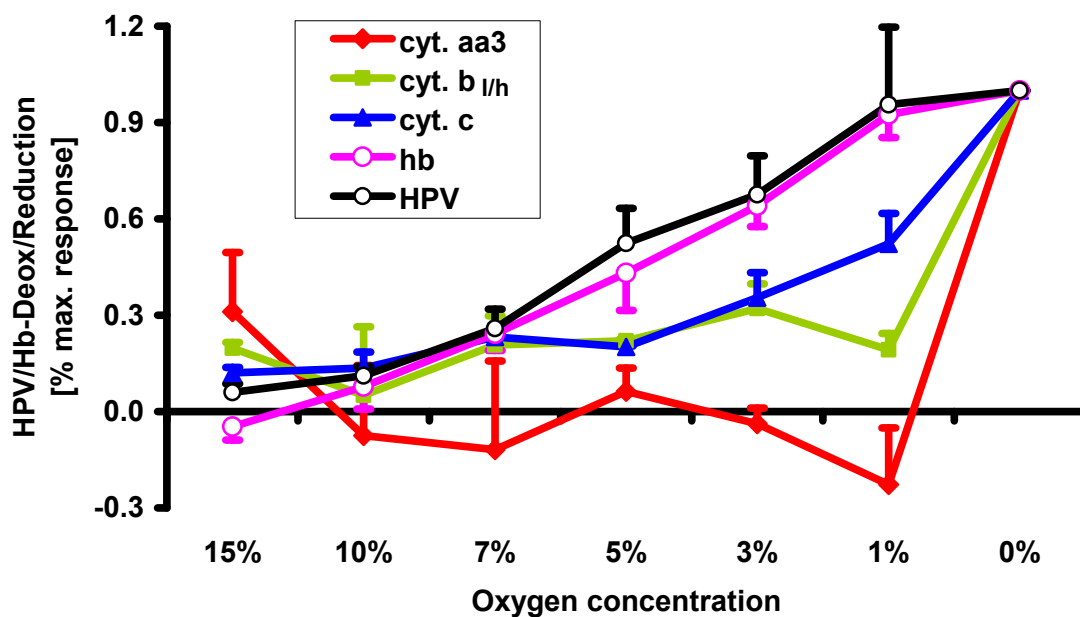


Figure 3.34 Comparison of the strength of HPV and the oxygenation state of hemoglobin

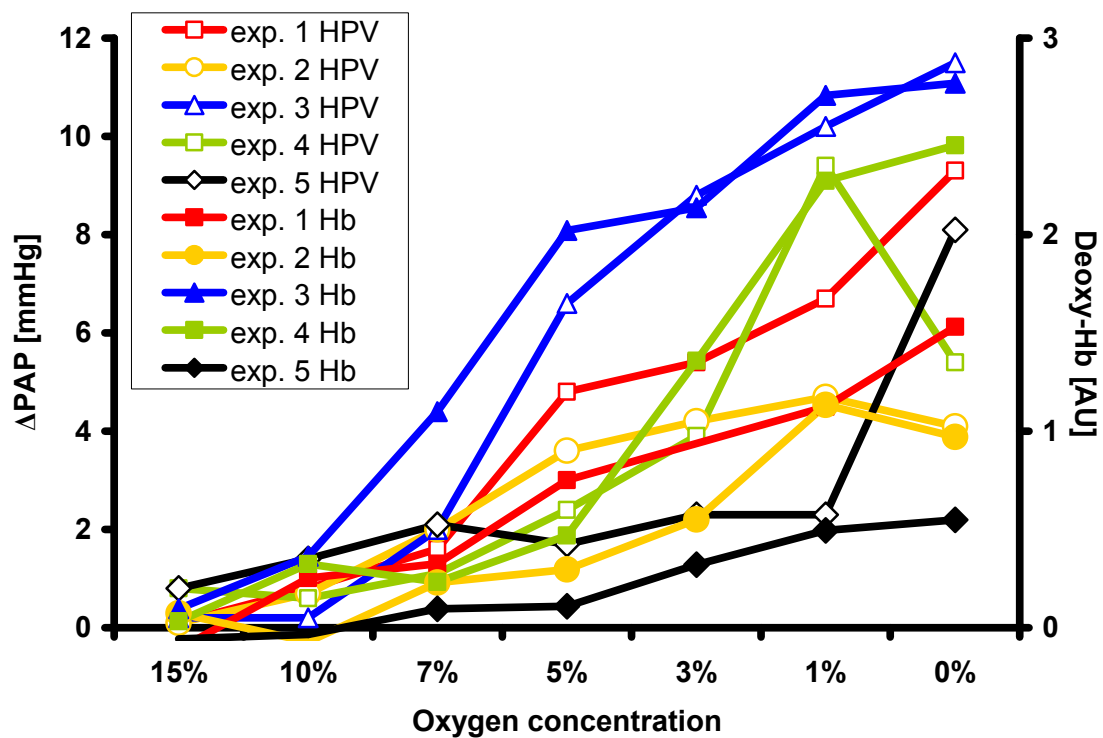


Figure 3.35 Comparison of HPV and amount of hemoglobin

Hypoxic pulmonary vasoconstriction (HPV) of different experiments (exp. 1-5) is illustrated in comparison with amount of deoxygenated hemoglobin (Hb) at specific O_2 concentrations. Data are from $n=5$ lung preparations (exp. 1-5) of lungs that showed signs of residual hemoglobin of different amount.

Therefore in isolated lungs oxygenation state and amount of hemoglobin might modulate HPV.

4 Discussion

Although mitochondria have long been thought to be involved in the O₂ sensing process underlying HPV [84, 108, 119, 122, 135], the possible mechanisms of their contribution are not yet resolved. In particular, the high O₂ affinity of mitochondria, ATP maintenance during HPV and contradictory findings of pharmacological complex IV inhibition have been considered to limit the importance of inhibition of mitochondrial respiration as a possible O₂ sensing mechanism [104]. Increased or decreased ROS production mainly at complex I and/or III are thought to be more promising pathways [14, 74, 86].

However, due to methodological limitations, it had thus far not been investigated if mitochondrial respiration and cytochrome redox state of the O₂ sensing cells of HPV are compromised during hypoxia-induced alterations in isolated lungs and HPV.

In the present study, remission spectroscopy was adapted to intact, isolated and blood-free perfused rabbit lungs to quantify redox alterations of mitochondrial cytochromes under graded hypoxia. Furthermore, combining this method with high resolution respirometry allowed correlation of the strength of HPV, as well as hypoxia-induced alterations in PASMC with respiration and cytochrome redox state of PASMC.

The current experiments yielded the following results:

- hypoxia induced HPV at O₂ concentrations $\leq 10\%$ ($pO_2 \leq 75$ mmHg) in isolated lungs and an increase of mitochondrial membrane potential, as well as mitochondrial matrix ROS production at O₂ concentrations $\leq 3\%$ ($pO_2 \leq 23$ mmHg) in isolated PASMC.
- mitochondrial respiration of PASMC was inhibited at O₂ concentrations $\leq 14\%$ ($pO_2 \leq 105$ mmHg), reaching $\geq 3 \pm 0 \%$ inhibition at O₂ concentrations of $\leq 3\%$ ($pO_2 \leq 23$ mmHg).
- cytochrome *aa3* of complex IV was significantly reduced by $\geq 11 \pm 3 \%$, cytochrome *c* by $\geq 10 \pm 4 \%$ at $\leq 3\%$ O₂ ($pO_2 \leq 23$ mmHg) in PASMC.
- cytochrome *b_h* was less reduced compared to cytochrome *aa3* and *c* at O₂ concentrations $\leq 3\%$ ($pO_2 \leq 23$ mmHg) in PASMC.
- RASMC differed from PASMC in that hypoxia inhibited their respiration less than that of PASMC and did not induce an increase of mitochondrial membrane potential or ROS production.
- application of cyanide, HQNO and rotenone resulted in dose-dependent inhibition of mitochondrial cytochrome reduction, correlating with the strength of HPV.

These findings suggest that hypoxia causes inhibition of complex IV resulting in alterations of cytochrome redox state, that initiate mitochondrial matrix superoxide release from complex III, by concomitant increase in mitochondrial membrane potential. This conclusion is based on the following facts: 1) the hypoxia-induced decrease of mitochondrial respiration paralleled HPV in isolated lungs; 2) the cytochrome reduction of cytochrome *c* and *aa3* (complex IV) and respiration in PASMC correlated to the hypoxia-dependent increase in mitochondrial superoxide levels as well as mitochondrial membrane potential; 3) cytochrome *b_{lh}* (complex III) was less reduced during hypoxia compared to cytochrome *c* and *aa3*; 4) these alterations were specific for PASMC, as RASMC displayed a lower decrease in respiration and no rise in matrix superoxide release and mitochondrial membrane potential; 5) pharmacological inhibition of mitochondria revealed analogous kinetics of cytochrome redox state and the strength of HPV.

4.1 Remission spectrophotometry

When measuring spectral alterations in lung tissue by remission spectrophotometry, the sum spectrum of all tissue cytochromes is detected. This included mitochondrial cytochromes, but also cytochrome *b₅₅₈* of NADPH oxidases, cytochrome P450 and cytochrome *b* of hemoglobin. In order to identify mitochondrial cytochromes in the isolated lung, the measured spectra were compared to published reference spectra and to difference spectra after application of specific inhibitors of the cytochromes. When comparing the spectral alterations in the lung at 0% O₂ (pO₂ 0 mmHg) with the spectra of the cytochromes, clear attribution to mitochondrial cytochromes could only be found in the wavelength range of 600-610 nm for cytochrome *aa3*. In the other wavelength ranges, the spectra of different cytochromes showed overlapping features, making it difficult to distinguish mitochondrial from non-mitochondrial cytochromes. To decrease the influence of hemoglobin as a prominent non-mitochondrial cytochrome, lungs were flushed with perfusate until the hemoglobin spectrum was no longer visible. Only these lungs were used for qualitative evaluation of oxygen dependency of mitochondrial cytochromes. However, the possibility that the difference spectrum of residual hemoglobin contributed to the spectral changes cannot be completely discounted. In measurements of lungs that showed signs of hemoglobin, the amount and oxygenation state of hemoglobin was semiquantitatively analyzed by fitting of the known hemoglobin difference spectra in the sum difference spectrum. Additionally, cytochrome *b₅₅₈* of NADPH oxidase peaking at 427 and 558 nm could not be distinguished from mitochondrial cytochrome *b_{lh}* with absorption maxima at 430 and 563/566 nm. However, reduction of

cytochrome b_{558} could only be detected by addition of SDT to anoxic tissue or cells, so that contribution of this cytochrome to the sum hypoxic spectrum is unlikely (see also 4.5).

In tissue remission spectrophotometry the spectrum is not only altered by absorption of light, but also by wavelength dependent scattering and reflection. For scattering by particles similar to or larger than the applied wavelength (e.g. as it occurs in milk or biological tissue), the Mie theory of scattering applies [205, 206]. This phenomenon results in higher intensities of backscattered light at high wavelengths, as seen in the measurement of backscattered light in milk. Light is additionally influenced by reflection at boundary layers in tissue. This occurs, for example, when crossing compartments of high and low water content. Furthermore, particularly in lung tissue, the density of scattering and absorption particles varies with ventilatory excursions and edema, such that the detected spectrum could be altered. If the scattering properties, reflection and tissue density do not change, they are constant during normoxia and hypoxia and can be eliminated from the measured spectrum by calculation of difference spectrum. The measured difference spectrum then only reflects absorption characteristics of the tissue. To eliminate the influence of ventilation, spectra were averaged over one minute. However, tissue water content can change during measurement and affect scattering, reflection and - due to density - absorption properties and thus result in spectral alterations that are not due to redox changes. Such spectral alterations have been proven in the present work to occur by variation of tissue water content elicited by increasing pulmonary venous pressure or reducing the intravascular fluid load and tissue density by induction of vasoconstriction with the thromboxane mimetic U-46619. The resulting spectra resembled remission spectra of lung tissue. This suggests decreased absorption (during volume load) or increased absorption (during vasoconstriction by thromboxane) due to lower or higher density of absorption particles in the measurement volume and/or increased reflection. Therefore, changes in tissue water content either by alteration of vascular tone or pulmonary edema must be taken into account when evaluating the redox spectra. The latter effect was avoided in the current study by only using lungs that showed no signs of edema. The first effect cannot be avoided and must be considered during interpretation of the respective results.

Therefore spectral alterations in the wavelength ranges of 410-440 nm and 520-590 nm may belong to non-mitochondrial cytochromes or scattering artefacts and only qualitative evaluation of spectral alterations in the lung seem to be adequate. However, when a high amount of hemoglobin is present and included into the fitting algorithm, semiquantitative evaluation of hemoglobin is possible due to its unique absorption characteristics at 590 nm and prominent absorbing character. The results of the less prominent cytochromes, with absorption features that overlap highly with other phenomena, particularly cytochrome $b_{1/h}$

interfering with hemoglobin at 560 nm and vasoconstriction induced alterations at 430 nm, cannot be evaluated in the isolated lung.

In contrast to the situation in the isolated lung, in cell suspensions of PASMC only mitochondrial cytochromes could be demonstrated. Reference absorption spectra for single cytochromes were determined in the closed chamber system by application of mitochondrial inhibitors and bovine cytochrome *c*. They resembled previously reported mitochondrial cytochrome difference spectra [207] (see also appendix). Thereby cytochrome *aa3*, *b_{lh}* and *c* could be identified. Cytochromes *a* and *a3* could not be distinguished, as determined by differential reduction of cytochrome *a* with cyanide. This effect is suggested to be caused by a much greater contribution in absorption from cytochrome *a* compared to cytochrome *a3* (80-90%) [185]. Cytochrome *c₁* and *b₅₆₀* of complex II was also not visible as reported previously [185].

In PASMC only mitochondrial cytochromes *aa3*, *b_{lh}* and *c* contribute to the sum difference spectrum measured during anoxia, as 1) it was found that recalculation of a sum spectrum with the derived reference spectra resembled the measured spectrum and 2) the spectral alterations after application of cyanide, which specifically reduces mitochondrial cytochromes, was almost identical with hypoxia-derived spectra.

For application of the fitting algorithm, therefore, cellular cytochromes of lower absorption coefficients that did not contribute detectably to the measured spectrum were neglected. Nevertheless, cytochrome *b₅₅₈* could be identified by reduction with SDT during anoxia, cytochrome P450 and sGC by CO. Other non-mitochondrial cytochromes (hemoglobin and myoglobin) could not be detected in PASMC (see 4.5).

Based on the identified mitochondrial difference spectra, changes in redox state were determined as follows: Attenuation of light intensity (i.e. difference spectrum) in cell suspensions is a non-linear function of absorption and scattering. However, for small changes of absorption and sufficient narrow-band consideration, the approach of Lambert-Beer, $A_{(\lambda)} \propto \ln(I_0(\lambda)/I_s(\lambda))$, $A_{(\lambda)} = \mu_a(\lambda) + \mu_s(\lambda)$, can be applied as first order approximation (λ : wavelength, A : light attenuation, I_0 : intensity of incident light, I_s : intensity of the backscattered light, $\mu_a(\lambda)$: absorption, $\mu_s(\lambda)$: scattering). According to this approximation, light attenuation depends linearly on absorption and scattering. The linear relationship between light attenuation and absorption was confirmed in the present experiments by successfully correlating difference spectra of cytochrome *c* with exogenously applied cytochrome *c* concentration in cell suspension. Absorption depends on chromophore concentration and redox state, scattering on particle size and concentration. Therefore, light attenuation (i.e., difference spectrum) is directly proportional to absorption when scattering is constant and conclusively directly proportional to changes in the redox state, when chromophore

concentration is constant. Changes in scattering cannot be completely controlled, as hypoxia may induce alterations of the shape of cells and/or mitochondria. However, since scattering effects are wavelength dependent, prominent scattering variations would result in differential absorption in the low and high wavelength ranges (415-460 nm and 500-620 nm, respectively), due to non-linear light attenuation in the low wavelength range. This was excluded in experiments with analysis of different wavelength ranges. However, only spectral measurements were included, in which differential calculation of low and high wavelength ranges showed identical results and spectral alterations of scattering could not be identified visually. The negligibility of the scattering effects was described previously in a similar system by Hollis *et al.* [185].

According to the above derived linear relationship between light attenuation, absorption and redox state, measured difference spectra were used to calculate changes in cytochrome redox states. Reference spectra of single cytochromes were fit in the measured sum difference spectrum by multi-wavelength least-square fitting. As the recalculated sum spectra were almost identical with the measured difference spectra, it can be concluded that the provided reference spectra were sufficient for semiquantitative evaluation of the contribution of the single cytochromes in the sum difference spectra.

4.2 Mitochondrial complex IV in oxygen sensing of HPV

In this study, mitochondrial respiration was inhibited at O₂ concentrations $\leq 14\%$ O₂ (pO₂ ≤ 105 mmHg) in PASMCM, correlating with the onset of HPV at $\leq 10\%$ O₂ (pO₂ ≤ 75 mmHg) in isolated lungs. Therefore, although the high O₂ affinity of mitochondria has been considered to exclude the inhibition of mitochondrial respiration as a possible mechanism underlying HPV in the past [104], inhibition of electron transfer to O₂ at complex IV can act as an O₂ sensor. However, the O₂ affinity is in the range of previously reported O₂ affinities [199], which results in very small inhibition of respiration under mild hypoxia ($\leq 3 \pm 0\%$ at $\geq 3\%$ O₂, pO₂ ≥ 23 mmHg). This is in line with the previously suggested hypothesis, that the inhibition of mitochondria may initiate a second messenger for O₂ sensing (e.g. a change in ATP/ADP ratio), rather than energy depletion during hypoxia acting as an O₂ sensing mechanism ([103, 106, 120], see introduction).

The redox alterations of complex IV (cytochrome *aa3*) in isolated PASMCM found in the investigations of this thesis support the findings of the respiration experiments that inhibition of complex IV can act as an O₂ sensor, as they 1) resembled the hyperbolic kinetics of respiration and 2) became significantly reduced at 3% O₂ (pO₂ 23 mmHg) in parallel with hypoxia-induced mitochondrial membrane hyperpolarization, ROS production, and calcium

increase in PASMC [208]. In isolated lungs the reduction of complex IV is difficult to detect due to interference of multiple spectral alterations, including non-mitochondrial cytochromes, other cell types beside PASMC and scattering artefacts. The spectral changes detected in the isolated lung at a PAO_2 of 10% O_2 (pO_2 75 mmHg) could not be observed in PASMC, which favors the suggestion that the spectral alterations in the wavelength range of 405-440 nm in isolated lungs under mild hypoxia (10% O_2 , pO_2 75 mmHg) are not attributed to cytochrome $b_{1/h}$ reduction in PASMC, but rather related to other cytochromes of the b class (hemoglobin, cytochrome b_{558}) in other cell types or scattering-induced alterations due to vasoconstriction, as evoked by application of the thromboxane mimetic. However, reduction of mitochondrial cytochrome $aa3$, peaking at 445 nm and 603/605 nm, could be clearly distinguished from other spectral alterations and could only be detected at a PAO_2 of 0 % O_2 (pO_2 0 mmHg). Visual evaluation of the spectral alterations provided the same result as fitting of the spectra of cytochrome $aa3$, $b_{1/h}$, c and hemoglobin in the hypoxic difference spectra of isolated lungs.

Therefore, despite the difficulties of discrimination of the mitochondrial cytochromes in the isolated lung, it can clearly be stated that complex IV reduction is detectable at anoxic ventilation. Integrating the results of PASMC, in higher O_2 concentrations small redox alterations of mitochondrial cytochromes can be expected, but are probably beyond the detection limit in the isolated lung. In summary, this study could show a small, but significant inhibition of respiration and reduction of complex IV in PASMC at O_2 concentrations, which induce HPV and/or hypoxia-induced cellular alterations.

In PASMC first hypoxia-induced alterations of mitochondrial membrane potential, ROS concentration and cellular calcium concentration were detectable at 3% O_2 (pO_2 23 mmHg), which correlated to a reduction of cytochrome c by 10 ± 4 %, cytochrome $aa3$ by 11 ± 3 % and respiration by 3 ± 0 %. Levels of hypoxia at which these alterations were detected in PASMC are well in line with the onset of HPV in the intact organ, since comparable O_2 values have been suggested to occur at the level of precapillary PASMC [3]. The range of onset of mitochondrial hyperpolarization and superoxide increase is similar to previous studies investigating the onset of hypoxia-induced cellular membrane depolarization, intracellular calcium increase and contraction of PASMC [21, 25]. Specifically the hypoxia-induced calcium increase in rabbit PASMC was reported to occur at a pO_2 of 16-21 mmHg (2-3 % O_2) [63] and of < 50 mmHg (7% O_2) with glucose free medium [26]. Therefore this study shows that inhibition of electron transfer at complex IV and reduction of respiration occur at O_2 concentrations that induce HPV, and it can be proposed that these alterations are initial steps of mitochondrial O_2 sensing in PASMC. The degree of inhibition seems to be too small for metabolic inhibition, but may result in signal initiation, for example, by AMP-dependent protein kinase activation [108], regulation of mitochondrial calcium release [209]

or ROS metabolism via regulation of cytochrome redox state. A subcellularly compartmentalized decrease of ATP, initiating a change in the redox state of the cell, has been suggested early to initiate HPV, due to the finding, that metabolic inhibition with 2-deoxyglucose (2-DOG) and reduced glutathione (GSH) inhibit the hypoxia-induced inhibition of K_v channels, with the limitation however, that the effect of GSH was not selective for PASMCM [24, 52]. The relevance for the localization of the mitochondria was recently emphasized [100], showing ATP- and magnesium dependent regulation of hypoxia sensitive K_v channels by near-by mitochondria [54]. Also in the O_2 sensing process of the carotid body mitochondrial complex IV has been suggested to serve as O_2 sensor for chemosensory discharge, as well as HIF-1 α stabilization [179].

In contrast, in fibroblasts of patients with decreased respiration due to impaired function of complex IV (Leigh Syndrome), no impairment of HIF-1 stabilization was found, suggesting that ATP production is not required for O_2 sensing [210].

Specifically in HPV, the importance of complex IV was questioned due to failure of cyanide to inhibit HPV in some investigations (see introduction, Table 1). However, this seems to be at least partially a dose dependent effect. In this study, cyanide inhibited HPV in the concentration range of 1-80 μ M (see 3.2.4.1.1).

4.3 Mitochondrial complex III in oxygen sensing of HPV

Due to the reported contradictory findings regarding pharmacological inhibition of complex IV and studies with agents interfering with ROS pathways, an increased or decreased ROS production mainly at complex I and/or III of mitochondria by a yet unresolved mechanism has been proposed as a pathway for O_2 sensing [14, 74, 86].

In the present investigations, results are in favor of increased ROS production at complex III, because 1) increased oxidation state of cytochrome b_{lh} compared to cytochrome $aa3$ and c was found, and 2) increased mitochondrial membrane potential and ROS production correlated to changes of mitochondrial redox state.

Cytochrome b_{lh} exhibited no signs of reduction even at severe hypoxia, whereas cytochrome c and $aa3$ had already been reduced. Although cytochrome b_{lh} has the lowest absorption coefficient according to these measurements, discernable changes were detectable according the equation for critical difference in the O_2 range of $\leq 3\%$ O_2 ($pO_2 \leq 23$ mmHg). This finding is in agreement with a hypoxia-induced increase in mitochondrial superoxide production at the semiubiquinone site at complex III and thus HPV as previously suggested [118, 118, 130, 133, 134, 211]. Furthermore, the results are in accordance with recent data

from Moncada and colleagues, who demonstrated a more pronounced reduction of cytochrome *aa3* and *c* compared to cytochrome *b_{lh}* in a monocyte cell line during inhibition of respiration by endogenous NO [212]. Increased mitochondrial membrane potential was suggested to support the resulting increase in ROS production [128], as also seen in the study presented in this thesis. Increased mitochondrial membrane potential may be caused by increased glycolytic ATP production [130]. Another hypothesis assumes that the mitochondrial proton leak decreases with low O₂ levels, leading to higher mitochondrial membrane potential than expected during hypoxia and, consequently, also to higher superoxide production [213].

Although it is not clarified yet how mitochondrial membrane hyperpolarization is achieved, the finding of the hyperpolarization is in line with previous studies by Michelakis et al. [23]. However, in contrast to the investigations in this thesis, Michelakis et al. [23] measured a decrease in ROS production in pulmonary artery rings. One difference between the studies is the use of fluorescent dyes specific for intracellular, but not mitochondrial ROS production. As illustrated in the introduction, this contradictory finding may be explained by the possibility that changes in ROS are dependent on subcellular localization, time course and degree of hypoxia. In general, the results of the present study support the conclusion that increased mitochondrial ROS production occurs under conditions of high membrane potential, highly reduced ubiquinone pool and decreased respiration (see introduction).

As a possible mechanism for ROS production at the quinol oxidase (Q_o) site of complex III, an unstable semiubiquinone could bypass the Q-cycle and directly reduce O₂, forming superoxide [214]. Inhibition of complex IV has been proposed to be insufficient for this mechanism, as complex IV inhibition results in cytochrome *c*₁ reduction, which may decrease electron inflow in complex III, due to a pivoting interaction of the iron-sulfur complex with cytochrome *c*₁ and the Q_o site depending on its redox state [133].

Thus, ROS production from complex III during complex IV inhibition appears to require an additional defect that increases oxidant production from the Q_o site of complex III. Functional alterations of the Q_o site can disrupt electron flux in this portion of complex III leading to “bypass reactions” of the Q_o site that enhance ROS production, with the rate-limiting step being the formation of a reactive species (probably a semiubiquinone), but not availability of O₂ [214]. However, it is not yet certain, which functional alterations of the Q_o site this could be under condition of hypoxia.

Another hypothesis questions this mechanism of semiubiquinone directly reducing O₂, as it doubts the existence of relevant amount of free semiubiquinone at the Q_o site. It proposes a reverse reaction of electron transfer from reduced cytochrome *b* onto O₂ via ubiquinone [211]. Conditions of ROS production would be favored by a partially oxidized ubiquinone pool to provide sufficient amounts of the redox mediator and a moderately high membrane

potential to increase the fraction of reduced heme b_L . In organs like the lung, where the ubiquinone pool is normally too oxidized for efficient ROS generation, already moderate O_2 limitation could directly increase the fraction of reduced ubiquinone to the critical level of about 75% ubiquinol. This would result in a burst of ROS production setting off the hypoxia signaling cascade [211].

Although the current work cannot exclude the relevance of ROS production from complex I for O_2 sensing, Q_o site of complex III has been suggested to be the dominant ROS production site, because ROS products are directed into the intermembrane space away from the antioxidant defenses of the matrix [133]. In this regard it has to be considered, that the measurements with MitoSox are limited for evaluation of this kind of mitochondrial ROS production, as MitoSox mainly determines mitochondrial matrix ROS production. Additionally MitoSox has to be judged critically under the conditions of this study, as its accumulation depends on mitochondrial membrane potential [215]. An effect, which may prove beneficial in this regard, may be that residual MitoSox in the cytosol and intermembrane space could contribute to the ROS signal and therefore also detect ROS released into the intermembrane space. This could explain the discrepancy with the measurements of Schumacker, who recently showed that ROS increased in cytosol and intermembrane space, but decreased in mitochondrial matrix in PASM and systemic cells [216]. Furthermore it is also generally accepted, that the Q_o site of complex III also releases ROS to the mitochondrial matrix site by an unresolved mechanism, and that the quinone reductase (Q_i) site can produce ROS, albeit to a much lower degree than at the Q_o site due to a higher stability of the semiubiquinone [132]. A convincing approach recently used siRNA against the iron-sulfur-complex of complex III, also demonstrating that the Q_o site of complex III is required for hypoxic stabilization of HIF-1 [140].

4.4 Comparison of PASM to arterial smooth muscle cells of the systemic vasculature

The present study found no evidence for differences between PASM and ASM with regard to redox alterations or O_2 affinity. ASM exhibited a smaller increase in mitochondrial membrane potential, no increase in ROS concentration and no calcium release [208]. RASM, that also showed no hypoxia-induced increase in calcium or ROS concentration, differed from PASM in the higher O_2 affinity and missing hypoxic mitochondrial membrane hyperpolarization, but not in mitochondrial redox state. Thus, it can be speculated, that for sufficient ROS release, an increase in mitochondrial membrane potential above a certain

threshold in combination with increased oxidation state of cytochrome b_{lh} is necessary. Only in the case of PASMC, when mitochondrial membrane potential and ROS release is increased, a hypoxia-induced intracellular calcium increase was detected [208]. The larger inhibition of respiration in hypoxia of PASMC compared to RASMC may promote these changes. However, specific downstream regulation of PASMC, (e.g. by different ion channel expression [217]) or specific regulation of ion channel function [218] may also underlie the differences between the cell types. The similar hypoxic behavior of PASMC and ASMC may be due to the fact, that ASMC are - like PASMC - exposed to rather high pO_2 in vivo with the aorta carrying well oxygenated blood.

A role of the culture conditions for the observed effects was largely excluded as only cells from passages 1 and 2 were used, no differences between these passages were detectable, and cultured cells showed expected physiological responses, e.g. with regard to the hypoxia-induced intracellular calcium increase [208].

4.5 Mitochondrial inhibition and HPV

The data presented in this study favor the conclusion that inhibition of respiration and reduction of mitochondrial cytochromes initiate signaling cascades in HPV. Differential regulation of the cytochromes may be essential for the signaling mechanism, as cytochrome b_{lh} was less reduced in hypoxia compared to cytochrome $aa3$ and c .

This hypothesis was investigated using inhibitors of the mitochondrial respiratory system that specifically prevent HPV (see introduction).

Application of cyanide in intact lungs decreased the strength of HPV to a similar degree as it induced mitochondrial cytochrome reduction. Cytochrome b_{lh} was significantly less reduced than was cytochrome c , suggesting that a differential regulation of redox states occurs also in the intact lung under condition of complex IV inhibition. In presence of HQNO, a dose-dependent reduction of cytochrome b_{lh} and oxidation of cytochrome c correlated well with the inhibition of HPV in isolated lungs. Rotenone did not result in any detectable changes of redox state during ventilation with normoxic or hypoxic gas of 3% O_2 (pO_2 23 mmHg) in the isolated lung. This can be explained by the fact that rotenone inhibits electron inflow into the respiratory chain and, therefore, no further oxidation could be detected [184] when the cytochromes are already completely oxidized in normoxia. Because mitochondrial cytochromes were also not significantly reduced at 3% hypoxia (pO_2 23 mmHg) in isolated lungs, inhibition of reduction (i.e. oxidation) could also not be measured during rotenone treatment in isolated lungs at this O_2 concentration. In contrast, cytochromes in isolated

PASMC were fully reduced in anoxia, and inhibition of electron inflow into the respiratory chain by application of rotenone resulted in decreased maximal possible reduction (i.e. higher oxidation compared to completely reduced anoxic cytochromes without rotenone). Furthermore in PASMC maximal possible reduction of the cytochromes during anoxia was decreased in a concentration-dependent manner by rotenone, and this inhibition correlated to HPV inhibition in the isolated lung. As anoxia cannot be achieved in the isolated lung, the effect of rotenone can only be measured and correlated to HPV in PASMC. In presence of cyanide and HQNO cytochrome redox state correlated to the strength of HPV in isolated lungs and to decreased redox alterations from normoxia to anoxia in PASMC. Small discrepancies between redox alterations in PASMC and inhibition of HPV may be due to different pharmacodynamics in isolated lungs and isolated cells.

In contrast to cytochrome reduction, the level of mitochondrial respiration in PASMC did not correlate to the strength of HPV, which supports the hypothesis that inhibition of mitochondrial respiratory chain initiates HPV, but subsequent regulation of cytochrome redox state is essential for signal transduction of HPV. The role of cytochrome b_{lh} was also highlighted by the inhibitor studies, as relative cytochrome b_{lh} oxidation is found during cyanide inhibition in the isolated lungs.

It remains unclear, how the differential regulation of cytochrome redox state and respiration is achieved.

Results of FCCP application support the importance of an intact mitochondrial membrane as a prerequisite for HPV. In high concentrations FCCP inhibited HPV, but did not change respiration or cytochrome reduction substantially. Therefore, it is concluded that, disruption of mitochondrial membrane potential by the uncoupling substance FCCP caused inhibition of HPV inhibition.

4.6 Identification of non-mitochondrial cytochromes

In isolated cells, only spectral alterations caused by mitochondrial cytochromes could be detected upon application of hypoxia. This was verified by comparison of hypoxic spectra with a) cyanide spectra, b) published mitochondrial spectra and c) spectra derived after application of inhibitors specific for complex III or IV. Nevertheless, non-mitochondrial cytochromes could be identified in PASMC and isolated lungs by application of certain interaction partners causing spectral shifts of non-mitochondrial cytochromes. In particular, reduced spectra of NADPH oxidase were visible after application of SDT to anoxic PASMC. It has been previously described that reduction of cytochrome b_{558} of NADPH oxidase is only observed to be rapid under anaerobic conditions when stimulated by NADPH [193].

Otherwise it is slow and incomplete even after several minutes of anoxia, due to conformational properties that allow electron inflow into the complex only in the presence of O₂ [219]. There was a question whether reduction of cytochrome *b*₅₅₈ provides insight into activity of NADPH oxidases at all [220].

Application of CO allowed demonstration of cytochrome P450 in isolated lungs, but not in isolated PASM. As cytochrome P450 has, however, been shown to 1) be present in PASM, 2) produce HETE [221], and 3) play a modulatory role in K_v channel activity [168], the concentration of cytochrome P450 may be too low to be identified in the experiments with addition of CO by the spectroscopic methods in the current study. In isolated lungs, no spectral alterations could be found at 450 nm during hypoxic ventilation, which indicates that binding of endogenous CO to cytochrome p450 does not occur in hypoxia. It therefore has to be taken into account that binding of endogenously produced CO could be obscured by relative low levels of cytochrome P450 compared to cytochrome aa₃, peaking at 445 nm. Furthermore, it cannot be excluded that cytochrome P450 plays a modulatory role in HPV via CO metabolism in the isolated lung. Substrate binding to cytochrome P450 (e.g. during activation of NADPH-dependent cytochrome P450 reductase-heme oxygenase signaling) may change the difference spectrum of the cytochrome P450, with a decreased or increased absorption at 420 nm ("type I" difference spectrum) or at 430 nm ("type II" spectrum) [222]. Such alterations could not be distinguished from other cytochromes in the isolated lung, but could also not be identified in isolated PASM. Therefore, within the limitations of the detection method, this study did not provide any evidence that cytochrome P450 played a role in O₂ sensing in PASM. This is in line with a previous study excluding a role of the cytochrome P450 reductase-hemoxygenase-BK_{Ca}-pathway as O₂ sensing mechanism by use of genetically modified mice [177]. Although cytochrome P450 seems not to be involved in O₂ sensing, the importance of the cytochrome P450-induced production of EETs as a modulator for HPV and pulmonary hypertension is well known [172], but may be beyond the detection limit of the applied spectrophotometric method in the isolated lung.

Spectral alterations that indicate involvement of sGC during O₂ sensing could not be detected in PASM. Although a b-type cytochrome peaking at 423 nm correlating to spectral alterations caused by sGC (see Table 3) could be detected during application of CO in PASM, these alterations were not present during hypoxia. NO binding would be expected to shift the absorption maximum of sGC from 431 nm (non-bound) to 398 nm (bound) [223], but could not be found in PASM. Hypoxia can shift the absorption maximum of sGC from 416 to 430 nm with maximal difference at 437 nm [189]. Although it is not possible to distinguish these alterations from other b-type cytochromes, (e.g. cytochrome *b*_{lh} of complex III), sGC seems unlikely to play a role in PASM given that the hypoxic spectrum resembles the cyanide spectrum. However, cyanide is not expected to cause spectral shifts of sGC.

The current investigations revealed no signs of the presence of myoglobin, neither in isolated lungs, nor in PASMC. It was not too long ago, when the existence of myoglobin in mammalian smooth muscle cells was discovered. However, it remains unclear, if this is also true for smooth muscle cells of pulmonary arteries, as in the cited study mRNA of myoglobin was not demonstrated in lung tissue [224].

The presence of hemoglobin measured in the isolated lung was found to be the only relevant non-mitochondrial cytochrome for modulation of HPV. Although methodologically challenging, it was successfully established that oxygenation state and amount of hemoglobin correlate with HPV. This fits the finding, that free oxygenated hemoglobin can scavenge NO, thereby enhancing HPV [225], yet deoxygenated hemoglobin can produce NO [226]. Considered with the results of the current thesis, it can be concluded that the sigmoidal stimulus-response relationship between pulmonary arterial pressure and the level of hypoxia could be the result of enhanced HPV in mild hypoxia by oxygenated Hb and attenuated HPV in severe hypoxia by deoxygenated Hb. It is important to mention, that even in visually hemoglobin-free perfused isolated lungs, spectral signs of persistent existence of hemoglobin are proven by spectrophotometry. Therefore even small amounts of hemoglobin, which went undetected in previous studies, could result in the different dynamics of HPV in isolated lungs versus pulmonary arteries or PASMC.

4.7 Conclusion

In conclusion, a new spectrophotometric technique was established in the presented work. This allows for the first time, to the best of the author's knowledge, the detection of O₂-dependence of mitochondrial respiration and redox state in isolated lungs, PASMC, ASMC and RASMC. As summarized in Figure 4.1, a small but significant decrease in mitochondrial respiration (1) and reduction of cytochrome *c* and *aa3* of complex IV (2) was found in the O₂ range of HPV and/or hypoxic reactions of PASMC. Thus, despite the high O₂ affinity of mitochondria, inhibition of mitochondrial respiration may act as a sensor in acute pulmonary O₂ sensing by O₂ deprivation at the physiological electron transfer site (complex IV). This may result in an increased electron backup and leak at complex III, indicated by an increased oxidation level of cytochrome *b_{llh}*. Together with increased mitochondrial membrane potential (3a) this can result in subsequent ROS production (3b) and increased cytosolic calcium levels. The higher O₂ affinity of RASMC and lower hypoxic mitochondrial membrane potential compared to PASMC and ASMC supports the hypothesis of differential mitochondrial behavior in different cell types. Modulation of HPV by hemoglobin (4) may play an important

role in isolated lungs. Alternative yet unidentified or established non-mitochondrial cytochromes were not detected, and thus are unlikely to be involved in O₂ sensing underlying HPV.

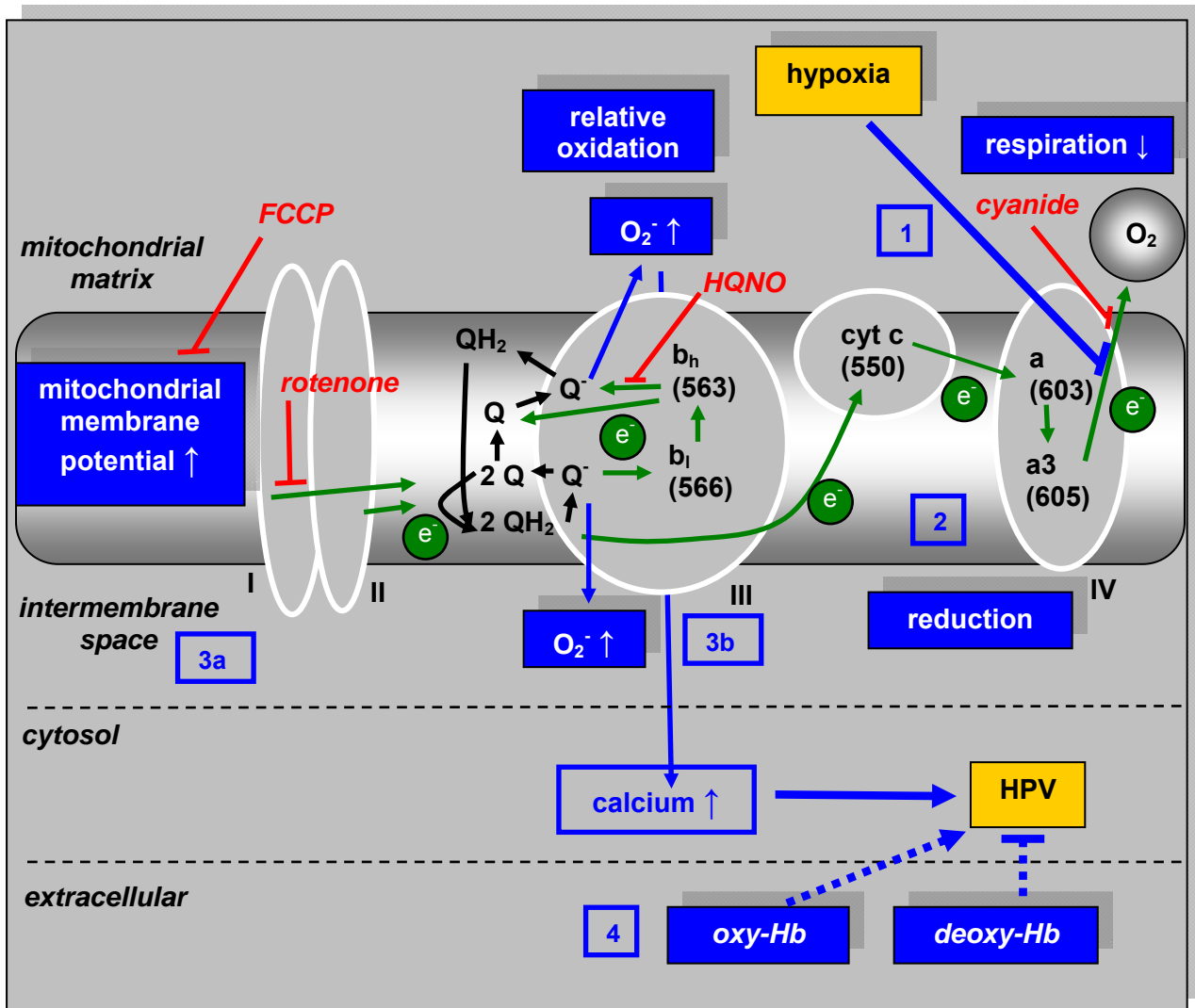


Figure 4.1 Proposed mitochondrial pathway of oxygen sensing in HPV
 For explanation please refer to the text.

5 Summary

Hypoxic pulmonary vasoconstriction (HPV) is an essential mechanism of the lung to match blood perfusion to alveolar ventilation and optimize pulmonary gas exchange. Mitochondria have been suggested as possible O₂ sensors of HPV. With regard to mitochondria the hypothesis of an increased or decreased production of reactive oxygen species (ROS) at complex I or III competes with the hypothesis of a localized small decrease of ATP production. Against this background, the present study investigated the O₂ dependent regulation of mitochondrial cytochrome redox state and respiration in isolated lungs and pulmonary arterial smooth muscle cells (PASMC).

Methodological limitations of the past were overcome by detection of mitochondrial cytochrome redox state under hypoxic and normoxic conditions using remission spectrophotometry in intact lungs and in PASMC. High-resolution respirometry was used to determine the respiration simultaneously in isolated cells. These alterations were compared to HPV and hypoxia-induced cellular responses, such as mitochondrial matrix superoxide release and mitochondrial membrane potential. Aortic and renal arterial smooth muscle cells (ASMC, RASMC) served as controls.

The hypoxia-induced decrease of mitochondrial respiration paralleled the increase in the strength of HPV in isolated lungs. In PASMC, reduction of respiration and mitochondrial cytochrome *c* and *aa3* (complex IV) matched an increase in matrix superoxide levels, as well as mitochondrial membrane hyperpolarization. Cytochrome *b_{1/h}* (complex III) was relatively more oxidized during hypoxia compared to cytochrome *c* and *aa3*. In contrast to PASMC, RASMC displayed a smaller decrease in respiration and no rise in superoxide or mitochondrial membrane potential. Pharmacological inhibition of mitochondria revealed analogous kinetics of cytochrome redox state and the strength of HPV.

The data of this thesis thus suggest inhibition of complex IV as an essential step in mitochondrial O₂ sensing of HPV. Concomitantly, increased superoxide release from complex III and mitochondrial membrane hyperpolarization may initiate the pathway underlying HPV.

In isolated lungs, HPV may be modulated by oxygenation state of hemoglobin, whereas there is no evidence for carbon monoxide playing a role via cytochrome P450.

6 Zusammenfassung

Die hypoxische pulmonale Vasokonstriktion (HPV) ist ein wesentlicher Mechanismus der Lunge, um die Perfusion an die alveoläre Ventilation anzupassen und so den pulmonalen Gasaustausch zu optimieren. Mitochondrien sind dabei möglicherweise die Sauerstoffsensoren der HPV. Derzeit bestehen konkurrierende Hypothesen bezüglich eines mitochondrialen Sensing-Mechanismus: Eine erhöhte oder erniedrigte Produktion von Sauerstoffradikalen am Komplex I oder III oder eine lokalisierte, leichte Abnahme der ATP Produktion könnten die Signalkaskade einleiten. Vor diesem Hintergrund, untersuchte die vorliegende Arbeit die sauerstoffabhängige Regulation des Redox-Status' mitochondrialer Cytochrome und der mitochondrialen Atmung in der isoliert perfundierten und ventilerten Lunge und in glatten Muskelzellen pulmonalarterieller Gefäße (PASMC).

Methodische Limitationen bisheriger Untersuchungen wurden durch die Anwendung von Remissionspektrometrie überwunden, wodurch der Redox-Status mitochondrialer Cytochrome während Hypoxie und Normoxie in intakten Lungen und PASMC bestimmt werden konnte. Mit hochauflösender Respirometrie wurde gleichzeitig die Atmung in isolierten Zellen erfasst. Veränderungen dieser Parameter wurden mit der Stärke der HPV und Hypoxie-induzierten zellulären Antworten in isolierten Zellen, wie Superoxidfreisetzung in der mitochondrialen Matrix und dem mitochondrialen Membranpotential, verglichen. Zur Kontrolle wurden glatte Gefäßmuskelzellen der Aorta und der Nierenarterie (ASMC, RASMC) herangezogen.

Eine hypoxie-induzierte Abnahme der mitochondrialen Atmung erfolgte gleichzeitig mit Beginn der HPV in der isolierten Lunge. In isolierten PASMC ging die Abnahme der Atmung und Reduktion der mitochondrialen Cytochrome *c* und *aa3* (Komplex IV) mit einem Anstieg der Superoxidkonzentration in der mitochondrialen Matrix, sowie einer mitochondrialen Membranhyperpolarisierung einher. Cytochrom *b_{lh}* (Komplex III) war bezogen auf Cytochrom *c* und *aa3* unter Hypoxie mehr oxidiert. Im Gegensatz zu PASMC, zeigten RASMC eine niedrigere Abnahme der Atmung und keinen Anstieg von Superoxid oder dem Membranpotential unter Hypoxie. Während pharmakologischer Inhibierung der Mitochondrien korrespondierte der cytochromale Redox-Status mit der Stärke der HPV.

Die Daten der vorliegenden Arbeit legen daher nahe, dass die Inhibierung von Komplex IV ein wesentlicher Schritt beim mitochondrialen Sauerstoffsensing der HPV ist. Gleichzeitig könnte ein Anstieg der Sauerstoffradikalfreisetzung von Komplex III und des mitochondrialen

Membranpotentials die der HPV zugrunde liegende Signaltransduktion initiieren. In isolierten Lungen ist die HPV ausserdem möglicherweise durch den Oxygenierungsstatus des Hemoglobin moduliert, während es keinen Hinweis darauf gibt, dass Kohlenmonoxid mittels Cytochrome P450 Interaktion eine Rolle spielt.

7 References

1. Naeije R, Brimiouille S. *Physiology in medicine: importance of hypoxic pulmonary vasoconstriction in maintaining arterial oxygenation during acute respiratory failure.* Crit Care 5(2): 67-71, 2001.
2. Carter EP, Hartsfield CL, Miyazono M, Jakkula M, Morris KG, Jr., McMurtry IF. *Regulation of heme oxygenase-1 by nitric oxide during hepatopulmonary syndrome.* Am J Physiol Lung Cell Mol Physiol 283(2): 346-53, 2002.
3. Marshall BE. *Hypoxic pulmonary vasoconstriction.* Acta Anaesthesiol Scand Suppl 94: 37-41, 1990.
4. Weissmann N, Akkayagil E, Quanz K, Schermuly RT, Ghofrani HA, Fink L, Hanze J, Rose F, Seeger W, Grimminger F. *Basic features of hypoxic pulmonary vasoconstriction in mice.* Respir Physiol Neurobiol 139(2): 191-202, 2004.
5. Weissmann N, Grimminger F, Walmrath D, Seeger W. *Hypoxic vasoconstriction in buffer-perfused rabbit lungs.* Respir Physiol 100(2): 159-69, 1995.
6. Lindgren L, Marshall C, Marshall BE. *Hypoxic pulmonary vasoconstriction in isolated rat lungs perfused with perfluorocarbon emulsion.* Acta Physiol Scand 123(3): 335-8, 1985.
7. Peake MD, Harabin AL, Brennan NJ, Sylvester JT. *Steady-state vascular responses to graded hypoxia in isolated lungs of five species.* J Appl Physiol 51(5): 1214-9, 1981.
8. Skovgaard N, Abe AS, Andrade DV, Wang T. *Hypoxic pulmonary vasoconstriction in reptiles: a comparative study of four species with different lung structures and pulmonary blood pressures.* Am J Physiol Regul Integr Comp Physiol 289(5): 1280-8, 2005.
9. Olson KR, Russell MJ, Forster ME. *Hypoxic vasoconstriction of cyclostome systemic vessels: the antecedent of hypoxic pulmonary vasoconstriction?* Am J Physiol Regul Integr Comp Physiol 280(1): 198-206, 2001.
10. Plumier L. *La circulation pulmonaire chez le chien.* Arch Int Physiol 1: 176-213, 1904.
11. Bradford JR, Dean HP. *The pulmonary circulation.* J Physiol (Lond) 16: 34-96, 1894.
12. Von Euler US, Liljestrand G. *Observations on the pulmonary arterial blood pressure in the cat.* Acta Physiol Scand 12: 301-20, 1946.
13. Motley HL. *The influence of short periods of induced acute anoxia upon pulmonary arterial pressure in man.* Am J Physiol 150(1947-1948): -315-20, 2007.
14. Weissmann N, Sommer N, Schermuly RT, Ghofrani HA, Seeger W, Grimminger F. *Oxygen sensors in hypoxic pulmonary vasoconstriction.* Cardiovasc Res 71(4): 620-9, 2006.
15. Hillier SC, Graham JA, Hanger CC, Godbey PS, Glenn RW, Wagner WW, Jr. *Hypoxic vasoconstriction in pulmonary arterioles and venules.* J Appl Physiol 82(4): 1084-90, 1997.
16. Staub NC. *Site of hypoxic pulmonary vasoconstriction.* Chest 88(4 Suppl): 240S-5S, 1985.
17. Kato M, Staub NC. *Response of small pulmonary arteries to unilobar hypoxia and hypercapnia.* Circ Res 19(2): 426-40, 1966.

18. Dawson CA, Grimm DJ, Linehan JH. *Influence of hypoxia on the longitudinal distribution of pulmonary vascular resistance.* J Appl Physiol 44(4): 493-8, 1978.
19. Madden JA, Dawson CA, Harder DR. *Hypoxia-induced activation in small isolated pulmonary arteries from the cat.* J Appl Physiol 59(1): 113-8, 1985.
20. Fike CD, Kaplowitz MR. *Developmental differences in vascular responses to hypoxia in lungs of rabbits.* J Appl Physiol 77(2): 507-16, 1994.
21. Murray TR, Chen L, Marshall BE, Macarak EJ. *Hypoxic contraction of cultured pulmonary vascular smooth muscle cells.* Am J Respir Cell Mol Biol 3(5): 457-65, 1990.
22. Madden JA, Vadula MS, Kurup VP. *Effects of hypoxia and other vasoactive agents on pulmonary and cerebral artery smooth muscle cells.* Am J Physiol 263(3 Pt 1): 384-93, 1992.
23. Michelakis ED, Hampl V, Nsair A, Wu X, Harry G, Haromy A, Gurtu R, Archer SL. *Diversity in mitochondrial function explains differences in vascular oxygen sensing.* Circ Res 90(12): 1307-15, 2002.
24. Yuan XJ, Tod ML, Rubin LJ, Blaustein MP. *Hypoxic and metabolic regulation of voltage-gated K⁺ channels in rat pulmonary artery smooth muscle cells.* Exp Physiol 80(5): 803-13, 1995.
25. Olschewski A, Hong Z, Nelson DP, Weir EK. *Graded response of K⁺ current, membrane potential, and [Ca²⁺]_i to hypoxia in pulmonary arterial smooth muscle.* Am J Physiol Lung Cell Mol Physiol 283(5): L1143-L1150, 2002.
26. Kang TM, Park MK, Uhm DY. *Characterization of hypoxia-induced [Ca²⁺]_i rise in rabbit pulmonary arterial smooth muscle cells.* Life Sci 70(19): 2321-33, 2002.
27. Sylvester JT, Gottlieb JE, Rock P., Wetzel R.C. Acute hypoxic responses. In: Abnormal Pulmonary Circulation, editor. Bergofsky EF. New York: Churchill-Livingstone; 1986. p. 127-65.
28. Stroud RC, Rahn H. *Effect of O₂ and CO₂ tensions upon the resistance of pulmonary blood vessels.* Am J Physiol 172(1): 211-20, 1953.
29. Fishman AP. *Hypoxia on the pulmonary circulation. How and where it acts.* Circ Res 38(4): 221-31, 1976.
30. Cutaia M, Rounds S. *Hypoxic pulmonary vasoconstriction. Physiologic significance, mechanism, and clinical relevance.* Chest 97(3): 706-18, 1990.
31. Davis MJ, Joyner WL, Gilmore JP. *Microvascular pressure distribution and responses of pulmonary allografts and cheek pouch arterioles in the hamster to oxygen.* Circ Res 49(1): 125-32, 1981.
32. Liu Q, Sham JS, Shimoda LA, Sylvester JT. *Hypoxic constriction of porcine distal pulmonary arteries: endothelium and endothelin dependence.* Am J Physiol Lung Cell Mol Physiol 280(5): 856-65, 2001.
33. Aaronson PI, Robertson TP, Ward JP. *Endothelium-derived mediators and hypoxic pulmonary vasoconstriction.* Respir Physiol Neurobiol 132(1): 107-20, 2002.
34. Weir EK, Olschewski A. *Role of ion channels in acute and chronic responses of the pulmonary vasculature to hypoxia.* Cardiovasc Res 71(4): 630-41, 2006.
35. Harder DR, Madden JA, Dawson C. *Hypoxic induction of Ca²⁺-dependent action potentials in small pulmonary arteries of the cat.* J Appl Physiol 59(5): 1389-93, 1985.
36. Savineau JP, Gonzalez de la Fuente P, Marthan R. *Cellular mechanisms of hypoxia-induced contraction in human and rat pulmonary arteries.* Respir Physiol 99(2): 191-8, 1995.

37. Ohe M, Ogata M, Shirato K, Takishima T. *Effects of verapamil and BAY K 8644 on the hypoxic contraction of the isolated human pulmonary artery*. *Tohoku J Exp Med* 157(1): 81-2, 1989.
38. Tucker A, McMurtry IF, Grover RF, Reeves JT. *Attenuation of hypoxic pulmonary vasoconstriction by verapamil in intact dogs*. *Proc Soc Exp Biol Med* 151(3): 611-4, 1976.
39. Weigand L, Foxson J, Wang J, Shimoda LA, Sylvester JT. *Inhibition of hypoxic pulmonary vasoconstriction by antagonists of store-operated Ca²⁺ and nonselective cation channels*. *Am J Physiol Lung Cell Mol Physiol* 289(1): L5-L13, 2005.
40. Wang J, Shimoda LA, Weigand L, Wang W, Sun D, Sylvester JT. *Acute hypoxia increases intracellular [Ca²⁺] in pulmonary arterial smooth muscle by enhancing capacitative Ca²⁺ entry*. *Am J Physiol Lung Cell Mol Physiol* 288(6): L1059-L1069, 2005.
41. Ward JP, Robertson TP, Aaronson PI. *Capacitative calcium entry: a central role in hypoxic pulmonary vasoconstriction?* *Am J Physiol Lung Cell Mol Physiol* 289(1): 2-4, 2005.
42. Yuan XJ, Goldman WF, Tod ML, Rubin LJ, Blaustein MP. *Hypoxia reduces potassium currents in cultured rat pulmonary but not mesenteric arterial myocytes*. *Am J Physiol* 264(2 Pt 1): 116-23, 1993.
43. Post JM, Hume JR, Archer SL, Weir EK. *Direct role for potassium channel inhibition in hypoxic pulmonary vasoconstriction*. *Am J Physiol* 262(4 Pt 1): 882-90, 1992.
44. Hasunuma K, Rodman DM, McMurtry IF. *Effects of K⁺ channel blockers on vascular tone in the perfused rat lung*. *Am Rev Respir Dis* 144(4): 884-7, 1991.
45. Patel AJ, Lazdunski M, Honore E. *Kv2.1/Kv9.3, a novel ATP-dependent delayed-rectifier K⁺ channel in oxygen-sensitive pulmonary artery myocytes*. *Embo J* 16(22): 6615-25, 1997.
46. Hulme JT, Coppock EA, Felipe A, Martens JR, Tamkun MM. *Oxygen sensitivity of cloned voltage-gated K(+) channels expressed in the pulmonary vasculature*. *Circ Res* 85(6): 489-97, 1999.
47. Archer SL, Souil E, Dinh-Xuan AT, Schremmer B, Mercier JC, El Yaagoubi A, Nguyen-Huu L, Reeve HL, Hampl V. *Molecular identification of the role of voltage-gated K⁺ channels, Kv1.5 and Kv2.1, in hypoxic pulmonary vasoconstriction and control of resting membrane potential in rat pulmonary artery myocytes*. *J Clin Invest* 101(11): 2319-30, 1998.
48. Reeve HL, Weir EK, Nelson DP, Peterson DA, Archer SL. *Opposing effects of oxidants and antioxidants on K⁺ channel activity and tone in rat vascular tissue*. *Exp Physiol* 80(5): 825-34, 1995.
49. Weir EK, Hong Z, Porter VA, Reeve HL. *Redox signaling in oxygen sensing by vessels*. *Respir Physiol Neurobiol* 132(1): 121-30, 2002.
50. Park MK, Bae YM, Lee SH, Ho WK, Earm YE. *Modulation of voltage-dependent K⁺ channel by redox potential in pulmonary and ear arterial smooth muscle cells of the rabbit*. *Pflugers Arch* 434(6): 764-71, 1997.
51. Olschewski A, Hong Z, Peterson DA, Nelson DP, Porter VA, Weir EK. *Opposite effects of redox status on membrane potential, cytosolic calcium, and tone in pulmonary arteries and ductus arteriosus*. *Am J Physiol Lung Cell Mol Physiol* 286(1): 15-22, 2004.
52. Yuan XJ, Tod ML, Rubin LJ, Blaustein MP. *Deoxyglucose and reduced glutathione mimic effects of hypoxia on K⁺ and Ca²⁺ conductances in pulmonary artery cells*. *Am J Physiol* 267(1 Pt 1): L52-L63, 1994.

53. Cox RH. *Molecular determinants of voltage-gated potassium currents in vascular smooth muscle*. Cell Biochem Biophys 42(2): 167-95, 2005.
54. Firth AL, Yuill KH, Smirnov SV. *Mitochondria-dependent regulation of Kv currents in rat pulmonary artery smooth muscle cells*. Am J Physiol Lung Cell Mol Physiol 295(1): L61-L70, 2008.
55. Post JM, Gelband CH, Hume JR. *[Ca²⁺]_i inhibition of K⁺ channels in canine pulmonary artery. Novel mechanism for hypoxia-induced membrane depolarization*. Circ Res 77(1): 131-9, 1995.
56. Gelband CH, Gelband H. *Ca²⁺ release from intracellular stores is an initial step in hypoxic pulmonary vasoconstriction of rat pulmonary artery resistance vessels*. Circulation 96(10): 3647-54, 1997.
57. Archer SL, London B, Hampl V, Wu X, Nsair A, Puttagunta L, Hashimoto K, Waite RE, Michelakis ED. *Impairment of hypoxic pulmonary vasoconstriction in mice lacking the voltage-gated potassium channel Kv1.5*. Faseb J 15(10): 1801-3, 2001.
58. Weissmann N, Dietrich A, Fuchs B, Kalwa H, Ay M, Dumitrascu R, Olschewski A, Storch U, Schnitzler M, Ghofrani HA, Schermuly RT, Pinkenburg O, Seeger W, Grimminger F, Gudermann T. *Classical transient receptor potential channel 6 (TRPC6) is essential for hypoxic pulmonary vasoconstriction and alveolar gas exchange*. Proc Natl Acad Sci U S A 103(50): 19093-8, 2006.
59. Ng LC, Wilson SM, Hume JR. *Mobilization of sarcoplasmic reticulum stores by hypoxia leads to consequent activation of capacitative Ca²⁺ entry in isolated canine pulmonary arterial smooth muscle cells*. J Physiol 563(Pt 2): 409-19, 2005.
60. Snetkov VA, Aaronson PI, Ward JP, Knock GA, Robertson TP. *Capacitative calcium entry as a pulmonary specific vasoconstrictor mechanism in small muscular arteries of the rat*. Br J Pharmacol 140(1): 97-106, 2003.
61. Morio Y, McMurtry IF. *Ca²⁺ release from ryanodine-sensitive store contributes to mechanism of hypoxic vasoconstriction in rat lungs*. J Appl Physiol 92(2): 527-34, 2002.
62. Jabr RI, Toland H, Gelband CH, Wang XX, Hume JR. *Prominent role of intracellular Ca²⁺ release in hypoxic vasoconstriction of canine pulmonary artery*. Br J Pharmacol 122(1): 21-30, 1997.
63. Dipp M, Nye PC, Evans AM. *Hypoxic release of calcium from the sarcoplasmic reticulum of pulmonary artery smooth muscle*. Am J Physiol Lung Cell Mol Physiol 281(2): 318-25, 2001.
64. Zheng YM, Wang QS, Rathore R, Zhang WH, Mazurkiewicz JE, Sorrentino V, Singer HA, Kotlikoff MI, Wang YX. *Type-3 ryanodine receptors mediate hypoxia-, but not neurotransmitter-induced calcium release and contraction in pulmonary artery smooth muscle cells*. J Gen Physiol 125(4): 427-40, 2005.
65. Zable AC, Favero TG, Abramson JJ. *Glutathione modulates ryanodine receptor from skeletal muscle sarcoplasmic reticulum. Evidence for redox regulation of the Ca²⁺ release mechanism*. J Biol Chem 272(11): 7069-77, 1997.
66. Du W, Frazier M, McMahon TJ, Eu JP. *Redox activation of intracellular calcium release channels (ryanodine receptors) in the sustained phase of hypoxia-induced pulmonary vasoconstriction*. Chest 128(6 Suppl): 556S-8S, 2005.
67. Favero TG, Zable AC, Abramson JJ. *Hydrogen peroxide stimulates the Ca²⁺ release channel from skeletal muscle sarcoplasmic reticulum*. J Biol Chem 270(43): 25557-63, 1995.

68. Wilson HL, Dipp M, Thomas JM, Lad C, Galione A, Evans AM. *Adp-ribosyl cyclase and cyclic ADP-ribose hydrolase act as a redox sensor. a primary role for cyclic ADP-ribose in hypoxic pulmonary vasoconstriction.* J Biol Chem 276(14): 11180-8, 2001.
69. Kaplin AI, Snyder SH, Linden DJ. *Reduced nicotinamide adenine dinucleotide-selective stimulation of inositol 1,4,5-trisphosphate receptors mediates hypoxic mobilization of calcium.* J Neurosci 16(6): 2002-11, 1996.
70. Wolin MS, Gupte SA, Oeckler RA. *Superoxide in the vascular system.* J Vasc Res 39(3): 191-207, 2002.
71. Wolin MS. *Interactions of oxidants with vascular signaling systems.* Arterioscler Thromb Vasc Biol 20(6): 1430-42, 2000.
72. Sylvester JT. *Hypoxic pulmonary vasoconstriction: a radical view.* Circ Res 88(12): 1228-30, 2001.
73. Sham JS. *Hypoxic pulmonary vasoconstriction: ups and downs of reactive oxygen species.* Circ Res 91(8): 649-51, 2002.
74. Waypa GB, Schumacker PT. *Hypoxic pulmonary vasoconstriction: redox events in oxygen sensing.* J Appl Physiol 98(1): 404-14, 2005.
75. Moudgil R, Michelakis ED, Archer SL. *Hypoxic pulmonary vasoconstriction.* J Appl Physiol 98(1): 390-403, 2005.
76. Ward JP. *Point: Hypoxic pulmonary vasoconstriction is mediated by increased production of reactive oxygen species.* J Appl Physiol 101(3): 993-5, 2006.
77. Weir EK, Eaton JW, Chesler E. *Redox status and pulmonary vascular reactivity.* Chest 88(4 Suppl): 249S-52S, 1985.
78. Weir EK, Will JA, Lundquist LJ, Eaton JW, Chesler E. *Diamide inhibits pulmonary vasoconstriction induced by hypoxia or prostaglandin F2 alpha.* Proc Soc Exp Biol Med 173(1): 96-103, 1983.
79. Archer SL, Peterson D, Nelson DP, DeMaster EG, Kelly B, Eaton JW, Weir EK. *Oxygen radicals and antioxidant enzymes alter pulmonary vascular reactivity in the rat lung.* J Appl Physiol 66(1): 102-11, 1989.
80. Weissmann N, Grimminger F, Voswinckel R, Conzen J, Seeger W. *Nitro blue tetrazolium inhibits but does not mimic hypoxic vasoconstriction in isolated rabbit lungs.* Am J Physiol 274(5 Pt 1): 721-7, 1998.
81. Weissmann N, Tadic A, Hanze J, Rose F, Winterhalder S, Nollen M, Schermuly RT, Ghofrani HA, Seeger W, Grimminger F. *Hypoxic vasoconstriction in intact lungs: a role for NADPH oxidase-derived H(2)O(2)?* Am J Physiol Lung Cell Mol Physiol 279(4): 683-90, 2000.
82. Jin N, Packer CS, Rhoades RA. *Reactive oxygen-mediated contraction in pulmonary arterial smooth muscle: cellular mechanisms.* Can J Physiol Pharmacol 69(3): 383-8, 1991.
83. Jones RD, Thompson JS, Morice AH. *The effect of hydrogen peroxide on hypoxia, prostaglandin F2 alpha and potassium chloride induced contractions in isolated rat pulmonary arteries.* Pulm Pharmacol Ther 10(1): 37-42, 1997.
84. Waypa GB, Guzy R, Mungai PT, Mack MM, Marks JD, Roe MW, Schumacker PT. *Increases in mitochondrial reactive oxygen species trigger hypoxia-induced calcium responses in pulmonary artery smooth muscle cells.* Circ Res 99(9): 970-8, 2006.
85. Sommer N, Dietrich A, Schermuly RT, Ghofrani HA, Gudermann T, Schulz R, Seeger W, Grimminger F, Weissmann N. *Regulation of hypoxic pulmonary vasoconstriction: basic mechanisms.* Eur Respir J 32(6): 1639-51, 2008.

86. Archer S, Michelakis E. *The mechanism(s) of hypoxic pulmonary vasoconstriction: potassium channels, redox O(2) sensors, and controversies*. *News Physiol Sci* 17: 131-7, 2002.
87. Oeckler RA, Kaminski PM, Wolin MS. *Stretch enhances contraction of bovine coronary arteries via an NAD(P)H oxidase-mediated activation of the extracellular signal-regulated kinase mitogen-activated protein kinase cascade*. *Circ Res* 92(1): 23-31, 2003.
88. Staniek K, Nohl H. *Are mitochondria a permanent source of reactive oxygen species?* *Biochim Biophys Acta* 1460(2-3): 268-75, 2000.
89. Archer SL, Nelson DP, Weir EK. *Simultaneous measurement of O₂ radicals and pulmonary vascular reactivity in rat lung*. *J Appl Physiol* 67(5): 1903-11, 1989.
90. Archer SL, Nelson DP, Weir EK. *Detection of activated O₂ species in vitro and in rat lungs by chemiluminescence*. *J Appl Physiol* 67(5): 1912-21, 1989.
91. Cadenas E, Arad ID, Fisher AB, Boveris A, Chance B. *Hydroperoxide-induced chemiluminescence of the perfused lung*. *Biochem J* 192(1): 303-9, 1980.
92. Spasojevic I, Liochev SI, Fridovich I. *Lucigenin: redox potential in aqueous media and redox cycling with O₂(-2) production*. *Arch Biochem Biophys* 373(2): 447-50, 2000.
93. Liu JQ, Sham JS, Shimoda LA, Kuppusamy P, Sylvester JT. *Hypoxic constriction and reactive oxygen species in porcine distal pulmonary arteries*. *Am J Physiol Lung Cell Mol Physiol* 285(2): 322-33, 2003.
94. Killilea DW, Hester R, Balczon R, Babal P, Gillespie MN. *Free radical production in hypoxic pulmonary artery smooth muscle cells*. *Am J Physiol Lung Cell Mol Physiol* 279(2): 408-12, 2000.
95. Waypa GB, Chandel NS, Schumacker PT. *Model for hypoxic pulmonary vasoconstriction involving mitochondrial oxygen sensing*. *Circ Res* 88(12): 1259-66, 2001.
96. Archer SL, Huang J, Henry T, Peterson D, Weir EK. *A redox-based O₂ sensor in rat pulmonary vasculature*. *Circ Res* 73(6): 1100-12, 1993.
97. Weissmann N, Kuzkaya N, Fuchs B, Tiyerili V, Schafer RU, Schutte H, Ghofrani HA, Schermuly RT, Schudt C, Sydykov A, Egemnazarow B, Seeger W, Grimminger F. *Detection of reactive oxygen species in isolated, perfused lungs by electron spin resonance spectroscopy*. *Respir Res* 6(1): 86, 2005.
98. Weissmann N, Zeller S, Schafer RU, Turowski C, Ay M, Quanz K, Ghofrani HA, Schermuly RT, Fink L, Seeger W, Grimminger F. *Impact of Mitochondria and NADPH Oxidases on Acute and Sustained Hypoxic Pulmonary Vasoconstriction*. *Am J Respir Cell Mol Biol*, 2005.
99. Waypa GB, Marks JD, Guzy R, Mungai PT, Schriewer J, Dokic D, Schumacker PT. *Hypoxia Triggers Subcellular Compartmental Redox Signaling in Vascular Smooth Muscle Cells*. *Circ Res*, 2009.
100. Firth AL, Gordienko DV, Yuill KH, Smirnov SV. *Cellular localization of mitochondria contributes to Kv channel-mediated regulation of cellular excitability in pulmonary but not mesenteric circulation*. *Am J Physiol Lung Cell Mol Physiol* 296(3): L347-L360, 2009.
101. Hampl V, Herget J. *Possible mechanisms of oxygen sensing in the pulmonary circulation*. *Physiol Res* 40(5): 463-70, 1991.
102. Leach RM, Sheehan DW, Chacko VP, Sylvester JT. *Energy state, pH, and vasomotor tone during hypoxia in precontracted pulmonary and femoral arteries*. *Am J Physiol Lung Cell Mol Physiol* 278(2): 294-304, 2000.

103. Buescher PC, Pearse DB, Pillai RP, Litt MC, Mitchell MC, Sylvester JT. *Energy state and vasomotor tone in hypoxic pig lungs*. J Appl Physiol 70(4): 1874-81, 1991.
104. Bell EL, Emerling BM, Chandel NS. *Mitochondrial regulation of oxygen sensing*. Mitochondrion 5(5): 322-32, 2005.
105. Waypa GB, Marks JD, Mack MM, Boriboun C, Mungai PT, Schumacker PT. *Mitochondrial reactive oxygen species trigger calcium increases during hypoxia in pulmonary arterial myocytes*. Circ Res 91(8): 719-26, 2002.
106. Leach RM, Hill HS, Snetkov VA, Ward JP. *Hypoxia, energy state and pulmonary vasomotor tone*. Respir Physiol Neurobiol 132(1): 55-67, 2002.
107. Leach RM, Hill HM, Snetkov VA, Robertson TP, Ward JP. *Divergent roles of glycolysis and the mitochondrial electron transport chain in hypoxic pulmonary vasoconstriction of the rat: identity of the hypoxic sensor*. J Physiol 536(Pt 1): 211-24, 2001.
108. Evans AM, Mustard KJ, Wyatt CN, Peers C, Dipp M, Kumar P, Kinnear NP, Hardie DG. *Does AMP-activated protein kinase couple inhibition of mitochondrial oxidative phosphorylation by hypoxia to calcium signaling in O₂-sensing cells?* J Biol Chem 280(50): 41504-11, 2005.
109. Robertson TP, Mustard KJ, Lewis TH, Clark JH, Wyatt CN, Blanco EA, Peers C, Hardie DG, Evans AM. *AMP-activated protein kinase and hypoxic pulmonary vasoconstriction*. Eur J Pharmacol 595(1-3): 39-43, 2008.
110. Emerling BM, Weinberg F, Snyder C, Burgess Z, Mutlu GM, Viollet B, Budinger GR, Chandel NS. *Hypoxic activation of AMPK is dependent on mitochondrial ROS but independent of an increase in AMP/ATP ratio*. Free Radic Biol Med 46(10): 1386-91, 2009.
111. Ward JP, Knock GA, Snetkov VA, Aaronson PI. *Protein kinases in vascular smooth muscle tone--role in the pulmonary vasculature and hypoxic pulmonary vasoconstriction*. Pharmacol Ther 104(3): 207-31, 2004.
112. Weissmann N, Voswinckel R, Hardebusch T, Rosseau S, Ghofrani HA, Schermuly R, Seeger W, Grimminger F. *Evidence for a role of protein kinase C in hypoxic pulmonary vasoconstriction*. Am J Physiol 276(1 Pt 1): 90-5, 1999.
113. Rathore R, Zheng YM, Niu CF, Liu QH, Korde A, Ho YS, Wang YX. *Hypoxia activates NADPH oxidase to increase [ROS]_i and [Ca²⁺]_i through the mitochondrial ROS-PKCε signaling axis in pulmonary artery smooth muscle cells*. Free Radic Biol Med 45(9): 1223-31, 2008.
114. Huang H, Frohman MA. *Lipid signaling on the mitochondrial surface*. Biochim Biophys Acta 1791(9): 839-44, 2009.
115. Olson KR, Dombkowski RA, Russell MJ, Doellman MM, Head SK, Whitfield NL, Madden JA. *Hydrogen sulfide as an oxygen sensor/transducer in vertebrate hypoxic vasoconstriction and hypoxic vasodilation*. J Exp Biol 209(Pt 20): 4011-23, 2006.
116. Salvaterra CG, Goldman WF. *Acute hypoxia increases cytosolic calcium in cultured pulmonary arterial myocytes*. Am J Physiol 264(3 Pt 1): 323-8, 1993.
117. Gnaiger E. *Oxygen conformance of cellular respiration. A perspective of mitochondrial physiology*. Adv Exp Med Biol 543: 39-55, 2003.
118. Weissmann N, Ebert N, Ahrens M, Ghofrani HA, Schermuly RT, Hanze J, Fink L, Rose F, Conzen J, Seeger W, Grimminger F. *Effects of mitochondrial inhibitors and uncouplers on hypoxic vasoconstriction in rabbit lungs*. Am J Respir Cell Mol Biol 29(6): 721-32, 2003.

119. Leach RM, Hill HM, Snetkov VA, Robertson TP, Ward JP. *Divergent roles of glycolysis and the mitochondrial electron transport chain in hypoxic pulmonary vasoconstriction of the rat: identity of the hypoxic sensor.* J Physiol 536(Pt 1): 211-24, 2001.
120. Fisher AB, Dodia C. *Lung as a model for evaluation of critical intracellular PO₂ and PCO.* Am J Physiol 241(1): E47-E50, 1981.
121. Shigemori K, Ishizaki T, Matsukawa S, Sakai A, Nakai T, Miyabo S. *Adenine nucleotides via activation of ATP-sensitive K⁺ channels modulate hypoxic response in rat pulmonary artery.* Am J Physiol 270(5 Pt 1): 803-9, 1996.
122. Weissmann N, Zeller S, Schafer RU, Turowski C, Ay M, Quanz K, Ghofrani HA, Schermuly RT, Fink L, Seeger W, Grimminger F. *Impact of Mitochondria and NADPH Oxidases on Acute and Sustained Hypoxic Pulmonary Vasoconstriction.* Am J Respir Cell Mol Biol, 2005.
123. Rounds S, McMurtry IF. *Inhibitors of oxidative ATP production cause transient vasoconstriction and block subsequent pressor responses in rat lungs.* Circ Res 48(3): 393-400, 1981.
124. Wang YX, Zheng YM, Abdullaev I, Kotlikoff MI. *Metabolic inhibition with cyanide induces calcium release in pulmonary artery myocytes and Xenopus oocytes.* Am J Physiol Cell Physiol 284(2): C378-C388, 2003.
125. Paddenberg R, Konig P, Faulhammer P, Goldenberg A, Pfeil U, Kummer W. *Hypoxic vasoconstriction of partial muscular intra-acinar pulmonary arteries in murine precision cut lung slices.* Respir Res 7: 93, 2006.
126. Han D, Antunes F, Canali R, Rettori D, Cadenas E. *Voltage-dependent anion channels control the release of the superoxide anion from mitochondria to cytosol.* J Biol Chem 278(8): 5557-63, 2003.
127. Aon MA, Cortassa S, Marban E, O'Rourke B. *Synchronized whole cell oscillations in mitochondrial metabolism triggered by a local release of reactive oxygen species in cardiac myocytes.* J Biol Chem 278(45): 44735-44, 2003.
128. Murphy MP. *How mitochondria produce reactive oxygen species.* Biochem J 417(1): 1-13, 2009.
129. Lenaz G. *The mitochondrial production of reactive oxygen species: mechanisms and implications in human pathology.* IUBMB Life 52(3-5): 159-64, 2001.
130. Erusalimsky JD, Moncada S. *Nitric oxide and mitochondrial signaling: from physiology to pathophysiology.* Arterioscler Thromb Vasc Biol 27(12): 2524-31, 2007.
131. Dawson TL, Gores GJ, Nieminen AL, Herman B, Lemasters JJ. *Mitochondria as a source of reactive oxygen species during reductive stress in rat hepatocytes.* Am J Physiol 264(4 Pt 1): C961-C967, 1993.
132. Jezek P, Hlavata L. *Mitochondria in homeostasis of reactive oxygen species in cell, tissues, and organism.* Int J Biochem Cell Biol 37(12): 2478-503, 2005.
133. Chen Q, Vazquez EJ, Moghaddas S, Hoppel CL, Lesnefsky EJ. *Production of reactive oxygen species by mitochondria: central role of complex III.* J Biol Chem 278(38): 36027-31, 2003.
134. Guzy RD, Schumacker PT. *Oxygen sensing by mitochondria at complex III: the paradox of increased reactive oxygen species during hypoxia.* Exp Physiol 91(5): 807-19, 2006.
135. Michelakis ED, Thebaud B, Weir EK, Archer SL. *Hypoxic pulmonary vasoconstriction: redox regulation of O₂-sensitive K⁺ channels by a mitochondrial O₂-sensor in resistance artery smooth muscle cells.* J Mol Cell Cardiol 37(6): 1119-36, 2004.

136. Paddenberg R, Ishaq B, Goldenberg A, Faulhammer P, Rose F, Weissmann N, Braun-Dullaeus RC, Kummer W. *Essential role of complex II of the respiratory chain in hypoxia-induced ROS generation in the pulmonary vasculature.* Am J Physiol Lung Cell Mol Physiol 284(5): 710-9, 2003.
137. Brookes PS, Yoon Y, Robotham JL, Anders MW, Sheu SS. *Calcium, ATP, and ROS: a mitochondrial love-hate triangle.* Am J Physiol Cell Physiol 287(4): 817-33, 2004.
138. Andrukhiv A, Costa AD, West IC, Garlid KD. *Opening mitoKATP increases superoxide generation from complex I of the electron transport chain.* Am J Physiol Heart Circ Physiol 291(5): H2067-H2074, 2006.
139. Weir EK, Archer SL. *The mechanism of acute hypoxic pulmonary vasoconstriction: the tale of two channels.* FASEB J 9(2): 183-9, 1995.
140. Bell EL, Klimova TA, Eisenbart J, Moraes CT, Murphy MP, Budinger GR, Chandel NS. *The Qo site of the mitochondrial complex III is required for the transduction of hypoxic signaling via reactive oxygen species production.* J Cell Biol 177(6): 1029-36, 2007.
141. Wang Q, Wang YX, Yu M, Kotlikoff MI. *Ca(2+)-activated Cl- currents are activated by metabolic inhibition in rat pulmonary artery smooth muscle cells.* Am J Physiol 273(2 Pt 1): 520-30, 1997.
142. Drummond RM, Tuft RA. *Release of Ca²⁺ from the sarcoplasmic reticulum increases mitochondrial [Ca²⁺] in rat pulmonary artery smooth muscle cells.* J Physiol 516 (Pt 1): 139-47, 1999.
143. Duchen MR. *Contributions of mitochondria to animal physiology: from homeostatic sensor to calcium signalling and cell death.* J Physiol 516 (Pt 1): 1-17, 1999.
144. Kang TM, Park MK, Uhm DY. *Effects of hypoxia and mitochondrial inhibition on the capacitative calcium entry in rabbit pulmonary arterial smooth muscle cells.* Life Sci 72(13): 1467-79, 2003.
145. Lassegue B, Clempus RE. *Vascular NAD(P)H oxidases: specific features, expression, and regulation.* Am J Physiol Regul Integr Comp Physiol 285(2): 277-97, 2003.
146. Mohazzab KM, Wolin MS. *Sites of superoxide anion production detected by lucigenin in calf pulmonary artery smooth muscle.* Am J Physiol 267(6 Pt 1): 815-22, 1994.
147. Griendling KK, Sorescu D, Ushio-Fukai M. *NAD(P)H oxidase: role in cardiovascular biology and disease.* Circ Res 86(5): 494-501, 2000.
148. Gabig TG, Bearman SI, Babior BM. *Effects of oxygen tension and pH on the respiratory burst of human neutrophils.* Blood 53(6): 1133-9, 1979.
149. Matsuzaki I, Chatterjee S, Debolt K, Manevich Y, Zhang Q, Fisher AB. *Membrane depolarization and NADPH oxidase activation in aortic endothelium during ischemia reflect altered mechanotransduction.* Am J Physiol Heart Circ Physiol 288(1): 336-43, 2005.
150. Petheo GL, Demarex N. *Voltage- and NADPH-dependence of electron currents generated by the phagocytic NADPH oxidase.* Biochem J 388(Pt 2): 485-91, 2005.
151. Shmelzer Z, Haddad N, Admon E, Pessach I, Leto TL, Eitan-Hazan Z, Hershinkel M, Levy R. *Unique targeting of cytosolic phospholipase A2 to plasma membranes mediated by the NADPH oxidase in phagocytes.* J Cell Biol 162(4): 683-92, 2003.
152. Marshall C, Marmay AJ, Verhoeven AJ, Marshall BE. *Pulmonary artery NADPH-oxidase is activated in hypoxic pulmonary vasoconstriction.* Am J Respir Cell Mol Biol 15(5): 633-44, 1996.

153. Thomas HM3, Carson RC, Fried ED, Novitch RS. *Inhibition of hypoxic pulmonary vasoconstriction by diphenyleneiodonium*. *Biochem Pharmacol* 42(7): 9-12, 1991.
154. Grimminger F, Weissmann N, Priestersbach R, Becker E, Rosseau S, Seeger W. *Effects of NADPH oxidase inhibitors on hypoxic vasoconstriction in buffer-perfused rabbit lungs*. *Am J Physiol* 268(5 Pt 1): 747-52, 1995.
155. Majander A, Finel M, Wikstrom M. *Diphenyleneiodonium inhibits reduction of iron-sulfur clusters in the mitochondrial NADH-ubiquinone oxidoreductase (Complex I)*. *J Biol Chem* 269(33): 21037-42, 1994.
156. Weir EK, Reeve HL, Cornfield DN, Tristani-Firouzi M, Peterson DA, Archer SL. *Diversity of response in vascular smooth muscle cells to changes in oxygen tension*. *Kidney Int* 51(2): 462-6, 1997.
157. Jones RD, Thompson JS, Morice AH. *The NADPH oxidase inhibitors iodonium diphenyl and cadmium sulphate inhibit hypoxic pulmonary vasoconstriction in isolated rat pulmonary arteries*. *Physiol Res* 49(5): 587-96, 2000.
158. Archer SL, Reeve HL, Michelakis E, Puttagunta L, Waite R, Nelson DP, Dinauer MC, Weir EK. *O₂ sensing is preserved in mice lacking the gp91 phox subunit of NADPH oxidase*. *Proc Natl Acad Sci U S A* 96(14): 7944-9, 1999.
159. Gupte SA, Kaminski PM, Floyd B, Agarwal R, Ali N, Ahmad M, Edwards J, Wolin MS. *Cytosolic NADPH may regulate differences in basal Nox oxidase-derived superoxide generation in bovine coronary and pulmonary arteries*. *Am J Physiol Heart Circ Physiol* 288(1): 13-21, 2005.
160. Ichinose F, Ullrich R, Sapirstein A, Jones RC, Bonventre JV, Serhan CN, Bloch KD, Zapol WM. *Cytosolic phospholipase A(2) in hypoxic pulmonary vasoconstriction*. *J Clin Invest* 109(11): 1493-500, 2002.
161. Jacobs ER, Zeldin DC. *The lung HETEs (and EETs) up*. *Am J Physiol Heart Circ Physiol* 280(1): H1-H10, 2001.
162. Birks EK, Bousamra M, Presberg K, Marsh JA, Effros RM, Jacobs ER. *Human pulmonary arteries dilate to 20-HETE, an endogenous eicosanoid of lung tissue*. *Am J Physiol* 272(5 Pt 1): 823-9, 1997.
163. Zhu D, Birks EK, Dawson CA, Patel M, Falck JR, Presberg K, Roman RJ, Jacobs ER. *Hypoxic pulmonary vasoconstriction is modified by P-450 metabolites*. *Am J Physiol Heart Circ Physiol* 279(4): 1526-33, 2000.
164. Harder DR, Narayanan J, Birks EK, Liard JF, Imig JD, Lombard JH, Lange AR, Roman RJ. *Identification of a putative microvascular oxygen sensor*. *Circ Res* 79(1): 54-61, 1996.
165. Tan JZ, Kaley G, Gurtner GH. *Nitric oxide and prostaglandins mediate vasodilation to 5,6-EET in rabbit lung*. *Adv Exp Med Biol* 407: 561-6, 1997.
166. Stephenson AH, Sprague RS, Weintraub NL, McMurdo L, Lonigro AJ. *Inhibition of cytochrome P-450 attenuates hypoxemia of acute lung injury in dogs*. *Am J Physiol* 270(4 Pt 2): 1355-62, 1996.
167. Zhu D, Bousamra M2, Zeldin DC, Falck JR, Townsley M, Harder DR, Roman RJ, Jacobs ER. *Epoxyeicosatrienoic acids constrict isolated pressurized rabbit pulmonary arteries*. *Am J Physiol Lung Cell Mol Physiol* 278(2): 335-43, 2000.
168. Yuan XJ, Tod ML, Rubin LJ, Blaustein MP. *Inhibition of cytochrome P-450 reduces voltage-gated K⁺ currents in pulmonary arterial myocytes*. *Am J Physiol* 268(1 Pt 1): 259-70, 1995.
169. Keseru B, Barbosa-Sicard E, Popp R, Fisslthaler B, Dietrich A, Gudermann T, Hammock BD, Falck JR, Weissmann N, Busse R, Fleming I. *Epoxyeicosatrienoic*

- acids and the soluble epoxide hydrolase are determinants of pulmonary artery pressure and the acute hypoxic pulmonary vasoconstrictor response.* FASEB J 22(12): 4306-15, 2008.
170. Weissmann N, Seeger W, Conzen J, Kiss L, Grimminger F. *Effects of arachidonic acid metabolism on hypoxic vasoconstriction in rabbit lungs.* Eur J Pharmacol 356(2-3): 231-7, 1998.
171. Chang SW, Dutton D, Wang HL, He LS, Stearns R, Hui A, Giacomini KM, Ortiz de Montellano P, Voelkel NF. *Intact lung cytochrome P-450 is not required for hypoxic pulmonary vasoconstriction.* Am J Physiol 263(4 Pt 1): 446-53, 1992.
172. Pokreisz P, Fleming I, Kiss L, Barbosa-Sicard E, Fisslthaler B, Falck JR, Hammock BD, Kim IH, Szelid Z, Vermeersch P, Gillijns H, Pellens M, Grimminger F, van Zonneveld AJ, Collen D, Busse R, Janssens S. *Cytochrome P450 epoxygenase gene function in hypoxic pulmonary vasoconstriction and pulmonary vascular remodeling.* Hypertension 47(4): 762-70, 2006.
173. Schenkman JB. *Spectral Analyses of Cytochromes P450.* Methods in Molecular Biology 320: 11-8, 2005.
174. Gilles-Gonzalez MA, Gonzalez G. *Heme-based sensors: defining characteristics, recent developments, and regulatory hypotheses.* J Inorg Biochem 99(1): 1-22, 2005.
175. Hoshi T, Lahiri S. *Cell biology. Oxygen sensing: it's a gas!* Science 306(5704): 2050-1, 2004.
176. Williams SE, Wootton P, Mason HS, Bould J, Iles DE, Riccardi D, Peers C, Kemp PJ. *Hemoxygenase-2 is an oxygen sensor for a calcium-sensitive potassium channel.* Science 306(5704): 2093-7, 2004.
177. Roth M, Rupp M, Hofmann S, Mittal M, Fuchs B, Sommer N, Parajuli N, Quanz K, Schubert D, Dony E, Schermuly RT, Ghofrani HA, Sausbier U, Rutschmann K, Wilhelm S, Seeger W, Ruth P, Grimminger F, Sausbier M, Weissmann N. *Heme oxygenase-2 and large-conductance Ca²⁺-activated K⁺ channels: lung vascular effects of hypoxia.* Am J Respir Crit Care Med 180(4): 353-64, 2009.
178. Tamayo L, Lopez-Lopez JR, Castaneda J, Gonzalez C. *Carbon monoxide inhibits hypoxic pulmonary vasoconstriction in rats by a cGMP-independent mechanism.* Pflugers Arch 434(6): 698-704, 1997.
179. Lahiri S, Antosiewicz J, Pokorski M. *A common oxygen sensor regulates the sensory discharge and glomus cell HIF-1alpha in the rat carotid body.* J Physiol Pharmacol 58 Suppl 5(Pt 1): 327-33, 2007.
180. Deinum G, Stone JR, Babcock GT, Marletta MA. *Binding of nitric oxide and carbon monoxide to soluble guanylate cyclase as observed with Resonance raman spectroscopy.* Biochemistry 35(5): 1540-7, 1996.
181. Attardi GM SM. *Mitochondrial Biogenesis and Genetics, Part a: 260 (Mitochondrial Biogenesis & Genetics).* San Diego, Academic Pr Inc., 1995.
182. Pon L, Schon E. *Mitochondria 2nd Edition.* Methods in Cell Biology 80. San Diego, Elsevier, 2007.
183. Brookes PS, Levonen AL, Shiva S, Sarti P, Darley-Usmar VM. *Mitochondria: regulators of signal transduction by reactive oxygen and nitrogen species.* Free Radic Biol Med 33(6): 755-64, 2002.
184. Lloyd D, Chance B. *Electron transport in mitochondria isolated from the flagellate Polytomella caeca.* Biochem J 107(6): 829-37, 1968.

185. Hollis VS, Palacios-Callender M, Springett RJ, Delpy DT, Moncada S. *Monitoring cytochrome redox changes in the mitochondria of intact cells using multi-wavelength visible light spectroscopy*. *Biochim Biophys Acta* 1607(2-3): 191-202, 2003.
186. Hutter E, Renner K, Jansen-Durr P, Gnaiger E. *Biphasic oxygen kinetics of cellular respiration and linear oxygen dependence of antimycin A inhibited oxygen consumption*. *Mol Biol Rep* 29(1-2): 83-7, 2002.
187. Bowen WJ. *The absorption spectra and extinction coefficients of myoglobin*. *J Biol Chem* 179(1): 235-45, 1949.
188. Guo Y, Guo G, Mao X, Zhang W, Xiao J, Tong W, Liu T, Xiao B, Liu X, Feng Y, Zou Q. *Functional identification of HugZ, a heme oxygenase from Helicobacter pylori*. *BMC Microbiol* 8: 226, 2008.
189. Boon EM, Huang SH, Marletta MA. *A molecular basis for NO selectivity in soluble guanylate cyclase*. *Nat Chem Biol* 1(1): 53-9, 2005.
190. Boon EM, Davis JH, Tran R, Karow DS, Huang SH, Pan D, Miazgowicz MM, Mathies RA, Marletta MA. *Nitric oxide binding to prokaryotic homologs of the soluble guanylate cyclase beta1 H-NOX domain*. *J Biol Chem* 281(31): 21892-902, 2006.
191. Yu L, Xu JX, Haley PE, Yu CA. *Properties of bovine heart mitochondrial cytochrome b560*. *J Biol Chem* 262(3): 1137-43, 1987.
192. Berry EA, Huang LS, DeRose VJ. *Ubiquinol-cytochrome c oxidoreductase of higher plants. Isolation and characterization of the bc1 complex from potato tuber mitochondria*. *J Biol Chem* 266(14): 9064-77, 1991.
193. Cross AR, Parkinson JF, Jones OT. *The superoxide-generating oxidase of leucocytes. NADPH-dependent reduction of flavin and cytochrome b in solubilized preparations*. *Biochem J* 223(2): 337-44, 1984.
194. Isogai Y, Iizuka T, Shiro Y. *The mechanism of electron donation to molecular oxygen by phagocytic cytochrome b558*. *J Biol Chem* 270(14): 7853-7, 1995.
195. OMURA T, SATO R. *A new cytochrome in liver microsomes*. *J Biol Chem* 237: 1375-6, 1962.
196. Rose F, Grimminger F, Appel J, Heller M, Pies V, Weissmann N, Fink L, Schmidt S, Krick S, Camenisch G, Gassmann M, Seeger W, Hanze J. *Hypoxic pulmonary artery fibroblasts trigger proliferation of vascular smooth muscle cells: role of hypoxia-inducible transcription factors*. *Faseb J* 16(12): 1660-1, 2002.
197. Fuchs B. *Die essentielle Bedeutung des „Classical Transient Receptor Potential 6“ (TRPC6)-Ionenkanals für die akute vaskuläre Hypoxiereaktion der Lunge - Untersuchungen an isolierten pulmonalerteriellen glatten Muskelzellen [PhD thesis]*. Giessen: Justus Liebig University, 2006.
198. Gnaiger E. *Bioenergetics at low oxygen: dependence of respiration and phosphorylation on oxygen and adenosine diphosphate supply*. *Respir Physiol* 128(3): 277-97, 2001.
199. Gnaiger E, Steinlechner-Maran R, Mendez G, Eberl T, Margreiter R. *Control of mitochondrial and cellular respiration by oxygen*. *J Bioenerg Biomembr* 27(6): 583-96, 1995.
200. Steinlechner-Maran R, Eberl T, Kunc M, Margreiter R, Gnaiger E. *Oxygen dependence of respiration in coupled and uncoupled endothelial cells*. *Am J Physiol* 271(6 Pt 1): C2053-C2061, 1996.
201. Reers M, Smiley ST, Mottola-Hartshorn C, Chen A, Lin M, Chen LB. *Mitochondrial membrane potential monitored by JC-1 dye*. *Methods Enzymol* 260: 406-17, 1995.

202. Mukhopadhyay P, Rajesh M, Yoshihiro K, Hasko G, Pacher P. *Simple quantitative detection of mitochondrial superoxide production in live cells*. *Biochem Biophys Res Commun* 358(1): 203-8, 2007.
203. Aviram I, Sharabani M. *Kinetic studies of the reduction of neutrophil cytochrome b-558 by dithionite*. *Biochem J* 237(2): 567-72, 1986.
204. Foroozan R, Ruedi JM, Babior BM. *The reduction of cytochrome b558 and the activity of the respiratory burst oxidase from human neutrophils*. *J Biol Chem* 267(34): 24400-7, 1992.
205. Bohren CF, Huffmann DR. *Absorption and scattering of light by small particles*. New York, Wiley-Interscience, 1983.
206. Beauvoit B, Chance B. *Time-resolved spectroscopy of mitochondria, cells and tissues under normal and pathological conditions*. *Mol Cell Biochem* 184(1-2): 445-55, 1998.
207. Chance B. *Spectra and reaction kinetics of respiratory pigments of homogenized and intact cells*. *Nature* 169(4293): 215-21, 1952.
208. Sommer N, Schörner S, Derfuss T, Krug A, Gnaiger E, Ghofrani H, Schermuly R, Huckstorf C, Seeger W, Grimminger F, Weissmann N. *Mitochondrial cytochrome redox states and respiration in acute pulmonary oxygen sensing*. *Eur.Respir.J.* 36(5):1056-66, 2010.
209. Ward JP, Snetkov VA, Aaronson PI. *Calcium, mitochondria and oxygen sensing in the pulmonary circulation*. *Cell Calcium* 36(3-4): 209-20, 2004.
210. Brunelle JK, Bell EL, Quesada NM, Vercauteren K, Tiranti V, Zeviani M, Scarpulla RC, Chandel NS. *Oxygen sensing requires mitochondrial ROS but not oxidative phosphorylation*. *Cell Metab* 1(6): 409-14, 2005.
211. Drose S, Brandt U. *The mechanism of mitochondrial superoxide production by the cytochrome bc1 complex*. *J Biol Chem* 283(31): 21649-54, 2008.
212. Palacios-Callender M, Quintero M, Hollis VS, Springett RJ, Moncada S. *Endogenous NO regulates superoxide production at low oxygen concentrations by modifying the redox state of cytochrome c oxidase*. *Proc Natl Acad Sci U S A* 101(20): 7630-5, 2004.
213. Gnaiger E, Mendez G, Hand SC. *High phosphorylation efficiency and depression of uncoupled respiration in mitochondria under hypoxia*. *Proc Natl Acad Sci U S A* 97(20): 11080-5, 2000.
214. Muller F, Crofts AR, Kramer DM. *Multiple Q-cycle bypass reactions at the Qo site of the cytochrome bc1 complex*. *Biochemistry* 41(25): 7866-74, 2002.
215. Robinson KM, Janes MS, Pehar M, Monette JS, Ross MF, Hagen TM, Murphy MP, Beckman JS. *Selective fluorescent imaging of superoxide in vivo using ethidium-based probes*. *Proc Natl Acad Sci U S A* 103(41): 15038-43, 2006.
216. Waypa GB, Marks JD, Guzy R, Mungai PT, Schriewer J, Dokic D, Schumacker PT. *Hypoxia triggers subcellular compartmental redox signaling in vascular smooth muscle cells*. *Circ Res* 106(3): 526-35, 2010.
217. Bonnet S, Archer SL. *Potassium channel diversity in the pulmonary arteries and pulmonary veins: implications for regulation of the pulmonary vasculature in health and during pulmonary hypertension*. *Pharmacol Ther* 115(1): 56-69, 2007.
218. Platoshyn O, Brevnova EE, Burg ED, Yu Y, Remillard CV, Yuan JX. *Acute hypoxia selectively inhibits KCNA5 channels in pulmonary artery smooth muscle cells*. *Am J Physiol Cell Physiol* 290(3): C907-C916, 2006.

219. Cross AR, Parkinson JF, Jones OT. *Mechanism of the superoxide-producing oxidase of neutrophils. O₂ is necessary for the fast reduction of cytochrome b-245 by NADPH.* Biochem J 226(3): 881-4, 1985.
220. Foroozan R, Ruedi JM, Babior BM. *The reduction of cytochrome b558 and the activity of the respiratory burst oxidase from human neutrophils.* J Biol Chem 267(34): 24400-7, 1992.
221. Zhu D, Effros RM, Harder DR, Roman RJ, Jacobs ER. *Tissue sources of cytochrome P450 4A and 20-HETE synthesis in rabbit lungs.* Am J Respir Cell Mol Biol 19(1): 121-8, 1998.
222. Omura T. *Cytochrome P-450: Second Edition.* Cambridge, VCH Publishers (UK) Ltd., 1993.
223. Ballou DP, Zhao Y, Brandish PE, Marletta MA. *Revisiting the kinetics of nitric oxide (NO) binding to soluble guanylate cyclase: the simple NO-binding model is incorrect.* Proc Natl Acad Sci U S A 99(19): 12097-101, 2002.
224. Qiu Y, Sutton L, Riggs AF. *Identification of myoglobin in human smooth muscle.* J Biol Chem 273(36): 23426-32, 1998.
225. Deem S, Min JH, Moulding JD, Eveland R, Swenson ER. *Red blood cells prevent inhibition of hypoxic pulmonary vasoconstriction by nitrite in isolated, perfused rat lungs.* Am J Physiol Heart Circ Physiol 292(2): H963-H970, 2007.
226. Cooper CE. *Radical producing and consuming reactions of hemoglobin: how can we limit toxicity?* Artif Organs 33(2): 110-4, 2009.
227. Liao GL, Palmer G. *The reduced minus oxidized difference spectra of cytochromes a and a₃.* Biochim Biophys Acta 1274(3): 109-11, 1996.
228. Huang LS, Borders TM, Shen JT, Wang CJ, Berry EA. *Crystallization of mitochondrial respiratory complex II from chicken heart: a membrane-protein complex diffracting to 2.0 Å.* Acta Crystallogr D Biol Crystallogr 61(Pt 4):380-7, 2005.
229. T'sai A, Palmer G. *Purification and characterization of highly purified cytochrome b from complex III of baker's yeast.* Biochimica et Biophysica Acta 681 (1982) 484-495

8 Appendix

8.1 Published reference spectra

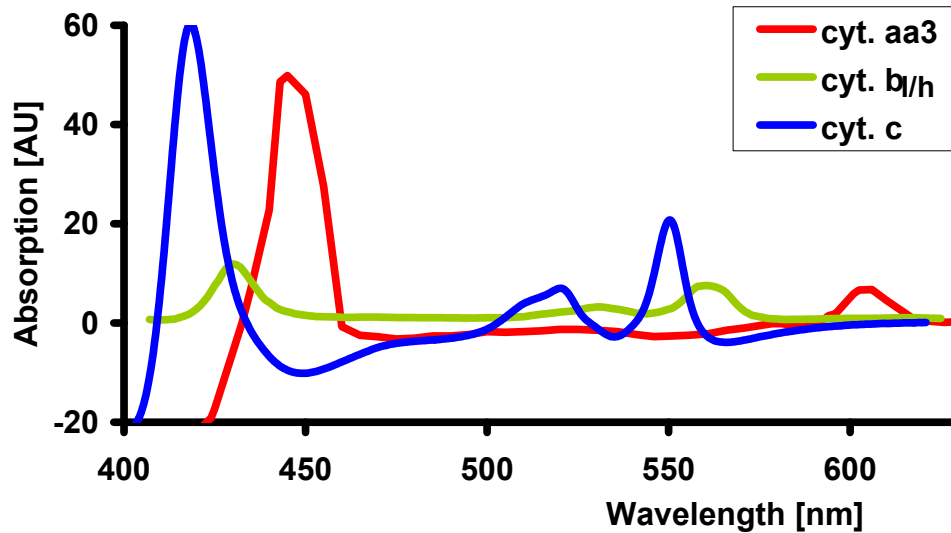


Figure 8.1: Published reference difference spectra

Reference spectra (reduced minus oxidized) are derived from the following sources: Liao et al. [227], Huang et al. [228], Palmer et al. [229] and University College London:

http://www.medphys.ucl.ac.uk/research/borl/research/NIR_topics/spectra/spectra.htm. Stand: 10.10.2010

8.2 Measured reference spectra

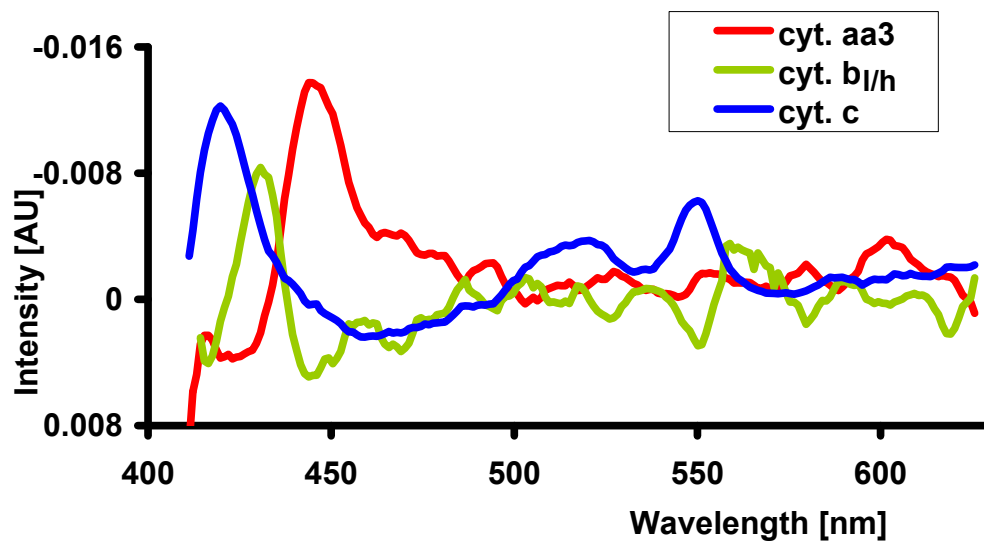


Figure 8.2 Measured reference difference spectra

Reference spectra (reduced minus oxidized) derived by application of mitochondrial inhibitors (see 3.1.3)

**Der Lebenslauf wurde aus der elektronischen
Version der Arbeit entfernt.**

**The curriculum vitae was removed from the
electronic version of the paper.**

Publications

1. **Sommer N**, Pak O, Schörner S, Derfuss T, Krug A, Gnaiger E, Ghofrani HA, Schermuly RT, Huckstorf C, Seeger W, Grimminger F, Weissmann N. Mitochondrial cytochrome redox states and respiration in acute pulmonary oxygen sensing. *Eur Respir J* 36(5):1056-66, 2010
2. Ketabchi F, Egemnazarov B, Schermuly RT, Ghofrani HA, Seeger W, Grimminger F, Shid, Moosavi M, Dehghani GA, Weissmann N, **Sommer N**. Effects of hypercapnia with and without acidosis on hypoxic pulmonary vasoconstriction. *Am J Physiol Lung Cell Mol Physiol* 297:L977-L983, 2009
3. Roth M, Rupp M, Hofmann S, Mittal M, Fuchs B, **Sommer N**, Parajuli N, Quanz K, Schubert D, Dony E, Schermuly RT, Ghofrani HA, Sausbier U, Rutschmann K, Wilhelm S, Seeger W, Ruth P, Grimminger F, Sausbier M, Weissmann N. Heme oxygenase-2 and large-conductance Ca²⁺-activated K⁺ channels: lung vascular effects of hypoxia. *Am J Respir Crit Care Med* 180:353-64, 2009
4. **Sommer N**, Dietrich A, Schermuly RT, Ghofrani HA, Gudermann T, Schulz R, Seeger W, Grimminger F, Weissmann N. Regulation of hypoxic pulmonary vasoconstriction: basic mechanisms. *Eur Respir J* 32:1639-51, 2008
5. Weissmann N, **Sommer N**, Schermuly RT, Ghofrani HA, Seeger W, Grimminger F. Oxygen sensors in hypoxic pulmonary vasoconstriction. *Cardiovasc Res* 71:620-9, 2006
6. **Sommer N**, Romano C, Jevtovic-Todorovic V. Chronic exposure to nitrous oxide increases [3H]MK801 binding in the cerebral cortex, but not in the hippocampus of adult mice. *Ann N Y Acad Sci* 1053:301-8, 2005
7. Walter B, Bauer R, Krug A, Derfuss T, Traichel F, **Sommer N**. Simultaneous measurement of local cortical blood flow and tissue oxygen saturation by Near infrared Laser Doppler flowmetry and remission spectroscopy in the pig brain. *Acta Neurochir Suppl* 81:197-9, 2002

Oral presentations

2nd Symposium of the Excellence Cluster Cardiopulmonary System (2009) Title: Differential Regulation of Mitochondrial Respiration and Cytochrome Redox State in Acute Pulmonary Oxygen Sensing

41st Annual Meeting of the German Society of Intensive Care and Emergency Medicine (2009) Title: Effects of Hypercapnia with and without Acidosis on Hypoxic Pulmonary Vasoconstriction

2nd Summer School on Mitochondrial Physiology (2008) Title: Simultaneous remission spectrophotometry and high-resolution respirometry

14th European Bioenergetics Conference (2006) Title: Simultaneous remission spectrophotometry and high-resolution respirometry. Respiratory control by oxygen and redox states of mitochondrial cytochromes in living cells

Abstracts and posters

Annual Meeting of the United Mitochondrial Disease Foundation (2009) Title: Mitochondrial alterations in pulmonary arterial smooth muscle cells in pulmonary arterial hypertension

105th International Conference of the American Thoracic Society (2009) Title: Differential regulation of mitochondrial respiration and cytochrome redox state in acute pulmonary oxygen sensing

104th International Conference of the American Thoracic Society (2008) Title: Hypoxic pulmonary vasoconstriction - Mitochondrial adaptations during acute and chronic hypoxia in oxygen sensing pulmonary arterial smooth muscle cells

16th European Bioenergetics Conference (2008) Title: Oxygen dependency of Mitochondrial Respiratory Chain Funktion in Hypoxic Pulmonary Vasoconstriction

103rd International Conference of the American Thoracic Society (2007) Title: Alterations in the redox state of pulmonary cytochromes in intact lungs during hypoxic vasoconstriction

Lung Science Conference of the European Respiratory Society (2007) Title: Hypoxic vasoconstriction –alterations in the redox state of pulmonary cytochromes in intact lungs during acute and sustained hypoxia

Lung Science Conference of the European Respiratory Society (2006) Titel: Role of mitochondrial respiratory chain in hypoxic vasoconstriction – In vivo observation of redox state of cytochromes in isolated perfused and ventilated lungs by remission spectrophotometry

10 Acknowledgements

I gratefully acknowledge my supervisor, Prof. Dr. Norbert Weissmann, for support in every respect during the experimental work in the lab, theoretical studies and composition of written works. It was always a great pleasure to work in an atmosphere of diligence and patience.

Thanks to the supervisors and teachers of the Graduate Program "Molecular Biology and Medicine of the Lung", that will provide the theoretical background for my research career in future.

In this regard, also many thanks to Prof. Dr. Werner Seeger, Director of the Department of Internal Medicine II, who made this program possible in combination with an excellent clinical education.

Most helpful work with inspiring character was performed by Oleg Pak, who I owe lots of thanks. He was always helping me and the other students with continuous cheerful mind.

I also want to thank my colleagues of the MBML, Bakytbek Egemnazarov, Manish Mittal and Sabine Lange for sharing time, fruitful discussions and entertainment in Giessen, Rauschholzhausen and at diverse conferences.

All the other people, who substantially contributed to the success of the work include particularly Karin Quanz, Ingrid Breitenborn-Müller, Carmen Homberger and Sabine Gräf-Höchst.

Special thanks also to Beate Fuchs, who established isolation of pulmonary arterial smooth muscle cells, Markus Roth for taking care of safety measures and Farzaneh Ketabchi for cooperation in hypercapnic studies.

Finally I would like to acknowledge the most dedicated medical students Julia Albus, Timm Hoeres, Susanne Schoerner, Phillip Krug and Sharon Waisbrod. May they also successfully finish their thesis soon!